WORKING PAPERS

N° 1378

December 2024

"The Welfare Consequences of Urban Traffic Regulations"

Isis Durrmeyer and Nicolás Martínez

Toulouse School of Economics

The Welfare Consequences of Urban Traffic Regulations

Isis Durrmeyer* Nicolás Martínez†

December 19, 2024

Abstract

We develop a structural model to represent individual transportation decisions, road traffic levels, and speeds in equilibrium within a city. The micro-founded model incorporates extensive heterogeneity: individuals differ in their access to transportation modes, travel time valuation, and scheduling constraints, while road congestion technologies vary across city zones. We estimate the model for the Paris area and predict the consequences of driving restrictions, uniform road tolls, and per-kilometer road tolls. We measure each policy's impact on welfare and its components - consumer surplus, toll revenue, and the value of emissions avoided- and benchmark these simple policies against welfare-maximizing personalized tolls.

JEL Classification: L9, R41, Q52

Keywords: structural model, policy evaluation, transportation, congestion, distributional effects, air pollution

*Toulouse School of Economics, Université Toulouse 1 Capitole. E-mail: isis.durrmeyer@tse-fr.eu

†Toulouse School of Economics, Université Toulouse 1 Capitole. E-mail: nicolas.martinez@tse-fr.eu

We would like to thank the Editor and three anonymous referees. We also thank Nano Barahona, Juan Camilo Castillo, Judy Chevalier, Philippe Gagnepain, Gaston Illanes, Luz Yadira Gómez-Hernández, Chenchen Huang, Myrto Kalouptsidi, Nicolas Koch, Lorenzo Magnolfi, Andrea Pozzi, Stef Proost, Valentina Reig, Mathias Reynaert, Marcelo Sant'Anna, Chenyu Yang, and Xin Zhang for their helpful comments and suggestions. We would also like to thank the participants of various seminars and conferences. We acknowledge financial support from the European Research Council under grant ERC-2019-STG-852815 "PRIDISP" and Agence Nationale de Recherche under grant ANR-17-EUR-0010 (Investissements d'Avenir program).

1 Introduction

Road traffic reduction is a key objective in large metropolitan areas due to the two main negative externalities cars generate: pollution and congestion. INRIX estimates that congestion costs an annual aggregate of 87 billion dollars in the U.S.[1] The effects of policies that aim to reduce congestion and pollution are difficult to predict since the road traffic levels are equilibrium outcomes of drivers' independent transportation decisions. Predicting individual reactions to changes in their transportation environment requires knowing how the road traffic equilibrium is modified after individuals make their transportation decisions. We define the transportation environment as all factors that affect individual transportation decisions and are exogenous to individuals, including the presence of urban traffic regulations. Observational studies that measure the direct impact of a change in the transportation environment are limited to comparing two equilibria. By contrast, we can separately identify individual reactions and the resulting equilibrium adjustments.

We develop a novel framework to analyze individual responses to changes in their transportation environments in equilibrium. It is a structural model representing equilibrium traffic conditions in a metropolitan area, with essential dimensions of heterogeneity at the individual and geographic levels. The first part of the model represents the choice of transportation mode and departure time by individuals with heterogeneous but fixed travel patterns (origin, destination, and itinerary). Since individuals have different travel patterns, transportation modes, preferences, and schedule flexibility, they react differently to changes in the transportation environment. Our model includes two key features that allow us to account for this heterogeneity. The first key feature is that different transportation modes are imperfect substitutes. The second key feature is the inclusion of individual schedule constraints, limiting their ability to substitute across departure times. We rely on a discrete choice nested logit model, containing heterogeneity in choice sets, sensitivities to trip duration and costs, and stochastic departure time constraints. The second part of the model represents the road congestion technologies which describe how driving speeds vary with changes in traffic level, represented by the total kilometers driven. Our model takes into account spatial heterogeneity by allowing the congestion technology to vary across areas of the city.

The model has the advantage of being transparent, tractable, and estimable with combinations of data that are typically publicly available for many metropolitan areas. We also provide a method to verify whether the model parameters are such that the equilibrium is unique. This model differs from existing ones in three key aspects. First, the model represents

[1] Source: https://www.cnbc.com/2019/02/11/americas-87-billion-traffic-jam-ranks-boston-and-dc-as-worst-in-us.html.

equilibrium transportation decisions for the entire metropolitan area rather than focusing on a specific road. Second, it accounts for different types of roads that may have different congestion technologies instead of considering one city-wide congestion technology. Third, all the model parameters are estimated and represent the joint distribution of preferences, schedule constraints, trip distances and itineraries, individual characteristics, and the available set of transportation mode choices. This joint distribution is key to analyze the effects of changes in the transportation environment at the individual level. To build a model with such individual heterogeneity, we must make some simplifications and consider some factors as exogenous. First, we consider only two departure times: peak and off-peak hours. Second, we hold fixed residential locations and trip destinations, i.e., we do not allow individuals to change where they live or work in response to a change in the transportation environment.[2] We focus on unavoidable trips (work or study trips), thus considering individuals who have to take their trips and do not model the number of trips. Consequently, the model does not micro-found the entire traffic; instead, we incorporate this by treating a portion of the traffic as unobserved. We believe that the population under study will be the most impacted by urban traffic regulations. Finally, we assume that the transportation modes available to an individual are fixed. While the choice of car ownership and car characteristics (e.g., fuel efficiency) may be affected by traffic regulations in the long term, we keep them constant in our analysis. Our welfare measures can be interpreted as short-run consequences of regulations.

We apply our model of transportation decisions and congestion to the Paris metropolitan area (Île-de-France region) and combine data from different sources to estimate the model parameters. We rely on transportation surveys conducted in 2010 and 2020, where respondents provided detailed information on all trips taken the day before the interview. We focus on the morning and work or study-related trips and construct a final sample of 15,470 individuals to estimate the transportation mode choice model. The surveys do not provide trip durations using the transportation modes that are not chosen or car trip durations for alternative departure times. To overcome this issue, we supplement the survey with data on expected travel times using Google Directions for public transport and the TomTom application programming interface (API, hereafter) for private vehicles during peak and off-peak hours. The surveys do not contain any information about individual schedule constraints. We assume that the ability to substitute between departure times depends on individual professional activity. We leverage additional workforce survey data to estimate the probability of being

[2]In our sample, the primary factor influencing residence choice is the price or size of the home, cited by 42.5% of respondents. This is followed by proximity to work, noted by 16.5%, and access to public transport, which is a priority for 1.9% of respondents.

flexible and therefore able to choose the departure time. The types of schedule constraints, i.e., whether individuals must commute during peak or off-peak hours when constrained, are jointly estimated with preference parameters, exploiting the distribution of departure times across socio-professional activities.

We estimate congestion technologies using two years of high-frequency data on traffic density and speed collected hourly from 1,359 traffic sensors across highways, ring roads, and the city center. Additionally, we use subway and suburban train ridership data to approximate overcrowding levels on metro and train lines during peak and off-peak hours.

We use our equilibrium model and estimated parameters to predict the effects of policy instruments that reduce road traffic, measuring changes in consumer surplus, toll revenue, and local and global pollutant emissions reductions valued at standard levels. We combine these three outcomes into a welfare function. While traffic reduction itself is not directly embedded in the welfare function, we treat it as the primary objective of these policies, maintaining a constant level of traffic reduction across different instruments. We analyze the effects of simple instruments: road tolls and simple driving restrictions.

Driving restrictions apply uniformly to all individuals, which is inefficient because even those who have limited alternatives are prevented from driving. Their advantage is implementation simplicity and ensuring that everyone contributes to traffic reduction, making them simple and effective policy instruments to decrease congestion. Such restrictions are often used as emergency schemes, which are temporary measures put in place under peak pollution episodes.[3] An alternative consists of sending price signals through road tolls. For instance, Stockholm and Singapore use congestion charges, restricting access to the city center during peak hours to those who pay a fee. Price mechanisms have the advantage of sorting individuals according to the benefits they get from driving: those who stop driving at peak hours have good transportation alternatives to driving or fewer schedule constraints, limiting the consumer surplus loss of traffic regulations. In addition, road tolls generate revenue that can be redistributed to individuals, mitigating consumer surplus losses.

In the main analysis, we compare the effects of driving restrictions with both fixed and variable tolls. These policies apply only during peak hours, allowing individuals unrestricted driving during off-peak times. We begin by examining the impacts of each policy across all possible levels of policy stringency. Under moderate stringency, both types of tolls improve welfare. This is not the case for driving restrictions, which always reduce welfare. Then, we

[3]Between 1997 and 2016, the Paris metropolitan area implemented alternate traffic restrictions based on license plate digits on six occasions. The longest of these schemes lasted four days, from December 6$^{\text{th}}$ to December 9$^{\text{th}}$, 2016. Since 2017, emergency plans activated during pollution peaks have instead imposed targeted driving restrictions based on vehicle age and fuel type.

decompose the welfare and evaluate its different components separately. All the regulations decrease consumer surplus, as speed gains cannot compensate for the consumer surplus losses due to the constraints imposed by the policies. From the consumer surplus perspective only, driving restrictions outperform the uniform tolls. Driving restrictions efficiently reduce traffic as they impose all drivers contribute to traffic reduction while a uniform toll requires a high value to reduce traffic as it mainly targets short-distance commuters. A high toll value generates high consumer surplus losses for all drivers. The variable toll is much more efficient since it targets long-distance commuters, who exert the largest congestion externalities. However, both tolls raise considerable revenue. Finally, the benefits of reducing emissions, computed using standard social values, are modest as they offset less than 6.8% of consumer surplus losses. In addition, w find that all policies are always progressive: the top 10% of high-income individuals lose more than those in the bottom 10%.

To further assess the effectiveness of the variable toll, we establish a first-best benchmark in which a social planner sets personalized tolls to maximize overall welfare. Our analysis shows that the variable toll performs well, capturing an average of 77.2% of potential welfare gains across different levels of stringency. However, the consumer surplus always decreases, and welfare improves only through the high toll revenues collected. Indeed, the social planner sets high tolls for individuals who are more likely to pay the toll in order to raise revenue. We also compare optimal policies conditional on each policy instrument. Here, we extend the set of policies analyzed and evaluate the performances of tolls with two parameters (fixed and variable parts, location-specific, and time-specific). We find that the fixed and variable toll achieves 86.4% of potential welfare gains; this is only one percent more than the variable toll. Location and time-specific tolls significantly improve the welfare gains relative to a uniform toll, which captures only 46.1% of potential welfare gains. Additionally, we explore personalized tolls that maximize consumer surplus and find some potential to reduce traffic while improving consumer surplus. The policy that maximizes consumer surplus sets prohibitively large tolls to a fraction of individuals while letting another share of individuals drive freely.

Finally, we fix a stringency level to go beyond the aggregate impacts of simple policy instruments and identify winners and losers. The analysis of consumer surplus changes under different policies shows that all policies result in a small fraction of winners. In a hypothetical vote on policy instrument, support would roughly be evenly distributed among driving restrictions, personalized tolls, and variable tolls, with no clear majority preference. Moreover, our analysis shows a U-shaped relationship between consumer surplus changes and income, indicating that middle-income individuals face the highest policy costs. Additionally, most emissions reductions stem from the far suburbs, implying that improving air quality in

the city center may be challenging.

We contribute to recent literature on modeling joint transportation decisions and traffic equilibrium in a city. Barwick et al. (2024) analyze the impact of tolls and driving restrictions on commuting choices and equilibrium congestion levels in Beijing. They endogenize individual housing location decisions and investigate the policies' effects on residential sorting. We consider housing locations fixed in our model but have a more flexible representation of congestion technology in the city and model departure time choice. Kreindler (2024) estimates a structural model of transportation decisions to analyze the welfare effects of congestion pricing in India. He leverages data from a field experiment to estimate preferences over departure times and the value of travel time. His model includes heterogeneous stochastic departure time preferences, costs for being early or late, and a switching cost parameter for route change. Our model focuses on the substitution between transportation modes and incorporates stochastic scheduling constraints and estimates heterogeneous sensitivities to travel time and trip cost. Almagro et al. (2024) consider a model similar to ours, but their analysis focuses on the combination of public transport policies and congestion charges. They utilize aggregate transportation data that do not contain any individual demographic characteristics, resulting in a more streamlined representation of individual preference heterogeneity compared to our approach.

Other papers with structural models of traffic equilibrium focus on a specific route or area rather than modeling the entire city. Tarduno (2022) models route and departure time choices for a bridge crossing but abstracts from mode substitution and ignores the effects of individual decisions on equilibrium speeds. Cook and Li (2023) evaluate the welfare effects of dynamic pricing on highway toll lanes with substitution across routes. Basso and Silva (2014) calibrates a single-road model where congestion varies with the choice of driving or taking the bus. Batarce and Ivaldi (2014) estimate a mode choice model with endogenous congestion, where the number of individuals driving generates congestion for the whole day.

Discrete choice models have been traditionally used to model transportation mode choices (McFadden, 1974, Small, 2012). Recent literature has relied on new data to estimate the value of travel time (VOT). Small et al. (2005) estimates individual VOT and valuations of travel time reliability using revealed and stated preferences data. Bento et al. (2020) use data from drivers entering an expressway subject to a toll to disentangle the value of urgency from the VOT of individuals. Buchholz et al. (2024) exploits data from a ride-sharing platform to retrieve individual VOT. Recent work has implemented field experiments to elicit directly travel time valuations (Goldszmidt et al., 2020, Kreindler, 2024, Hintermann et al., 2024). While our estimates of the VOT rely on the model structure, our results are consistent with

the estimates from this literature.

Our model for the congestion technology extends the work from the literature in two ways. First, we do not impose a linear or log-linear relationship between speed and traffic density as in Russo et al. (2021), Yang et al. (2020), Couture et al. (2018), Akbar and Duranton (2017). We estimate the relationships between speed and traffic density flexibly and find that the marginal impact of traffic on speed is not constant. Second, we estimate area-specific congestion technologies and model the equilibrium traffic level in each area and each period. Both differences have important consequences: the marginal cost of congestion varies with traffic level and city area.

This paper relates to the literature measuring the impacts of existing traffic regulations using direct policy evaluation methods. The initial literature focused on driving restrictions in developing countries (Davis, 2008, Gallego et al., 2013). Recent studies evaluate European policies such as low emissions zones, congestion charges, and road closures (Galdon-Sanchez et al., 2021, Tassinari, 2024, Herzog, 2023, Bou Sleiman, 2021). Our analysis differs, as we evaluate hypothetical policies, the heterogeneity of the their effects across individuals, and provide estimates for unobserved outcomes that are a function of the model parameters, such as consumer surplus.

Other empirical models that represent transportation decisions and congestion are based on the bottleneck model of Arnott et al. (1990) and Arnott et al. (1993) (Van Den Berg and Verhoef, 2011, Hall, 2018, and Hall, 2021). These models carefully describe congestion dynamics for a single road but ignore the substitution between driving and other transportation modes. Anderson (2014) shows that the substitution between cars and public transport significantly affects congestion levels. Van Den Berg and Verhoef (2011), Hall (2018) and Hall (2021) show that congestion pricing can improve consumer surplus without toll revenue redistribution. By contrast, we find that simple road tolls do not increase aggregate consumer surplus without redistributing the toll revenue, while personalized tolls can raise aggregate consumer surplus. Our finding that simple tolls can never increase aggregate consumer surplus is nevertheless consistent with Kreindler (2024), Barwick et al. (2024) and Almagro et al. (2024) who estimate models that are closer to ours.[4]

Previous literature on urban traffic policies in Paris (De Palma and Lindsey, 2006, Kilani et al., 2014) models equilibrium traffic level with a less detailed characterization of individual

[4]One important difference with bottleneck models is that we analyze traffic at the city level instead of studying a representative road - typically a highway where the speed improvements may be higher. Moreover, we model traffic levels at the period level instead of using a continuous time measure, ignoring the sorting of individuals within the period, which may generate extra consumer surplus. Furthermore, we consider that all roads are tolled while Hall (2018) and Hall (2021) consider only a fraction of the roads to be tolled.

preferences and limited mode substitution. De Palma et al. (1997) and Javaudin and de Palma (2024) incorporate a version of the bottleneck model into a calibrated citywide traffic simulator. De Palma et al. (2017) and Haywood and Koning (2015) study the role of public transport quality in Paris for driving decisions. Finally, while our model differs from general spatial equilibrium models, the analysis in our paper could be useful for models representing the locations choices of individuals when accounting for the role of transportation policies (see Allen and Arkolakis, 2022, Tsivanidis, 2022, Herzog, 2023, and Carstensen et al., 2022).

2 A structural model of transportation decisions and traffic conditions

We develop an equilibrium model representing the individual choice of a transportation mode and departure time. The model considers car trip durations as endogenous and dependent on the congestion levels on the roads, which are directly related to the number of drivers and how long they drive. We approximate this by the number of kilometers individuals drive in each time period. To represent the relationship between speed and traffic density, we model road congestion technologies for different areas in the city. Finally, we describe how to solve for the equilibrium of the model and check whether the equilibrium is unique. Table 18 in Appendix A includes an index of the mathematical notation used in the paper.

2.1 Transportation mode choice model

We introduce the structural model representing individuals choosing which transportation mode to use and their departure time for their morning commute trip. We consider that the origins and destinations of trips are given and exogenous. We also make the assumption that the itinerary from the origin to the destination is fixed. The city is split into A mutually exclusive areas. We do not allow for an outside option, as we model the choice of individuals facing unavoidable trips. We make the simplification that individuals choose between T discrete periods. There are J different transportation modes. Our model is a nested discrete choice model, and we follow the standard distributional assumptions from the literature (see Train, 2009). The nests correspond to the different transportation modes. We assume individuals choose a transportation mode and then decide when they leave home. The consequence of this modeling assumption is that we allow individuals to have correlated preference shocks for the same transportation mode across departure periods. The utility function of an individual n associated with transportation mode j, and departure time t is assumed to be a function of the mode and departure period characteristics X_{njt} (which

includes the trip cost, trip duration, and mode and period specific intercepts):

$$u_{njt} = \beta_n' X_{njt} + \epsilon_{njt}. \tag{1}$$

β_n is a vector of coefficients of preferences for these variables for consumer n and ϵ_{njt} is a random idiosyncratic term. This assumption implies that the different modes and departure periods are imperfect substitutes. We allow for correlation between these idiosyncratic terms across different periods by decomposing the preference shocks into a mode-specific shock ζ_{nj} common to all departure periods and a mode and period-specific shock $\tilde{\epsilon}_{njt}$:

$$\epsilon_{njt} = \zeta_{nj} + \sigma\tilde{\epsilon}_{njt}. \tag{2}$$

σ represents the degree of independence between the preference shocks ϵ_{njt} across different periods for the same transportation mode and is a parameter to estimate. When $\sigma = 1$, the preference shocks are independent, while if $\sigma = 0$, the preference shocks are identical within a mode and the departure periods are perfect substitutes. We assume here a simple correlation structure where there is a common mode specific shock. This implies that different period preference shocks have the same correlation. Distant periods might be less substitutable than closer ones; our model captures this through the mode and period-specific constants that should be more similar. There is another assumption behind Equation (2): σ does not depend on the mode and thus the preference shocks ϵ_{njt} have the same correlation across all transportation modes.

Each individual has a choice set which comprises all transportation modes ($\mathcal{J}_n$) and periods ($\mathcal{T}_n$) she can access. Individuals may have schedule constraints that make them unable to travel at certain periods. Each individual chooses the combination of mode j^* and departure time t^* that maximizes their utility:

$$\{j^*, t^*\} = \underset{j\in\mathcal{J}_n, t\in\mathcal{T}_n}{\arg\max}\, u_{njt}.$$

We assume that $\tilde{\epsilon}_{njt}$ are identically and independently distributed across individuals and follow a type one extreme value distribution. We assume that ζ_{nj} follows the only distribution such that ϵ_{njt} is also distributed according to an extreme value (see Cardell, 1997). The probability that individual n chooses the transportation mode j and departure time t is:

$$s_{njt|\mathcal{T}_n} = \frac{\exp\left(\frac{\beta_n' X_{njt}}{\sigma}\right)}{D_{nj}^{1-\sigma}\sum_{j'\in\mathcal{J}_n} D_{nj'}^{\sigma}}, \tag{3}$$

where $D_{nj'} = \sum_{t \in \mathcal{T}_n} \exp\left(\frac{\beta_n' X_{nj't}}{\sigma}\right)$.

In the following, we consider that individual schedule constraints are stochastic, which means that they may vary daily. Another interpretation of the stochastic constraints is that there are unobserved constraints, and the model approximates this unobserved level of individual heterogeneity (see Crawford et al., 2021 for a survey on unobserved choice set heterogeneity). There are L possible combinations of periods. We denote by π_{nl} the probability that individual n has access to the subset of periods $\mathcal{T}_l$. In this model, the expected probability of choosing the combination of mode and period j and t is:

$$s_{njt} = \sum_{l=1}^{L} \pi_{nl} s_{njt|\mathcal{T}_l} = \sum_{l=1}^{L} \pi_{nl} \frac{\exp\left(\frac{\beta_n' X_{njt}}{\sigma}\right)}{D_{njl}^{1-\sigma} \sum_{j' \in \mathcal{J}_n} D_{nj'l}^{\sigma}}, \tag{4}$$

where $D_{njl} = \sum_{t' \in \mathcal{T}_l} \exp\left(\frac{\beta_n' X_{njt'}}{\sigma}\right)$.

To ease notation, when referring to driving as a transportation mode, we use index **d**. Therefore, the probability of individual n driving in period t is $s_{n\mathbf{d}t}$. The individual probabilities of choosing a mode depend on trip durations. The individual car trip duration is the sum of the duration driven in each area, which itself is the distance divided by the driving speed in that area:

$$\text{duration}_{n\mathbf{d}t} = \sum_{a=1}^{A} \frac{k_n^a}{v_t^a} \times \rho_{nt}. \tag{5}$$

k_n^a represents individual n's distance in area a and v_t^a is the speed in period t. If the itinerary of an individual does not include an area, distance is set to 0. ρ_{nt} represents an individual and period-specific multiplicative speed shock, which constitutes another structural parameter of the model. It captures individual-specific unobserved trip characteristics that make an individual average speed lower or higher than the average. We assume these shocks are exogenous to the traffic conditions and hold them constant when we simulate new traffic equilibria. We denote by $\mathbf{v}$ the vector of speeds for the different areas and periods and write the probability of driving at period t for individual n as $s_{n\mathbf{d}t}(\mathbf{v})$.

In our data, we observe a sample of N individuals, who represent the entire population in the metropolitan area using the individual weights $\omega_1, ..., \omega_N$. The total number of kilometers driven in period t within area a, K_t^a, is given by:

$$K_t^a = \sum_{n=1}^{N} \omega_n k_n^a s_{n\mathbf{d}t}(\mathbf{v}). \tag{6}$$

2.2 Road traffic conditions and congestion technology

We model congestion technology at the local level, with A mutually exclusive areas. The driving speed in an area depends on the congestion technology and the traffic level in that area only. Following the transportation literature, we base our congestion technology model on the fundamental traffic diagram (see Small et al., 2007). Geroliminis and Daganzo (2008) empirically show the existence of a fundamental traffic diagram at the city level, called a "macroscopic fundamental traffic diagram". Other applications include Yang et al. (2020), Couture et al. (2018), and Anderson and Davis (2020). We follow their approach but allow for heterogeneity within the city by considering area-specific congestion technologies.

Congestion levels can be different throughout the day, but we consider that congestion technology is fixed over time. Congestion technology represents all the elements that determine the speed at which individuals can drive at a given traffic level. It represents the type of road (highway or city road), the presence of traffic lights and intersections, and the number of entries or exits that may force drivers to slow down. In area a, the traffic level in period t is given by the total number of kilometers driven by the individuals in our sample, K_t^a, and from another unobserved source (trucks, buses, non-commuters) that we denote by K_{0t}^a. Thus the total traffic level is $K_t^a + K_{0t}^a$. K_t^a is given by Equation (6) and depends on speeds. By contrast, we assume that K_{0t}^a is fixed so that it does not depend on speeds. Formally, we define the speed in area a at time t, v_t^a to be a function of the total traffic level:

$$v_t^a = f^a(K_t^a + K_{0t}^a). \tag{7}$$

f^a represents the congestion technology that indicates how the speed decreases when the number of kilometers driven increases.

2.3 Equilibrium of the model

This model's equilibrium consists of individual probabilities to drive in all periods and speeds for all areas and periods. We substitute the total number of kilometers driven, defined in Equation 6 as a function of the individual probabilities, in the speed function defined in Equation 7. We can thus express the equilibrium in terms of speeds only and get the following system of non-linear equations:

$$v_t^a = f^a\left(\sum_{n=1}^{N} \omega_n k_n^a s_{n\mathbf{d}t}(\mathbf{v}) + K_{0t}^a\right). \tag{8}$$

There is no general result that guarantees that the system of non-linear equations always

has a unique solution. However, there are two special cases where the speed equilibrium is unique. The first case is when there is only one period and one area, so we have a single non-linear equation to solve. Because the speed function f^a is weakly decreasing, we are sure that if a speed equilibrium exists, it is unique. The second case is when we have one area and multiple periods. The proof of uniqueness relies on the fact that the Jacobian of the system of equations has positive terms on the diagonal and negative terms off-diagonal. The property of the Jacobian of the system of equations is the consequence of two key features of our model: the speed function is decreasing, and the different departure periods are substitutes. We provide the proofs of uniqueness under these two particular cases in Appendix B.

Even though there is no proof of the uniqueness of the equilibrium for the general model, we provide a method to check if the system of equations in speeds has a unique solution given our set of estimated parameters. The approach consists of defining the function:

$$g_t^a(\mathbf{v}, \kappa) = \kappa v_t^a + (1 - \kappa) f^a(\mathbf{v})$$

and check whether there exists $\kappa \in [0, 1[$ such that $\mathbf{g}(.) = \left(g_1^1 \cdots g_T^1 \cdots g_1^A \cdots g_T^A\right)'$ is a contraction. By the Banach fixed-point theorem, if g is a contraction and there exists $\mathbf{v}^*$ such that $\mathbf{g}(\mathbf{v}^*, \kappa) = \mathbf{v}^*$, the solution $\mathbf{v}^*$ is unique. This is a sufficient condition for equilibrium uniqueness. Recall that a function $\mathbf{g}(.)$ is a contraction if it is K-Lipschitz, with $K<1$, implying that $\forall \mathbf{v} \in [\underline{\mathbf{v}}, \overline{\mathbf{v}}]$ (the support of the speeds):

$$||\mathbf{g}(\mathbf{v}', \kappa) - \mathbf{g}(\mathbf{v}, \kappa)|| \leq K||\mathbf{v}' - \mathbf{v}||.$$

We use the supremum norm, so the Lipschitz coefficient K is given by:

$$\max_{a \in 1,\dots A} \max_{t \in 1,\dots,T} \max_{a' \in 1,\dots,A} \max_{t' \in 1,\dots,T} \max_{\mathbf{v} \in [\underline{\mathbf{v}}, \overline{\mathbf{v}}]} \left| \frac{\partial g_t^a(\mathbf{v}, \kappa)}{\partial v_{t'}^{a'}} \right|.$$

Suppose we can find $\kappa \in [0, 1[$ such that $K < 1$, the function $\mathbf{g}(.)$ is a contraction. Therefore, if the iteration process converges, it converges to a unique solution of the system of equations. If we find a set of κ such that the function $\mathbf{g}(.)$ is K-Lipschitz with $K < 1$, we should select the value of κ that implies the lowest coefficient K to ensure the maximum speed of convergence. Therefore, we solve for:

$$\min_{\kappa \in [0,1[} \max_{a \in 1,\dots A} \max_{t \in 1,\dots,T} \max_{a' \in 1,\dots,A} \max_{t' \in 1,\dots,T} \max_{\mathbf{v} \in [\underline{\mathbf{v}}, \overline{\mathbf{v}}]} \left| \frac{\partial g_t^a(\mathbf{v}, \kappa)}{\partial v_{t'}^{a'}} \right|.$$

In practice, we do a grid search over some possible values of κ between 0 and 1. We do a

non-linear optimization over speeds, and the objective function we maximize is the highest value of the absolute value of the elements of the Jacobian of $\mathbf{g}(.)$.

In this equilibrium model, only car trip durations are endogenous. We assume that the durations in public transport are fixed and unaffected by changes in traffic equilibrium. This assumption seems reasonable in our setting since, in the Paris metropolitan area, public transport itineraries very often rely on the railway system.[5] However, individuals may care about the comfort of public transport, which depends on overcrowding levels. In our application, we construct a proxy of the metro and train line-specific overcrowding levels to assess individual sensitivity to public transit comfort. However, we do not endogenize the overcrowding levels because our sample is not representative at the metro or train line level. We still explore, in robustness, how changes in overcrowding may change the results of our counterfactual analysis.

3 Specification and estimation of the transportation choice model

We estimate the transportation choice model parameters using a combination of two main datasets. First, we rely on data on individual commuting patterns in the Paris area from the 2010 and 2020 survey waves of "Enquête Globale Transport" (EGT hereafter). They are combined with a second self-constructed dataset on expected trip durations and itineraries for cars and public transport from TomTom and Google Directions APIs. Additionally, we leverage several ancillary datasets to complement the information about the different transportation modes and individual characteristics.

3.1 Overview of the data

The EGT data contains information about the departure time, precise origin and destination locations, transportation mode, and motive for every trip. In addition, the survey records household and individual socio-demographic characteristics such as age, professional activity, household size, income class, and housing characteristics. We model the choice of transportation mode and departure time for the morning commute. We consider that two possible departure times: peak and off-peak hours, denoted t_1 (peak hours) and t_2 (off-peak hours). We consider 7-8.59 a.m. to be peak hours while 6-6.59 a.m. and 9-9.59 a.m. are off-peak hours, and assume individuals choose only one mode of transportation. If individuals take

[5] In our sample, 75.5% of the trips by public transport involves the usage of a railway-based mode (subway, train, tramway).

multiple modes, we keep the one reported as the primary mode.[6] To focus on unavoidable trips, we restrict the sample to trips related to work or study motives.[7]

We pick the individual as the observation unit rather than the household, assuming that individual decisions are independent within families. However, individuals from the same home still share access to the same transportation modes and household demographic characteristics. This assumption implies that two people can take the same car to make their respective trips without incurring any delay. In this case, we consider two vehicles are on the road.[8] While this simplification ignores potential cost savings and detours associated with carpooling, modeling such joint decisions would add too much complexity to the model.

We consider five transportation mode alternatives: biking, public transport, two-wheeled motor vehicles (motorcycles), walking, and driving.[9] If the household does not own a car or a motorcycle, the alternative is considered unavailable to the individual. If walking or biking takes more than 2.5 hours, we also define those alternatives as unavailable. If Google Directions cannot provide a public transport itinerary, we consider the option unavailable (this occurs for 13.4% of the final sample that combines 2010 and 2020).

We obtain a final sample of 15,470 individual trips, 12,353 from the 2010 survey and 3,117 from the 2020 survey.[10] Using the weights provided by the surveys, we have transportation decisions representing 3.8 million individuals in both survey waves, corresponding to approximately one-third of the total population of the Paris metropolitan area (11.9 million inhabitants in 2011). We provide more information about the EGT data in Appendix C.1.

Since the EGT data only provides trip durations for chosen transportation modes, we must rely on additional data to compute travel times. For consistency across alternatives, we ignore self-reported trip durations. Instead, we consider predicted travel times for chosen and non-chosen transportation modes. We use Google Directions API to provide expected trip durations and itineraries by public transport and use TomTom API for expected driving times and itineraries.[11] We specify the trip query to a future date, so the predictions are not

[6] Only 7.7% (6.1%) of public transport trips in the 2010 (2020) survey also use a car. Around 1% of public transport trips also use a bicycle or motorcycle.

[7] Unavoidable trips cover a large share of transportation decisions. In the 2010 survey, they represent 66% of the trips (67.2% in the 2020 survey) and 72.3% of the total distance traveled during peak hours. For the off-peak period (between 6 and 7 and 9 and 10 a.m.), unavoidable trips account for 50.1% of the trips in 2010 (50.9% in the 2020 survey) and 67.5% of the distance traveled (55% in the 2020 survey).

[8] In our sample, only 7.2% (6.8%) of individuals report using a car as a passenger in 2010 (2020).

[9] Recent literature highlights the role of ridesharing and taxis on congestion levels (Rosaia, 2024 and Mangrum and Molnar, 2020). In the EGT data, only 0.12% (0.37%) of the trips in 2010 (2020) use a taxi or ridesharing. We thus ignore these transportation modes.

[10] The Covid crisis stopped early the data collection of the 2020 survey and thus only contains interviews made in 2019.

[11] We did the queries in November 2023. These APIs can only provide trip durations now or for a future

subject to the current traffic conditions and their idiosyncrasies. The predictions nevertheless rely on the expected traffic level to predict car trip durations. We thus use the predicted car trip durations at 8:30 a.m. for peak hours and 6:30 a.m. for off-peak hours. We provide more details about the queries in Appendix C.2.

The EGT surveys do not include information on individual schedule constraints. We complement our data with the "Enquête Emploi" workforce survey for 2019 and 2022 (workforce survey, hereafter).[12] These surveys explicitly ask workers if they can choose starting and ending working times. Since schedule constraints are likely specific to the occupation, we calculate the fraction of individuals with flexible work hours for 16 socio-professional categories (SPC hereafter). This dataset does not include information for students. We assume the students in high school or below have the lowest flexibility observed among workers. We assume that students in higher education have the largest observed flexibility. Appendix C.3 contains additional information about the workforce survey and how we aggregate a few SPCs.

3.2 Functional form assumptions, identification and estimation

We now explain how we estimate the parameters of the utility function presented in Equation 1. First, we parameterize the individual heterogeneity in preferences and assume that β_n are functions of a finite number of observable demographic characteristics. σ, which represents the correlation of individual preference shocks across periods, is another parameter to estimate. $\boldsymbol{\theta}$ denotes the vector that regroups these parameters.

In Section 2.1, we consider a model where individuals face stochastic constraints regarding their departure times. From an estimation perspective, the challenge arises due to the lack of information about whether individuals are schedule-constrained on the data collection day. We consider the schedule constraints depend only on the SPC of individual n, denoted by $c(n)$. There are C SPCs. We let $\phi_{c(n)}$ denote the probability of being schedule-constrained, i.e., the individual has to commute at a specific time, and $1 - \phi_{c(n)}$ the probability of being unconstrained. Conditional on being schedule-constrained, the individual has a probability $\pi_{c(n)}$ that she has to commute during peak hours. The probability of having to commute during peak or off-peak hours is also a function of the SPC only. There are three possible combinations for the departure times available to individual n, $\mathcal{T}_n$: $\mathcal{T}_{12} = \{t_1, t_2\}$, $\mathcal{T}_1 = \{t_1\}$, or $\mathcal{T}_2 = \{t_2\}$ with probabilities that are respectively $1 - \phi_{c(n)}$, $\phi_{c(n)}\pi_{c(n)}$, $\phi_{c(n)}(1 - \pi_{c(n)})$.

In the workforce survey, we observe the probabilities of being schedule-constrained $(\phi_c)_{c=1,\dots,C}$,

date, we cannot have expected trip durations that correspond exactly to the survey years.

[12] We do not exploit 2020 and 2021 data because the Covid crisis might have temporarily affected the working conditions.

but we need to estimate the probabilities that under schedule constraints, the individuals must commute during peak hours $\boldsymbol{\pi} = (\pi_1, ..., \pi_C)$. We leverage the shares of individuals choosing peak hours conditional on the SPC by writing π_c as a function of the vector of parameters of preferences $\boldsymbol{\theta}$. We start by expressing the probability of choosing to travel at peak hours conditional on the SPC c that we denote μ_c and is observed:

$$\mu_c = \phi_c \pi_c + (1 - \phi_c) \frac{\sum_{n \in \mathcal{C}} \omega_n \sum_{j \in \mathcal{J}_n} s_{njt_1|\mathcal{T}_{12}}(\boldsymbol{\theta})}{\sum_{n \in \mathcal{C}} \omega_n},$$

where $\mathcal{C}$ denotes the set of individuals with the SPC c. $s_{njt|\mathcal{T}_{12}}(\boldsymbol{\theta})$ corresponds to the mode shares conditional of having no schedule constraints, defined in Equation 3. Thus, we can write π_c as function of μ_c, ϕ_c and $\boldsymbol{\theta}$:

$$\pi_c(\boldsymbol{\theta}) = \frac{\mu_c}{\phi_c} - \frac{(1 - \phi_c)}{\phi_c} \frac{\sum_{n \in \mathcal{C}} \omega_n \sum_{j \in \mathcal{J}_n} s_{njt_1|\mathcal{T}_{12}}(\boldsymbol{\theta})}{\sum_{n \in \mathcal{C}} \omega_n}$$

Since we need $\pi_c(\boldsymbol{\theta}) \in [0, 1]$, we define:

$$\pi_c^*(\boldsymbol{\theta}) = \pi_c(\boldsymbol{\theta}) \mathbb{1}\{\pi_c(\boldsymbol{\theta}) \in [0, 1]\} + \mathbb{1}\{\pi_c(\boldsymbol{\theta}) > 1\}. \tag{9}$$

This allows us to write the probability that individual n chooses the combination j and t as function of the parameters:

$$\begin{aligned} s_{njt}(\boldsymbol{\theta}) =& \phi_{c(n)} \pi^*_{c(n)}(\boldsymbol{\theta}) s_{njt|\mathcal{T}_1}(\boldsymbol{\theta}) + \phi_{c(n)}(1 - \pi^*_{c(n)}(\boldsymbol{\theta})) s_{njt|\mathcal{T}_2}(\boldsymbol{\theta}) \\ &+ (1 - \phi_{c(n)}) s_{njt|\mathcal{T}_{12}}(\boldsymbol{\theta}). \end{aligned}$$

The equation above is the same as Equation 4, but it is adjusted to our setting with two periods and partially observed schedule constraints. When individuals are schedule-constrained, they only choose a transportation mode, and the model becomes a logit, so the probabilities do not depend on σ. It implies that the identification of σ is only possible when the probability of being schedule-constrained is below one.

The identification of the unobserved schedule constraints represented by $\boldsymbol{\pi}^*$ comes from observing the departure time by SPC and the probability of having flexible hours (from the workforce survey). Controlling for schedule constraints and preference heterogeneity within SPCs, observed departure times conditional on a SPC reveal the type of schedule constraints faced by individuals in that SPC. The key assumption for identification of $\boldsymbol{\pi}^*$ is that preferences do not systematically differ across socio-professional categories.

Finally, an individual n contribution to the likelihood is:

$$l_n = \Pi_{j \in \mathcal{J}_n} \Pi_{t=\{t_1,t_2\}} \left(s_{njt}(\boldsymbol{\theta})\right)^{y_{njt}},$$

where $y_{njt} = 1$ when the mode j and the period t are chosen and 0 otherwise. We estimate $\boldsymbol{\theta}$ using the method of maximum likelihood; we want to find the values of the parameters that best rationalize the observed choices given the theoretical probabilities. We maximize the log-likelihood function:

$$LL(\boldsymbol{\theta}) = \sum_{n=1}^{N} \sum_{j \in \mathcal{J}_n} \sum_{t=\{t_1,t_2\}} \omega_n y_{njt} \log\left(s_{njt}(\boldsymbol{\theta})\right). \tag{10}$$

We recall that ω_n corresponds to the sample weight of the individual n. The identification of the parameters in $\boldsymbol{\theta}$ comes from observing a cross-section of individuals with different choice sets, trip characteristics, and demographic characteristics, making different choices.[13]

The maximum likelihood method requires that the individual preference shocks are uncorrelated to the mode and period observed characteristics:

$$\mathbb{E}(\epsilon_{njt}|X_{njt}) = 0.$$

This means that individual shocks that affect the decision to drive should be uncorrelated with individual car trip duration. However, this contradicts the theoretical equilibrium model, where individual driving times are an equilibrium outcome. Unobserved factors may simultaneously affect individual preferences for driving and speeds (e.g., rain) or all individuals' preferences simultaneously and thus speeds (e.g., an important event). Our data structure mitigates these concerns for two reasons. First, we do not rely on observed car trip durations but on expected trip durations from TomTom on a future date. This prediction is based on the expected traffic level and is not subject to real-time traffic or speed shocks (e.g., caused by rain). Second, individuals are surveyed on different days throughout the year (outside school holiday periods), so their unobserved preference shocks are less likely to be correlated.

In addition, our specification allows for a rich set of interactions between demographics, cost and travel time. Controlling for such individual-level heterogeneity is important to have independence of the unobserved preferences shocks and mode characteristics.

[13] Our application is centered around policies influencing car usage. While we could adopt a simplified model in which individuals choose between driving and public transport, identifying preferences in such a model would be more difficult due to the limited variation in mode characteristics and the lack of variation in choice sets.

To further mitigate the risk of endogeneity of car trip durations, we use 93 zone fixed effects for the individual origins and destinations interacted with the car alternatives. These fixed effects capture unobserved driving conditions, since individuals with a high preference for driving might live or work in areas with better road infrastructure, where driving time is low. Barwick et al. (2024) also use such fixed effects to mitigate endogeneity concerns.

Additionally, we use a control function approach to deal with the potential endogeneity of car trip durations. We construct a set of instruments and apply the control function approach suggested by Petrin and Train (2010). The control function method is a widespread approach to deal with endogeneity while relying on individual data and using the maximum likelihood estimation method (Agarwal, 2015, Dubois et al., 2018, Buchholz et al., 2024). Our instruments are inspired by Berry et al. (1995): they are characteristics of the choice sets of other individuals living in the origin or destination zone. We also use the free-flow duration as in Almagro et al. (2024). In Appendix D.1, we provide details on the control function approach and the underlying assumptions.

3.3 Utility specification and variable constructions

We specify the utility as a linear function of the following variables: transportation mode-and-departure-time-specific intercepts, the trip monetary cost, the trip duration and some public transport characteristics. We consider a flexible functional form for the trip duration by interacting it with the trip distance using a local linear functional form. More specifically, we split the trip distance into five intervals and allow the parameters of the interaction between duration and distance to vary on each segment of the interval. Spending one additional minute might be different depending on the trip distance. We also allow the sensitivities to the trip duration and cost to vary with six age classes and nine income brackets.

We add some controls to represent the characteristics of public transport. We use the overcrowding level in the metro and suburb trains, a dummy if the public transport itinerary relies on the railway system only (instead of using the bus or tramway), and the number of layovers. Following the literature on public transport congestion, such as De Palma et al. (2017) and Haywood and Koning (2015), we assume the utility is linear in the level of overcrowding on public transit.

Except for the mode and departure time dummies, none of the variables in the utility function are readily available in the EGT data and need to be constructed. We rely on the self-constructed dataset on expected trip durations for driving and public transport. To estimate trip durations for walking and bicycle trips, we compute the average speed for individuals who chose to bike or walk using their declared trip durations and distances. We

find a walking speed of 3.4 km/hr and 8.2 km/hr for biking.[14] These average speeds are combined with distance to compute trip durations for the two modes. Finally, we use the predicted car durations at off-peak hours for motorcycles, assuming they can bypass traffic.

The EGT data contains information on some characteristics of cars and motorcycles: vintage, fuel type, and horsepower. Using additional data, we estimate the fuel consumption and emissions per kilometer driven for the vehicles from these characteristics (see Appendix C.4). Fuel consumption is essential to estimate the cost of driving, while the emissions are used in counterfactual simulations to predict the environmental benefits of reducing traffic. For the cost of driving, we follow a similar approach as the American Automobile Association and construct a per-kilometer cost that includes fuel consumption, car depreciation, maintenance, and insurance. Car prices are not observed in the EGT data, so we predict them from the vintage, fuel type, and horsepower using additional proprietary data on car sales. The EGT contains household-level data on the annual maintenance and insurance costs and information on the number of kilometers driven annually. The precise methodology and related assumptions to estimate the driving costs are provided in Appendix C.5.1.

The survey also records whether individuals own a public transport pass and the type of subscription. Since public transit users are more likely to own a subscription and thus to pay a cheaper price, we control for the selection into public transport subscription by predicting the cost of the trip net of the subscription rebate. We present our methodology in Appendix C.5.2.

Walking is always free, while biking is free only for households owning bicycles. If the individual has an annual bike-sharing subscription, we consider the per-trip cost of the subscription is the annual cost divided by twice the number of working days. In other cases, we consider biking to have the price of a single bike-sharing ticket, €1.7. Our final cost estimates are trip and individual-specific and account for the public transport subscription rebates, vehicle characteristics, and trip distances. Finally, we deflate the cost of the 2020 trips to 2010 euros.[15]

We construct a measure of overcrowding for all the subway and urban railway transit lines to capture the potential disutility of overcrowding in public railway transport. We use publicly available data from 2015 on passenger flows (the oldest year available) combined with historical data on hourly public transit schedules and train capacities. A train's capacity

[14]Speeds are computed using the reported duration and trip distances. We check that the speeds are not sensitive to rounding errors in the reported trip durations by excluding observations reporting a multiple of five minutes.

[15]The value of the deflator comes from the French National Institute of Statistics and Economic Studies. See https://www.insee.fr/fr/statistiques/2122401.

is the number of passengers in a train for a density of four persons per square meter. We approximate the overcrowding level by the hourly number of passengers divided by the line's capacity. A line's capacity is a function of two factors: train frequencies and train physical capacities. Since different lines operate different trains and have different frequencies, we obtain important heterogeneity in capacities across metro and train lines. We obtain individual overcrowding levels from the urban railway line-level overcrowding estimates by weighting the line-level overcrowding measures by the percentage of the trip duration spent on the line. We provide details on the data used and the construction of the overcrowding variable in Appendix C.6. Table 20 on the same Appendix C.6 provides the time-specific overcrowding measures for each line. On average, across metro and train lines, public railway transport is at 73% capacity at off-peak hours and reaches 180% at peak hours.

The EGT provides the household monthly income in ten brackets. We follow the approach of the French National Institute of Statistics and Economic Studies to calculate consumption units in a household. We count the first individual in a household as one consumption unit, other adults represent half a consumption unit, and children represent 0.3 consumption units. We divide the midpoint of each income bracket by the number of consumption units to obtain an estimate of income at the individual level. We then reclassify the individuals into the initial income categories. Taking into account the household size is important as only 19.9% of the sample remains in their initial income category. Finally, we aggregate the two highest income classes (between €4,500 and €5,500 and above €5,500) because there are few observations in the highest income bracket (0.5% of the sample).

Table 1 shows the distribution of trip characteristics and mode shares across the different demographic categories. We see that the youngest category (below 18 years old) have, on average, trip distances three to four times lower than the rest of the population. This can be explained by the proximity of schools to their residences. Car usage increases with age, while public transport usage decreases with it. Trip duration also monotonically decreases with age from 18 onwards. This could be related to older individuals having higher sensitivity to travel time.

Car usage is at least ten percentage points lower for the two lowest income categories than for the rest of the population. Meanwhile, public transport is popular across low and middle-level income categories. The lowest public transport usage corresponds to individuals with an income between €3,500 and €4,500. Across SPC, we see large heterogeneity in the share of trips made during peak hours, with less than half of qualified workers traveling at peak, while almost all students at high school or below travel during peak hours.

Table 1: Summary statistics by demographic groups

		Mean		Mode & period shares		
	Freq.	**Dist.**	**Duration**	**Car**	**Pub. trans.**	**Peak**
Age						
Age $\leq$ 18	31.6	4.1	24.4	19.9	35.1	90.6
Age $\in$]18, 30]	17.3	15.3	39.7	22.4	67.4	70.7
Age $\in$]30, 40]	17.2	16.1	37.3	37.5	49.5	66.5
Age $\in$]40, 50]	17.6	16	36.3	41.4	46.6	70.7
Age $\in$]50, 60]	14	15.7	35.1	43.6	43.8	71.8
Age $>$ 60	2.27	12.8	32.7	44.5	41.7	72.3
Income						
Income $\leq$ 800	10.5	8.08	32.1	16.9	47.1	77.3
Income $\in$ [800, 1,200[	12.69	10.05	32.53	23.84	48.72	75.76
Income $\in$ [1200, 1,600[	15.6	11.8	31.8	35.5	41.5	74.2
Income $\in$ [1600, 2,000[	15.3	13.4	33.5	36.3	46.4	73.6
Income $\in$ [2000, 2,400[	14.2	13.5	34.6	33.4	47.1	75.1
Income $\in$ [2400, 3,000[	11.4	13.6	34.6	32.1	51.5	75.7
Income $\in$ [3000, 3,500[	8.62	12.3	33	29.1	50.6	79.9
Income $\in$ [3500, 4,500[	7.56	13	32.8	35.5	43.8	81.6
Income $>$ 4,500	4.18	14.5	34.5	37.9	48.3	77.6
Socio-professional category						
Farmers	0.11	14.2	32.7	36.4	29.4	82.3
Craftspeople	0.698	19.8	31	81.2	12.3	54.1
Shopkeepers	0.517	15.7	34.6	46.7	30.9	50.2
Entrepreneurs	1.45	13.4	32.6	36.2	37.8	66.9
Public executives	6.96	13.8	35.6	31.2	53.8	72.7
Private executives	12.9	17.2	38.9	31.8	58.3	76.7
Education, health	8.25	13.3	33	42	43.1	76.6
Administrative professions	7.21	17.1	38.8	32.5	59.6	74.8
Technicians	3.54	18.3	38.1	48	41.4	62.3
First-line supervisors	1.24	19.1	40.5	50.8	40.8	61.3
Public employees	5.55	13.3	35.6	37.6	45.2	71.1
Private employees	4.69	18.7	38.8	34.9	58.5	80.3
Retail employees	1.16	15.3	36.6	38.2	49.7	59.9
Services	1.71	9.76	33.2	17.4	59.6	60.3
Qualified workers	5.27	15.8	34.4	55.6	36.2	47.3
Unqualified workers	1.6	12.8	34.4	37.3	48.9	48.1
Students in high school or below	31.6	3.89	23.9	20.4	33.6	91
Students in higher education	5.59	15.1	43.7	9.73	80.7	73.5
Average		12.1	33.2	30.9	47.1	76.2

Note: Durations in minutes, distances in km, monthly income in € per consumption unit. Frequencies and mode shares are in %. Distances and durations are those of the chosen transportation modes. All statistics are for the pooled 2010-2020 sample and are computed using survey weights.

Across socio-professional categories, we see a large variation in the usage of cars and public transport. We also observe large variation in the share of trips done at peak hours. Workers (qualified and unqualified), and individuals working in services have a lower rates of departure at peak hours than the average. By contrast, executives and individuals working in health have higher rates of departure during peak hours. We take this as evidence of differences in schedule flexibility across socio-professional categories. Mode availability, as well as the distribution of durations and costs by mode, are given in Appendix C.7.

One possible concern with using the 2010 and 2020 waves of the EGT survey is that transportation patterns could have changed in the ten years between the surveys. The last panel of Table 21 in Appendix C.7 provides the availability and mode shares. We do not observe major changes across the two survey waves, with the difference between shares being less than 2.5 percentage points.

3.4 Estimation results

We estimate the transportation choice model by maximizing the log-likelihood defined by Equation (10). Only differences in utilities are identified in this discrete choice model. Thus, we consider walking at peak hours as the baseline option and normalize its intercept to 0. The mean utility of an individual walking at peak hours is not normalized to 0 because the utility contains the trip duration. In the estimation, we impose that the sensitivities to duration and trip cost are always negative.

We present in Table 2 the results from four different specifications. The first corresponds to our main specification with stochastic schedule constraints governing departure time substitution. The second specification uses a control function approach to deal with duration endogeneity. In the third one, all individuals can substitute across departure periods. Finally, in the last specification, individuals cannot substitute across departure periods. The last two specifications make extreme assumptions regarding the ability of individuals to substitute across periods. The differences between them and our preferred model inform us about the role of incorporating stochastic schedule constraints. All specifications include a rich set of fixed effects: the zones of origin and destination interacted with driving.

The table also provides the median value of travel time (or opportunity cost of time) in €/hr. The VOT represents how much an individual should receive (in €) to compensate for the decrease in utility related to an increase in travel time by an hour. Given our functional form assumptions and the unit for duration (ten minutes), the VOT is simply the ratio between the sensitivity to duration and the sensitivity to the trip monetary cost multiplied by six. The sensitivity to duration depends on individual specific demographic characteristics and trip distance.

Table 2: Estimation results for the utility parameters

Coefficients	**(1)**		**(2)**		**(3)**		**(4)**	
Duration	-0.538**	(0.033)	-0.537**	(0.033)	-0.9**	(0.089)	-0.531**	(0.033)
Cost	-0.53**	(0.049)	-0.533**	(0.049)	-0.871**	(0.102)	-0.533**	(0.049)
Bicycle, peak	-3.47**	(0.075)	-3.46**	(0.076)	-5.8**	(0.429)	-3.47**	(0.076)
Public transport, peak	-1**	(0.062)	-0.995**	(0.063)	-1.79**	(0.157)	-0.994**	(0.062)
Motorcycle, peak	-3.43**	(0.112)	-3.43**	(0.113)	-5.66**	(0.406)	-3.49**	(0.113)
Car, peak	-2.68**	(0.527)	-2.71**	(0.528)	-4.54**	(0.935)	-2.72**	(0.528)
Car, off-peak	-3.88**	(0.544)	-3.95**	(0.563)	-6.27**	(0.95)	-3**	(0.535)
Public transport, off-peak	-1.9**	(0.174)	-1.94**	(0.221)	-2.96**	(0.164)	-1.16**	(0.098)
Walking, off-peak	-0.737**	(0.154)	-0.779**	(0.195)	-1.81**	(0.055)	0	(0)
Bicycle, off-peak	-4.15**	(0.16)	-4.18**	(0.188)	-7**	(0.438)	-3.37**	(0.133)
Motorcycle, off-peak	-3.73**	(0.162)	-3.75**	(0.18)	-6.31**	(0.412)	-2.74**	(0.164)
Duration × income ∈ [800, 1,200[	-0.03	(0.03)	-0.03	(0.03)	-0.036	(0.05)	-0.036	(0.03)
Duration × income ∈ [1,200, 1,600[	-0.115**	(0.032)	-0.115**	(0.032)	-0.158**	(0.053)	-0.116**	(0.032)
Duration × income ∈ [1,600, 2,000[	-0.072*	(0.031)	-0.071*	(0.031)	-0.083	(0.051)	-0.073*	(0.031)
Duration × income ∈ [2,000, 2,400[	-0.075*	(0.032)	-0.075*	(0.032)	-0.1†	(0.052)	-0.08*	(0.032)
Duration × income ∈ [2,400, 3,000[	-0.083*	(0.034)	-0.084*	(0.034)	-0.09†	(0.054)	-0.088**	(0.034)
Duration × income ∈ [3,000, 3,500[	-0.102**	(0.035)	-0.103**	(0.036)	-0.102†	(0.057)	-0.118**	(0.036)
Duration × income ∈ [3,500, 4,500[	-0.141**	(0.041)	-0.143**	(0.042)	-0.134*	(0.063)	-0.169**	(0.042)
Duration × income ≥ 4,500	-0.169**	(0.058)	-0.174**	(0.06)	-0.139†	(0.082)	-0.241**	(0.061)
Duration × age ∈ [18, 30]	-0.138**	(0.025)	-0.137**	(0.025)	-0.257**	(0.046)	-0.136**	(0.025)
Duration × age ∈]30, 40]	-0.311**	(0.029)	-0.308**	(0.03)	-0.54**	(0.058)	-0.291**	(0.03)
Duration × age ∈]40, 50]	-0.26**	(0.029)	-0.259**	(0.029)	-0.446**	(0.054)	-0.262**	(0.03)
Duration × age ∈]50, 60]	-0.327**	(0.033)	-0.326**	(0.033)	-0.532**	(0.06)	-0.322**	(0.034)
Duration × age > 60	-0.38**	(0.073)	-0.38**	(0.074)	-0.598**	(0.113)	-0.35**	(0.074)
Duration × distance	0.223**	(0.023)	0.223**	(0.023)	0.356**	(0.048)	0.22**	(0.023)
Duration × (dist-d_2) × (dist≥d_2)	-0.265**	(0.041)	-0.262**	(0.041)	-0.426**	(0.071)	-0.239**	(0.042)
Duration × (dist-d_3) × (dist≥d_3)	-0.031	(0.062)	-0.035	(0.063)	-0.048	(0.092)	-0.042	(0.064)
Duration × (dist-d_4) × (dist≥d_4)	0.099	(0.114)	0.105	(0.115)	0.104	(0.171)	0.118	(0.113)
No. layovers in Pub. transport	-0.486**	(0.041)	-0.488**	(0.041)	-0.778**	(0.09)	-0.49**	(0.041)
Railway only	0.015	(0.063)	0.011	(0.063)	0.143	(0.095)	-0.011	(0.065)
Pub. transport overcrowding	-0.066*	(0.033)	-0.064†	(0.033)	-0.199**	(0.041)	-0.046	(0.036)
Cost × income ∈ [800, 1,200[	-0.013	(0.036)	-0.014	(0.036)	-0.016	(0.059)	-0.012	(0.036)
Cost × income ∈ [1,200, 1,600[	-0.059†	(0.036)	-0.059†	(0.036)	-0.085	(0.06)	-0.055	(0.036)
Cost × income ∈ [1,600, 2,000[	-0.023	(0.034)	-0.024	(0.034)	-0.025	(0.057)	-0.015	(0.034)
Cost × income ∈ [2,000, 2,400[	-0.093**	(0.036)	-0.094**	(0.036)	-0.146*	(0.06)	-0.088*	(0.036)
Cost × income ∈ [2,400, 3,000[	-0.085*	(0.037)	-0.086*	(0.037)	-0.126*	(0.062)	-0.079*	(0.037)
Cost × income ∈ [3,000, 3,500[	-0.07†	(0.039)	-0.071†	(0.039)	-0.095	(0.064)	-0.061	(0.039)
Cost × income ∈ [3,500, 4,500[	-0.059	(0.04)	-0.06	(0.04)	-0.065	(0.066)	-0.056	(0.04)
Cost × income ≥ 4,500	0.017	(0.043)	0.016	(0.043)	0.064	(0.07)	0.016	(0.043)
Cost × age ∈ [18, 30]	0.301**	(0.044)	0.304**	(0.044)	0.459**	(0.078)	0.306**	(0.044)
Cost × age ∈]30, 40]	0.384**	(0.043)	0.389**	(0.044)	0.606**	(0.083)	0.391**	(0.044)
Cost × age ∈]40, 50]	0.45**	(0.043)	0.455**	(0.044)	0.717**	(0.088)	0.451**	(0.044)
Cost × age ∈]50, 60]	0.408**	(0.044)	0.412**	(0.045)	0.655**	(0.087)	0.407**	(0.045)
Cost × age > 60	0.385**	(0.063)	0.389**	(0.064)	0.616**	(0.113)	0.398**	(0.063)
σ	0.816**	(0.16)	0.87**	(0.217)	0.603**	(0.043)		
Residual control function duration peak			-0.006	(0.008)				
Residual control function duration off-peak			-0.013	(0.016)				
Log-likelihood	-17,441		-9,664		-17,923		-14,513	
Median VOT (in €/hr)	15.6		15.7		15.2		15.6	

*Notes: (1): Baseline specification, with stochastic schedule constraints. (2): Stochastic schedule constraints and control function for duration. (3): Full flexibility, all individuals can substitute across departure periods. (4): No substitution across departure periods. In this specification the mode dummies are identical across periods. Walking at peak hours is the baseline alternative. "income" represents the monthly individual income, "dist" is the distance, in 10 km and d_2, d_3 and d_4 are the inner values that split the distance interval equally in five. The reference categories are individuals with age < 18, with an income below €800. Duration measured in 10 minutes. Cost in €. Significance levels: **: 1%, *: 5%, †: 10%.*

Baseline sensitivities to duration and cost are very similar across specifications (1), (2) and (4). In specification (3), individuals in the base category appear to be more sensitive to price and travel time. This is intuitive because the model, without schedule constraints, rationalizes the fact that only 76.2% of individuals choose to commute during peak hours with a high sensitivity to duration. We take the results from specification (3) as evidence of a possible bias from assigning the option to substitute across departure times to individuals who cannot. However, the median VOT remains very close to our baseline estimate.

Furthermore, all four specifications suggest qualitatively the same heterogeneity in preferences. When looking at the estimates from our preferred specification, the interactions between the trip duration and individual characteristics reveal that the sensitivity to trip duration is more heterogeneous across age than across income categories. Older and higher income individuals are more sensitive to trip duration. Older individuals are also less sensitive to trip cost. We find little heterogeneity across income brackets on the cost sensitivity and the heterogeneity suggests a u-shaped curve: individuals with middle incomes (€2,000-€3,000) are the most sensitive to trip cost.

Our baseline specification suggests a preference shock correlation between periods of 0.82, indicating that leaving at peak and off-peak hours are subject to relatively independent shocks and thus constitute imperfect substitutes. Yet, the coefficient is lower than one, confirming the relevance of the nest to represent substitution patterns between different transportation modes and departure times. With the control function, the estimated σ is slightly higher (0.87). Under the assumption of full schedule flexibility, σ equals 0.60, suggesting a greater correlation of preferences within modes.

Finally, the included residuals from the first stage of the control function are not significant. Due to these factors, we prefer to use specification (1) as our main specification for the remaining analysis. Overall, the results from the different specifications are reassuring that our assumptions about the presence or absence of schedule constraints, as well as the control function, do not have large impacts on the estimated coefficients.

The transportation mode dummies reveal significant differences in the stand-alone preferences for different transportation alternatives. Consistently across transportation modes, we find that peak hours are always preferred to off-peak hours. The public transport controls have the expected signs: the number of layovers and overcrowding reduce the utility of public transport. The railway dummy is positive but not significant. Overcrowding has a small impact on choices. Indeed, the average willingness to pay to decrease the overcrowding level by 10% during peak hours is €0.064. By contrast, the average willingness to pay to reduce the trip duration by 10% is €0.97.

Table 3 presents the estimated probabilities of being schedule-constrained (obtained from the workforce survey) and those of commuting during peak-hour only when schedule-constrained (calculated from the estimated parameters according to Equation (9)). The least schedule-constrained socio-professional categories are craftspeople, entrepreneurs, and private sector executives. The most schedule-constrained workers are public and retail employees and unqualified workers. When workers are schedule-constrained, we find that 78% of the time, they have to commute during peak hours. However, craftspeople and shopkeepers always have to make their trip during off-peak hours when schedule-constrained. Entrepreneurs, self-employed, qualified and unqualified workers also tend to be constrained to off-peak hours when they are schedule-constrained. By contrast, schedule-constrained private executives always have to commute during peak hours. We also find that farmers, private employees, and students in high school or below are most likely to have only peak-hour travel available if they are schedule-constrained.

Table 3: Estimated probabilities of being schedule-constrained and having to commute at peak-hours

Socio-professional category	**Prob. of being schedule-constrained** ($\hat{\phi}_c$)	**Std. error**	**Prob. of being constrained to peak-hour commute** ($\hat{\pi}^*_c$)	**Std. error**
Farmers	0.302	0.011	0.991	0.031
Craftspeople	0.109	0.007	0	0
Shopkeepers	0.143	0.009	0	0
Entrepreneurs, self-employed	0.13	0.008	0.338	0.075
Public executives	0.382	0.008	0.732	0.017
Private executives	0.135	0.004	1	0
Education, health	0.636	0.006	0.785	0.006
Administrative professions	0.447	0.008	0.784	0.013
Technicians	0.473	0.01	0.515	0.013
First-line supervisors	0.527	0.014	0.519	0.011
Public employees	0.849	0.004	0.707	0.002
Private employees	0.624	0.009	0.852	0.007
Retail employees	0.884	0.006	0.581	0.002
Services	0.738	0.007	0.556	0.004
Qualified workers	0.793	0.005	0.406	0.003
Unqualified workers	0.869	0.006	0.444	0.003
Students $\leq$ high school	0.884	0.006	0.932	0.002
Students in higher education	0.109	0.007	0.748	0.088
Average	0.579		0.779	

Notes: $\hat{\phi}_c$ corresponds to the empirical share of respondents with constrained work schedules according to the workforce survey. $\hat{\pi}^*_c$ are estimates from our preferred specification, specification (1). Standard-errors for $\hat{\phi}_c$ correspond to the standard-error for the mean. Standard-errors for $\hat{\pi}^*_c$ computed using the delta-method and takes into account the variance of $\hat{\phi}_c$.

We further test the sensitivity of our estimation results to alternative model assumptions. These additional robustness checks and their results are presented and discussed in Appendix D.2. To account for the possible role of unobservables correlated with trip duration, we check that adding weather variables or a measurement of travel time reliability as controls do not affect our estimates. We also study the effect of using a different cost definition for motorized

vehicles and the impact of not including the correction to the public transport cost. We also provide the estimation results when we use the two periods as nests, and check that our estimates are robust to alternative choice set definitions. Finally, we validate our assumption that schedule flexibility is only related to professional activity by showing that additional individual controls do not provide significant extra explanatory power.

3.5 Values of travel time and substitution across modes and periods

Table 4 presents detailed information about the distribution of the VOT across individuals. We present the VOT distribution for the 2010 sample, which is used for the policy analysis. Due to the low number of observations in the 2020 survey, we limit counterfactual analysis to the 2010 data.[16] We obtain an average value of travel time of €17.9/hr, which is slightly higher than the median value of €16.4/hr. The mean value represents 75% of the mean wage in 2012 in the Paris metropolitan area (€23.9/hr).[17] This is equal to the ratio found by Goldszmidt et al. (2020) of 75% using natural field experiments on 13 U.S. cities. Barwick et al. (2024) find a ratio of 95.6% for commuters in Beijing. Buchholz et al. (2024) estimate an average VOT of $13.2/hr which represents 139% of the hourly wage in Prague.[18] Finally, our estimate aligns with Almagro et al. (2024), who find an average of $15/hr for Chicago, and with Kilani et al. (2012), who estimate an average of €17/hr for a working father in Paris.

We observe substantial heterogeneity in how individuals value their time in transport, reflected by the extreme minimum and maximum opportunity costs of time (€1.58/hr and €90.3/hr). Figure 10 of Appendix D.3 shows the distributions of VOT as functions of age, income, and distance. We find important heterogeneity in terms of age. Young individuals have the lowest VOT, and the VOT rapidly increases until 45. Regarding income, we see little heterogeneity for incomes below €3,000. Then, the VOT increases quickly with income due to the low sensitivity to the trip cost. Finally, the VOT is not monotonic in distance; the lowest VOTs are for very short and middle-length trips (20 km).

We compute the own and cross elasticities to driving duration and cost to better understand the substitution across departure periods for driving. These elasticities are crucial to predict individual reactions to tolls. Table 4 presents the distributions of these elasticities in the population for 2010. The duration elasticities for driving are highly heterogeneous across individuals. For instance, the duration elasticity at peak hours is between -7.1 and -0.01. The

[16] This explains why we obtain different median VOT in Tables 2 and 4.

[17] Source for the average hourly wage in Paris: https://www.lemonde.fr/les-decodeurs/article/2016/11/28/en-ile-de-france-le-salaire-horaire-depasse-de-41-celui-des-autres-regions_5039717_4355770.html.

[18] This study is rather specific because the VOT is estimated on a sample of cab riders.

heterogeneity partly reflects the differences in the trip distance, which is highly correlated to duration. It is also the consequence of the heterogeneity in preferences, schedule constraints, availability and characteristics of the substitutes for driving. We obtain an average of -1.01, slightly lower than the value obtained by Almagro et al. (2024) (-1.44 for peak hours). The driving cost elasticities at peak hours are even more dispersed, between -13 and -0.004. The cost elasticities with values close to zero correspond to individuals with electric cars, who pay zero fuel costs, and thus only pay for depreciation, maintenance, and insurance costs. The cost elasticities are, on average, -0.58 at peak hours, very similar to the -0.55 found by Almagro et al. (2024).

In the bottom panel, we provide the cross elasticities with and without conditioning on the ability to do intertemporal substitution. Individuals are more elastic to changes in duration at peak hours than at off-peak hours, indicating strong preferences for driving at peak hours. The cross elasticities of driving at peak hours to the trip duration at off-peak hours are very low (0.1 on average), indicating low inter-temporal substitution. This is the consequence of important schedule constraints that limit inter-temporal substitution. We obtain average elasticities almost three times larger when conditioning on the ability to substitute across departure times. This highlights the critical role of schedule constraints in limiting individual responses to duration and cost changes.

Table 4: Distributions of values of travel time and elasticities to driving duration and cost

	Min	**p1%**	**Mean**	**Median**	**p99%**	**Max**
Value of travel time	1.58	2.74	17.9	16.4	52.8	90.3
Own elasticities						
$\mathcal{E}^{\text{duration}}_{t_1,t_1}$	-7.13	-4.93	-1.01	-0.54	-0.07	-0.01
$\mathcal{E}^{\text{duration}}_{t_2,t_2}$	-6.07	-3.74	-0.84	-0.57	-0.1	-0.03
$\mathcal{E}^{\text{cost}}_{t_1,t_1}$	-12.99	-3.97	-0.58	-0.28	-0.02	-0.004
$\mathcal{E}^{\text{cost}}_{t_2,t_2}$	-12.82	-4.12	-0.65	-0.35	-0.03	-0.005
Cross elasticities						
$\mathcal{E}^{\text{duration}}_{t_1,t_2}$	0.0004	0.0008	0.1	0.05	0.71	2.23
$\mathcal{E}^{\text{duration}}_{t_2,t_1}$	0.005	0.01	0.28	0.15	1.54	3
$\mathcal{E}^{\text{cost}}_{t_1,t_2}$	0.0001	0.0007	0.06	0.02	0.45	1.36
$\mathcal{E}^{\text{cost}}_{t_2,t_1}$	0.0004	0.003	0.15	0.07	0.93	3.33
Cross elasticities, conditional on $\mathcal{T}_{12}$						
$\mathcal{E}^{\text{duration}}_{t_1,t_2}$	0.004	0.009	0.24	0.18	1.32	2.63
$\mathcal{E}^{\text{duration}}_{t_2,t_1}$	0.03	0.08	0.68	0.55	2.49	5.55
$\mathcal{E}^{\text{cost}}_{t_1,t_2}$	0.0009	0.004	0.15	0.11	0.8	1.76
$\mathcal{E}^{\text{cost}}_{t_2,t_1}$	0.003	0.01	0.36	0.25	1.93	7.72

Note: Value of travel time in €/ hr. Elasticities in %. "t_1" represents peak hours and "t_2" off-peak hours. All statistics computed using survey weights for 2010 sample. Cross elasticities, conditional on $\mathcal{T}_{12}$ correspond to individuals who can substitute across departure periods.

3.6 Individual speed shocks

The last primitives of the transportation mode choice model to recover are the individual and time-specific driving speed shocks represented by ρ_{nt} in Equation (5). We take the logarithm of Equation (5):

$$\log(\text{duration}_{n\mathbf{d}t}) = \log\left(\sum_{a=1}^{A} \frac{l_n^a}{v_t^a}\right) + \tilde{\rho}_{nt}.$$

where $\tilde{\rho}_{nt} = \log(\rho_{nt})$. We use the TomTom durations and trip distances by area to estimate the inverse of the initial speeds, $\tilde{v}_t^a = 1/v_t^a$. We use the non-linear least squares method, which amounts to solving for each period t:

$$\min_{(\tilde{v}_t^a)_{a=1,\dots,A}} \sum_{n=1}^{N} \left(\tilde{\rho}_{nt}(\tilde{v}_t^a)\right)^2. \tag{11}$$

This regression provides us with the individual speed shocks $\tilde{\rho}_{nt}$, considered policy-invariant parameters. We also obtain the initial speeds by area and period reported in Table 5. Speeds are always higher during off-peak hours than peak hours. The difference is the largest on the highways, followed by the ring roads, far suburbs, close suburbs, and finally, in the city center.

Table 5: Estimated average speeds from TomTom data

	Peak hours		**Off-peak hours**	
Area	**Average speed**	**Std. error**	**Average speed**	**Std. error**
Highways	58.6	0.82	84.6	1.06
City center	13.2	0.13	17.4	0.148
Ring roads	28.5	0.565	48.8	0.899
Close suburb	15.9	0.101	20.1	0.11
Far suburb	24.6	0.126	28.6	0.127

Note: Speeds in km/hr. Standard errors are computed using the delta-method from the estimates of the inverse of speeds.

4 Estimation of the road traffic congestion technologies

4.1 Overview of the data

We split the Paris area into five areas: the city center, the ring roads, the close suburb, the far suburb, and the main highways that connect the city center to the suburbs. We estimate the congestion technology for the city center, ring roads, and highways. Due to the absence of data, we cannot directly estimate a congestion technology for the suburbs. However, we still allow for adjustment of the equilibrium speeds in the suburbs by making additional functional form assumptions on their congestion technologies. More specifically, we assume the congestion technology in the suburbs is a convex combination of those on the highways

and the city center. We provide the map that shows the areas and the locations of road traffic sensors in Appendix D.4.1.

To estimate the road congestion technologies, we rely on hourly data on traffic conditions from 1,359 road traffic sensors for 2016 and 2017. We use 2016 and 2017 data from traffic sensors since it is the earliest year available for highways.[19] The road traffic sensors typically record up to four variables: the traffic flow (in vehicles per hour), the traffic density (in vehicles per kilometer), the occupancy rate, i.e., the percentage of time during which the traffic sensor detects a car (in percentage per hour), and the speed (in km/hr). We provide more details about these variables and their theoretical relationships in Appendix D.4.2. We rely on two key variables: speed (in km/hr) and road occupancy rate. We use the occupancy rate to represent the traffic level since it seems more appropriate because we aggregate different roads. We use these two variables to estimate the relationship between speed and occupancy rate denoted $\tilde{f}^a$. This function differs from the speed function f^a defined in Equation (7) because the latter requires the number of kilometers driven as an argument. Section 4.4 defines a mapping between the occupancy rate and the number of kilometers driven K_t^a.

4.2 Speed-occupancy rate relationship

For the estimation, we observe a sample of $i = 1, ..., I$ independent observations of speed v_i^a and occupancy rate τ_i^a. There are unobserved speed shocks ν_i^a, so that we can write the speed as:

$$v_i^a = \tilde{f}^a(\tau_i^a) + \nu_i^a.$$

We make minimal functional form assumptions on $\tilde{f}^a$ by relying on basis polynomials. More specifically, we use Bernstein basis polynomials of degree Q^a:

$$v_i^a = \sum_{q=0}^{Q^a} c_q^a B_q(\tau_i^a) + \nu_i^a. \tag{12}$$

The coefficients c_q^a are the parameters of interest, and B_q are the Bernstein basis polynomials given by:

$$B_q(\tau) = \binom{Q^a}{q} \tau^q (1-\tau)^{Q^a - q}.$$

Since the occupancy rate τ_i^a and speeds are simultaneously determined in equilibrium, τ is

[19] We use data from 2010 for the city center and the ring roads to evaluate the differences in traffic between the two periods. We find that the average speed decreased by only 5.5% and 5.1% at peak and off-peak hours in the city center between 2010 and 2016. In the ring roads, we find an increase of 0.7% at peak hours and a decrease of 3.7% during off-peak hours.

correlated to the speed shock ν. We thus rely on instruments and use the general method of moments to estimate the parameters $\mathbf{c}^a = (c_q^a)_{q=0,...,Q^a}$ in Equation 12. We rely on the matrix of P instruments $Z = (z^1, ..., z^P)$ to form empirical counterparts of moment conditions:

$$m(\mathbf{c}^a)^p = \sum_{i=1}^{I} \nu_i(\mathbf{c}^a) z_i^p.$$

We estimate $\mathbf{c}^a$ by minimizing:

$$\mathbf{m}(\mathbf{c}^a)' W \mathbf{m}(\mathbf{c}^a), \tag{13}$$

where $m(\mathbf{c}^a) = (m(\mathbf{c}^a)^1, ..., m(\mathbf{c}^a)^P)'$ is the vector of moments and W is a weighting matrix. We implement the two-step GMM to use the efficient weighting matrix, starting with the identity matrix. In addition, we impose that the speed functions are weakly decreasing. This can be imposed by restricting that $c_q^a \geq 0$ and $c_{q+1}^a \leq c_q^a \quad \forall q \in \{0, ..., Q^a - 1\}$.

The relationship between speed and traffic is identified from the local variation in traffic conditions in the data, conditional on the instruments. Since our instruments are all dummy variables, interpreting the orthogonality conditions is straightforward. We exploit several dimensions of variation between observations in the traffic data. We observe data for different roads, at different hours, on different days, and with different exogenous shifters of traffic level.

The order of the Bernstein polynomial approximation, Q^a, is selected to minimize the mean squared forecast error (MSFE). We follow Hansen (2014) and use the leave-one-out estimator of the MSFE, which can be summarized by the following cross-validation criteria:

$$Q^a = \underset{1 \leq p \leq \bar{Q}}{\arg\min} \left\{ \frac{1}{I^a} \sum_{i=1}^{I^a} \frac{\hat{e}_{ip}^2}{\left(1 - h_{ip}^a\right)^2} \right\},$$

where $\bar{Q}$ is the maximum degree of the polynomial considered and I^a is number of observations in area a. $\hat{e}_{ip}^2$ is the squared prediction error for observation i under a polynomial basis of order p. h_{ip}^a is the leverage value for observation i given by the i^{th} diagonal element of the projection matrix $\mathcal{B}_p^a \left(\mathcal{B}_p^{a\prime} \mathcal{B}_p^a\right)^{-1} \mathcal{B}_p^{a\prime}$ where $\mathcal{B}_p^a = (B_0^a, ..., B_p^a)$ is a matrix containing the values of the Bernstein basis polynomials $B_p(\tau)$ for all observations.

To mitigate concern about speed shocks affecting simultaneously traffic level and speed, we exclude from our sample the observations with extreme weather conditions. For instance, snow may discourage individuals from driving and reduce their speed. Extreme weather conditions are defined by either snow, temperatures below the 5th percentile or above the 95th percentile of the entire temperature distribution, or wind or rain intensity above the

95th percentile of the entire wind or rain distribution. To be conservative, we drop the observations with an extreme weather event during the hour or up to three hours before and after.

Then, we construct instruments to estimate the parameters of the Bernstein polynomial. Valid instruments are variables uncorrelated with speed shocks but affect the traffic level. We use the following dummies: hour, day-of-the-week, school holidays, bank holidays, low public transport (number of daily passengers below the 25th percentile), days with a driving restriction in place, an accident in a donut of 1 to 1.5 km radius (3 to 5 km on the highways), an accident in a 1.5 km radius (5 km on the highways) during the previous hour, a temperature between 19 and 25° celsius, temperatures between 4 and 9° celsius. All these variables presumably shift the traffic level exogenously and are not correlated with speed shocks. For instance, cold weather is likely to increase car usage. However, driving speeds are affected only by changes in the level of traffic and not directly by low temperatures. Kreindler (2024) also uses hour of the day dummies. In the same spirit, we use bank holidays and school holidays. The low number of public transport passengers represents a proxy for a strike event. An accident close to the traffic sensor is likely to affect traffic level and speed simultaneously. This is why we use a donut around the traffic sensor to capture changes in traffic due to re-routing and accidents in the previous hour. Finally, we also use the interactions between the dummies if there are more than 500 observations with positive values. Ultimately, we use 391 instruments for the highways, 380 for the ring roads and 390 for the city center.

We make several assumptions to estimate the congestion technologies in the close and far suburbs, where we do not have detailed traffic data. First, we assume the close and far suburbs share the same congestion technology. Second, we assume this technology is a convex combination of the congestion technologies of the city center and highways. We pin down the parameter of the convex combination by relying on a limited dataset we obtained from the Seine-Saint-Denis department, one of the four departments composing the close suburbs. The data contains one week of hourly observations for road traffic sensors in 2023. Instead of providing speed measurements, the data assigns each car to intervals such as 0 to 30 km/hr. These large intervals do not allow us to estimate a speed-traffic curve like in the other areas. We still use this dataset to compute peak and off-peak hours average speeds and occupancy rates. We calibrate the parameter of the convex combination to be the closest to the two speed-occupancy rate data points. The parameter reflects a weight of 17.7% for the highways technology and 82.3% for the city center technology.

4.3 Summary statistics and estimation results

We explain how we construct the final sample to estimate the congestion technologies in Appendix D.4.3. It contains 3.84 million hourly observations from 643 traffic sensors for the highways, 1.2 million observations from 117 traffic sensors for the ring roads, and 5.12 million observations from 599 traffic sensors for the city center.

Table 6 provides the summary statistics for the speeds and occupancy rates in the different areas. We focus on 8:00 to 8:59 a.m. for peak hours and on 6:00 to 6:59 a.m. for off-peak hours to be comparable with the TomTom queries. We observe significant heterogeneity across areas, suggesting that our partition is relevant. Speeds at peak and off-peak hours significantly differ, supporting our differentiation across periods. In addition to providing evidence of heterogeneity across areas, the traffic speeds and occupancy rates are highly variable; we leverage these forms variation to estimate flexible road congestion technologies, given that the variability is still important after conditioning on the instruments.

Table 6: Road traffic conditions by area

		Peak	**Off-peak**	**All sample**		
	Area	**Mean**	**Mean**	**Mean**	**Median**	**Std. dev.**
Speed	Highways	41.7	66.7	67.7	76	33.3
	City center	19.8	29.4	22.8	17.8	17.7
	Ring roads	30.5	56.7	44.1	44.6	21.1
Occupancy rate	Highways	24.6	14	15	10.7	11
	City center	18.9	6.7	14.2	10.1	11.6
	Ring roads	32.5	15.6	22.6	20.6	12.1

Note: Speed is in km/hr, and occupancy rate is in %. Averages at peak and off-peak hours are computed using our final sample and weighted by the average traffic flow of the traffic sensor. Peak hours are between 8:00 and 8:59 a.m., and off-peak hours are between 6:00 and 6:59 a.m.

In Figure 1, we provide the congestion technologies for the different areas (the close and far suburbs have the same technology, but they do not have the same equilibrium traffic conditions). The initial traffic conditions are obtained from the average speeds obtained from TomTom trip durations (see Table 5). From the initial speeds, we back out the initial occupancy rates by inverting the congestion technologies:

$$\tau_t^a = \left(\tilde{f}^a\right)^{-1}(v_t^a).$$

τ_t^a is unique since $\tilde{f}^a$ is monotonically decreasing in speed at the initial speed value. Understanding which occupancy rates reflect a congested road helps interpret the congestion technology graph. The authorities consider the traffic fluid if the occupancy rate is below 15%, pre-saturated if between 15% and 30%, and saturated if above. According to this definition, the traffic is pre-saturated during peak and off-peak hours in all areas except on the highways (fluid during off-peak hours) and the ring roads (saturated at peak hours).

Figure 1: Estimated congestion technologies and initial traffic conditions

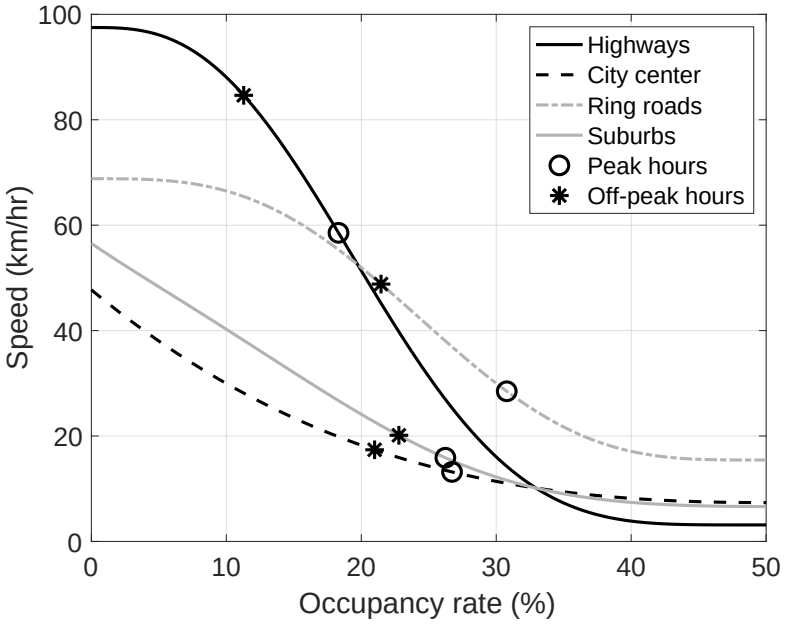

Note: Initial conditions are average speeds at peak and off-peak hours from TomTom predicted durations. We provide the initial conditions in the close suburbs on the suburbs congestion technology curve.

As Figure 1 shows, the estimated values of the maximum speeds are consistent with the speed limits in each area. We estimate it to be 97.5 km/hr for highways compared to speed limits that vary between 90 and 130 km/hr depending on the road and the location. The speed limit is typically 70 km/hr on the ring roads, which is close to our 68.8 km/hr estimate. Lastly, the speed limit is usually between 30 and 50 km/hr in the city center, close to our estimate of 47.7 km/hr. In the suburbs, the maximum speed is 56.5 km/hr. We provide the R^2 and the polynomial degrees of the models for each area in Appendix D.4.4. The fits are particularly good for the highways and ring roads (with R^2 of 0.63 and 0.65, respectively), and the degrees of the polynomial are high (8 and 7, respectively). By contrast, we select a polynomial of degree 3 in the city center and explain only 18% of the variance.

Our congestion technologies show heterogeneity across areas. Clearly, our estimates reject the assumption of a single, city-wide congestion technology and show that congestion technologies do not follow simple functional forms. We have a high speed for low traffic levels on highways, but it becomes slower than ring roads for occupancy rates above 19.7%, and slower than any other area for occupancy rates above 32.9%. This can be explained by the role of interchanges, entries, and exits on highways, which may slow down driving speeds quickly when the traffic increases.

The congestion curve for ring roads remains flat initially: the slope remains higher than -0.72 until an occupancy rate of 10%. By contrast, the speed in the city center displays a

convex relation, with speeds decreasing faster for lower occupancy rates than for larger ones. In the suburbs, speeds are higher than in the city center for occupancy rates below 32.9%. Then, suburb speeds become only slightly below those in the city center.

4.4 Mapping between occupancy rate and kilometers driven

To estimate f^a, we need a mapping from the number of kilometers driven to the occupancy rate τ_t^a in each area. We assume an affine relation between the occupancy rate and the total number of kilometers driven. Formally, we introduce a scale parameter ϕ^a such that :

$$\tau_t^a = \phi^a \times (K_t^a + K_{0t}^a). \tag{14}$$

where K_t^a is the number of kilometers driven in the area a at time t predicted by our transportation choice model and K_{0t}^a represents the rest of traffic that we do not model (irreducible traffic). We can thus obtain f^a as:

$$f^a = \tilde{f}^a \left(\phi^a \times (K_t^a + K_{0t}^a)\right).$$

We can only identify two parameters per area because we observe individual choices and speeds for only two periods.[20] We impose that the irreducible traffic level is identical at peak and off-peak hours: $K_{0t}^a = K_0^a$. We could, alternatively, impose some restrictions across areas and let the irreducible traffic level vary with the period. However, given that the areas have very different sizes and may be subject to different levels of irreducible traffic, our assumption seems more appropriate.

With two linear equations and two unknowns, we can find a unique pair of parameters for each area. We further impose that the irreducible traffic implies occupancy rates between 0 and 50% and use the constrained least-squares method that minimizes the sum of square deviations from Equation 14:

$$\begin{aligned} &\min_{\phi^a, K_0^a} \sum_{t=t_1,t_2} \left[\tau_t^a - \phi^a \times (K_t^a + K_0^a)\right]^2 \\ \text{s.t. } &\phi^a \times K_0^a \leq 50 \\ &\phi^a \times K_0^a \geq 0. \end{aligned} \tag{15}$$

The calibrated parameters are presented in Table 7. We obtain a relatively sizeable irreducible share of traffic in the suburbs (76.6% and 78.7% of traffic for the close and far suburbs,

[20] We only use the 2010 EGT sample. The 2020 EGT sample has too few observations, which compromises the sample representativity at the area level.

respectively). At the same time, we estimate lower levels of irreducible traffic for the city center and the ring roads (36.6% and 33.4%, respectively). Finally, we estimate a tiny share of 1.11% on the highways.

Table 7: Calibrated parameters of the mapping between road occupancy rates and driven distances

Area	**Scale parameter** ($\phi^a \times 10{,}000$)	**Irreducible traffic** ($K_0^a/10,000$)	**Irreducible traffic share (%)** ($K_0^a/(K_0^a + K_{t_1}^a) \times 100$)
Highways	0.036	5.57	1.11
City center	0.426	23	36.6
Ring roads	0.361	28.2	33.4
Close suburb	0.043	465	76.6
Far suburb	0.01	1,491	78.7

Notes: The share of irreducible traffic is in % of the distance driven at peak hours.

4.5 Fit of the model

By construction, our model almost exactly predicts the average speeds that rationalize TomTom's expected trip durations. The imperfect prediction comes from the constraint of bounding the traffic below 50% when estimating the parameters of the mappings between road occupancy rates and the distances driven. This implies that the equilibrium speeds differ slightly from those obtained in Table 5. The individual trip durations are thus slightly different from TomTom. We see negligible differences between Columns 2 and 3 of Table 8. This table also suggests that the model delivers good predictions of aggregate shares. Indeed, all the differences between observed and predicted shares are at most 0.7 percentage points. These results give us confidence in the ability of the model to predict equilibrium transportation mode shares.

Table 8: Shares of transportation modes observed and predicted by the model

	Observed	**Predicted with TomTom durations**	**Predicted with Equilibrium speeds**
Pub. transport, peak	34	33.9	33.7
Car, peak	24.4	23.9	24
Walk, peak	15.2	14.9	14.9
Bicycle, peak	1.59	1.89	1.88
Motorcycle, peak	1.35	1.29	1.28
Pub. transport, off-peak	11.7	11.7	11.6
Car, off-peak	8.46	8.35	8.48
Walk, off-peak	2.11	2.77	2.77
Bicycle, off-peak	0.446	0.568	0.566
Motorcycle, off-peak	0.644	0.763	0.756

Note: in %. All shares computed using survey weights for 2010.

We further assess the fit of our model by comparing the distances driven in each area. If our model predicts the number of individuals driving well, the distance analysis reveals whether we can also predict who is driving. Table 9 shows that we get very close estimates across all areas during peak hours, with the difference being smaller than 4.1% in all locations. We

obtain slightly more extensive differences during off-peak hours. In particular, we underpredict distances driven on the highways and the city center but overpredict the amount driven through the ring roads. We do not consider these differences large enough to signal the model's inability to predict counterfactual equilibrium outcomes.

Table 9: Observed and predicted distances driven

	Peak hours		Off-peak hours	
Area	**Observed**	**Predicted**	**Observed**	**Predicted**
Highways	502	497	307	270
City center	39.7	39.9	26.2	21.9
Ring roads	57.1	56.3	31.3	33.8
Close suburbs	148	142	67.9	65.5
Far suburbs	418	405	170	162

Note: in 10,000 of kilometers.

Table 10 compares the average speeds from road traffic sensor data and those predicted from the model equilibrium (for the highways, city center, and ring roads where we have the data). This comparison constitutes an external validity check since the average speed data from road traffic sensors are not directly used in the estimation. We find that our estimates are not perfectly aligned with the average speeds but are fairly similar. Our estimates are optimistic for the highways but conservative for ring roads and the city center, particularly during off-peak hours. Nevertheless, we predict speeds in the same order of magnitude as those recorded by the sensor data, and we correctly predict the speed ranking between areas for both periods.

Table 10: Predicted equilibrium speeds and average speeds from traffic data

	Peak hours		Off-peak hours	
Area	**Traffic data**	**Eq. speeds**	**Traffic data**	**Eq. speeds**
Highways	46.9	59.3	68.4	88.2
City center	22.5	13.1	31.4	19.1
Ring roads	31.8	29	57.5	46.8
Close suburbs		16.2		20.3
Far suburbs		24.8		28.8

Note: in km/hr.

4.6 Equilibrium uniqueness check

We now apply the method developed in Section 2.3 to verify that our algorithm is a contraction. Given the estimated model parameters, we check that the model has a unique equilibrium. We provide in Appendix D.5.1 the analytical formula for the Jacobian of $\mathbf{g}(.)$.

We compute the Lipschitz coefficients for values of the algorithm tuning parameter κ between 0 and 0.99 with a step of 0.01. We solve for these coefficients at the equilibrium speeds without policy and under different policy environments we consider in section 5. We

calculate:

$$\max_{a\in A}\max_{t\in T}\max_{a'\in A}\max_{t'\in T}\left|\frac{\partial g_t^a(\mathbf{v}^*,\kappa)}{\partial v_{t'}^{a'}}\right|,$$

where $\mathbf{v}^*$ denotes the vector of equilibrium speeds. Panel (a) of Figure 2 shows that only when κ is equal to 0, i.e., when we only iterate on the speed function, the algorithm is not a contraction. We also find that the policies decrease the Lipschitz coefficients of the algorithm so that the no-policy environment requires the highest κ to have a contraction.

We also check for which values of the tuning parameters our algorithm is a contraction in the entire set of possible speed values. This time we calculate:

$$\max_{a\in 1,\ldots,A}\max_{t\in 1,\ldots,T}\max_{a'\in 1,\ldots,A}\max_{t'\in 1,\ldots,T}\max_{\mathbf{v}\in[\underline{\mathbf{v}},\overline{\mathbf{v}}]}\left|\frac{\partial g_t^a(\mathbf{v},\kappa)}{\partial v_{t'}^{a'}}\right|,$$

where $[\underline{\mathbf{v}},\overline{\mathbf{v}}]$ denotes the speed interval for the speed vector $\mathbf{v}$. Due to the computational intensity of the optimization, we do a coarser grid search over the values of κ between 0.5 and 0.95, with a step of 0.05. We use 20 random speed vectors as initial values to avoid local minima. Panel (b) of Figure 2 shows that from $\kappa = 0.9$, the algorithm is a contraction under any environment. The no-policy environment is associated with the smallest set of κ that ensures our algorithm is a contraction. This can be explained by the policies making individuals less reactive to speed changes. We use the value 0.9 to solve the equilibrium speeds. The resulting algorithm takes on average 160 iterations and converge in 2.3 seconds (see Figure 12 in Appendix D.5.2).

Figure 2: Lipschitz coefficients at the equilibrium speed and for any speed

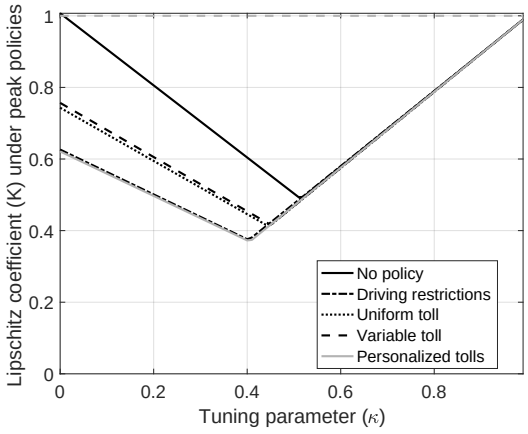

(a) At the equilibrium speeds

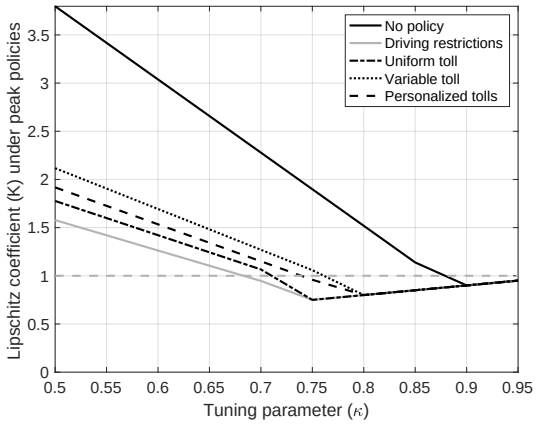

(b) In the space of all possible speeds

5 Quantifying the welfare consequences of the regulations

Our model predicts individual probabilities of choosing each transportation mode and the equilibrium driving speeds at peak and off-peak hours in the five areas. Thus, we do not predict counterfactual choices but individual choice probabilities, which we use to compute the expected number of individuals choosing each transportation mode and departure period. First, we evaluate how severe congestion problems are and study the role of scheduling constraints on congestion. Second, we compare the effects of simple policies across all stringency levels. Third, we compare the performance of these instruments relative to personalized tolls designed to maximize either welfare or consumer surplus. Finally, we study the differences across policy instruments for distributional effects and emissions reduction.

5.1 Value of driving and marginal costs of congestion

We measure the value of driving at the initial equilibrium speeds by relying on consumer surplus changes when we remove the driving option or modify speeds. We provide the formula for consumer surplus in Appendix E.1. We measure the value of driving at peak hours under the maximum speeds possible given the irreducible portion of traffic. The speed improvements lead to a total surplus increase of €10 million, €3.3 per potential driver. Relaxing congestion generates a total reduction in expected travel time of 203,000 hours, equivalent to an average of four minutes per individual.

We define the marginal costs of congestion for an area at a given period as the total consumer surplus losses associated with one additional kilometer driven or an extra driver in that area. For the case of an extra driver, we add the average number of kilometers driven by a potential driver in that area. Table 11 shows area-specific marginal costs for an additional kilometer are between €0.16 and €1.3 during peak hours. Highways and suburbs have the lowest marginal costs. This is the effect of large area size, as one additional kilometer has a tiny impact on the traffic level. The costs associated with an extra driver are between €0.32 (for far suburbs during off-peak hours) and €4.4 (for highways at peak hours). The existence of preferences and constraints for driving at peak hours explains why the costs of congestion are higher at peak hours than off-peak hours. Finally, we also compute the marginal cost of congestion by adding an individual with the average itinerary (i.e., distance traveled in each area) among car owners. The average costs are €6.4 at peak hours and €1.8 during off-peak hours.

Our estimates of the marginal costs of congestion are higher than Couture et al., 2018

($0.035 for several U.S. cities). Our marginal cost estimates are, however, similar to Yang et al., 2020 (3 yuan or approximately €0.36 for Beijing) and Koch et al. (2023) (between €0.45 and €0.73 for Berlin between 6 and 10 a.m.).[21] Koch et al. (2023) also estimate the marginal cost of an additional average driver to be €4.5 in Berlin, close to the average between our values of €1.8 for the off-peak period and €6.4 during peak hours.

Table 11: Estimated initial marginal costs of congestion by area

	One kilometer		One average driver	
Area	**Peak**	**Off-peak**	**Peak**	**Off-peak**
Highways	0.418	0.065	4.39	0.683
City center	1.3	0.553	4.26	1.81
Ring roads	0.983	0.28	4.24	1.2
Close suburbs	0.513	0.195	1.57	0.599
Far suburbs	0.155	0.056	0.893	0.323
Average			6.38	1.84

Note: in €. "Average" is the marginal cost for the average driver itinerary across areas.

Finally, to assess the importance of schedule constraints, we compute the new equilibrium if individuals are always or never able to choose their departure time. Removing the schedule constraints increases the average individual surplus by €1.2. The share of individuals commuting during off-peak hours increases by 2.9 percentage points. By contrast, if individuals can never substitute inter-temporally, the average surplus decreases by €1, and the share of individuals choosing peak hours increases by 1.8 percentage points.

5.2 Main outcomes of interest and policy overview

We measure policy impacts on consumer surplus, toll revenue, and emissions. We define an aggregate welfare measure W that is the sum of the change in aggregate consumer surplus, toll revenues and the benefits from avoided emissions valued at standard levels. Our estimated welfare effects are for one trip per person for the entire population of commuters in the Paris area.[22]

We rely on a 2019 report from the European Commission (Van Essen et al., 2019) for the social costs of emissions that provides the values specific to urban areas in France. Table 12 contains the social costs of the different pollutants. On average, in our sample, the social cost of emissions per km for a gasoline car is €0.34, while for a diesel car it corresponds to €0.45. Additional details on the emissions costs are provided in Appendix E.2.

[21] We use the average 2014 CNY-EUR exchange rate from https://www.exchangerates.org.uk/CNY-EUR-spot-exchange-rates-history-2014.html.

[22] There are, on average, 224 working days annually and two commuting trips per day. We should multiply the welfare effects by 448 to convert them into annual terms.

Table 12: Social costs of emissions

	CO_2	NO_X	HC	PM
Social cost (€/ton)	189	27,200	1,500	407,000

We study the welfare effects of three policies: (1) driving restrictions banning a fraction of cars randomly, (2) uniform tolls, and (3) variable tolls linear in the trip distance (or per-kilometer toll).[23] We focus on policies applicable at peak hours only so that driving during off-peak hours is never constrained or charged.[24] We focus on peak-hour policies in the main analysis for three reasons. First, congestion is most severe at peak hours, leading to high pollution levels and exacerbated congestion effects. Second, our model allows individuals to substitute across periods. This model feature is rarely covered in the literature and is particularly relevant when regulations are period-specific. Finally, several real-life examples of congestion charges have greater tolls during peak hours.[25]

We also study the importance of accounting for speed adjustments to accurately predict the transportation policies' effects. In Appendix E.3.1 we compare the congestion levels and driving rates predicted by our model against those obtained under a simpler model with constant speeds. The comparison highlights the importance of considering the policies' effects on speeds, as they influence substitution patterns between transportation modes and departure periods.

5.3 Comparison of simple instruments across policy levels

First, we compare policies that achieve the same traffic reduction during peak hours to make a fair comparison. We interpret the traffic reduction as the policy stringency level, which is directly comparable across policies. The regulator may seek to reduce traffic beyond the emissions concern, or the emissions avoided may have much higher benefits than standard values because of severe local pollution (e.g., during a pollution peak episode). The comparison results would be very similar if we considered policies that generate the same reduction in emissions costs instead of considering the traffic reduction outcome.[26]

Figure 3 presents the welfare changes, consumer surplus changes, and toll revenues associated with the three simple instruments. Panel (a) shows that the two types of tolls have positive

[23] 0.068% of the individuals in our sample do not have an alternative to cars. To avoid an empty choice set when simulating driving restrictions under schedule constraints, we assign to these individuals a public transport option using the fifth percentile of the distribution of public transport speeds (8.5 km/hr).

[24] Appendix E.5.1 presents the same analysis for policies applicable across all periods. The results are qualitatively similar.

[25] Santiago, Stockholm, Oslo, Bergen and Singapore are examples of cities with congestion pricing schemes that include a specific peak-hour price.

[26] Panel (a) of Figure 4 below shows that the policies have very similar effects on the emissions cost reductions.

impacts on welfare for moderate stringency levels. By contrast, driving restrictions always generate welfare losses. The variable toll is always better than the uniform toll for welfare, and has a broader range of welfare-enhancing policy stringency levels. We obtain welfare gains for traffic reductions below 30.6% with a uniform toll. The corresponding tolls are below €5.4. With a variable toll, we can improve welfare by reducing traffic up to 51.6%, with per-km tolls below €0.455/km.

Panel (b) provides the changes in consumer surplus. All policy instruments generate consumer surplus losses across all policy stringency levels. Even if the policies relax congestion problems, the speed improvements for individuals who drive never compensate for the consumer surplus losses from tolls or driving restrictions. This is due to two main reasons. First, the speed improvements at peak hours are modest, particularly in the city center and the suburbs, as shown by Figure 15 in Appendix E.3.2. In addition, speeds during off-peak hours decrease. Second, the value of travel time savings does not compensate for the toll cost or the cost of being restricted a fraction of the time. Indeed, as Figure 16 in Appendix E.3.2 suggests, the gains from speed changes cover at most 44.7% of the consumer surplus losses from the policies. For the uniform tolls and the driving restrictions, the speed gains are lower than 31.1% and 27.2%, respectively. The gains, in relative terms, always decrease with the policy stringency level. Speed changes negatively affect consumer surplus at very stringent policy levels because individuals drive predominantly during off-peak hours when the speeds are lower than in the absence of policy.

Policy rankings by consumer surplus change are different than ranking by welfare. The uniform toll always generates the largest consumer surplus losses, followed by the driving restrictions and the variable tolls. This is the consequence of needing to impose very high uniform tolls to trigger traffic reductions. Panel (a) of Figure 4 shows that the average variable toll is always significantly lower than the uniform toll.

Panel (c) of Figure 3 shows that the welfare gains come from the ability of the tolls to generate extensive revenues and the assumption that toll revenues can be redistributed. We obtain Laffer curves as the total toll revenue decreases from certain policy stringency levels. The maximum toll revenues occur under fairly stringent policies, indicating that it takes high toll values to discourage individuals from driving at peak hours. Finally, for most policy levels, the uniform toll is better at generating revenue than the variable toll. This can be explained by the higher average toll paid by individuals under the uniform toll than the variable toll (see Panel (a) of Figure 4 below).

Under the optimal uniform and variable tolls, the toll revenues cover 117% and 135% of the total consumer surplus losses, respectively. With the value of emissions avoided, the

excess toll revenue implies that these optimal tolls are welfare-improving with shadow costs of public funds below 18.2% and 31% for the uniform and variable tolls, respectively.[27]

Panel (b) of Figure 4 shows the average distances driven at peak hours under the regulations are quite different. The average distance only slightly increases under driving restrictions, while it increases under the uniform toll and decreases under the variable toll. This is helpful to understand who is targeted by each policy. Driving restrictions force all individuals to contribute to traffic reductions. However, since this policy targets individuals randomly, we observe a relatively constant average trip distance across stringency levels. The uniform toll discourages short-distance trips, making this policy inefficient at reducing traffic. The regulator must set high uniform tolls to trigger a response from individuals and traffic reduction. By contrast, by pricing based on distance, the variable toll discourages long-distance trips and thus efficiently decreases traffic.

Finally, Panel (c) of Figure 4 shows that the emissions gains are modest across policies. They are always below €343,000, while the consumer surplus losses are up to €7.2 million. Across policy levels, the emissions gains cover at most 6.8% of the consumer surplus losses as shown by Panel (b) of Figure 16 in Appendix E.3.2. At the optimal variable toll, the emissions gains only cover 6.6% of the consumer surplus losses. The results imply that emissions should be valued 15.2 times more to justify the optimal variable toll if we do not include toll revenue in the welfare computation.

Figure 3: Change in welfare, consumer surplus, and toll revenue

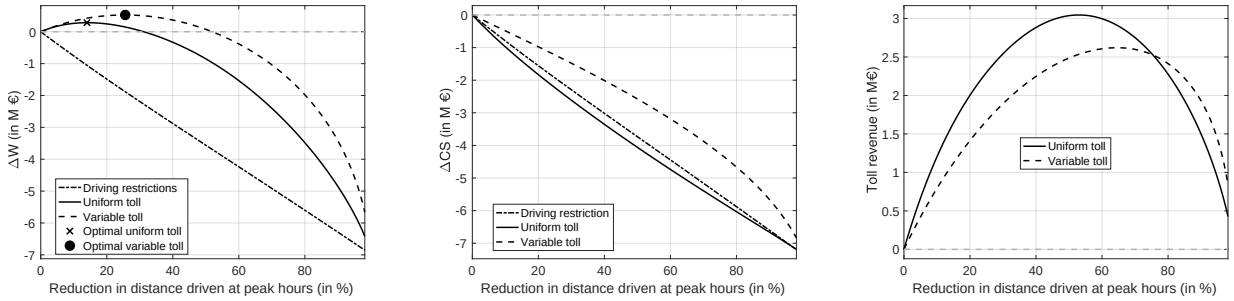

(a) Welfare (b) Consumer surplus (c) Toll revenue

[27]The maximum shadow costs $\tilde{\lambda}$ are the solutions to: $\Delta CS + \Delta E + (1 - \tilde{\lambda})T = 0$, where T denotes the toll revenue.

Figure 4: Additional policy outcomes

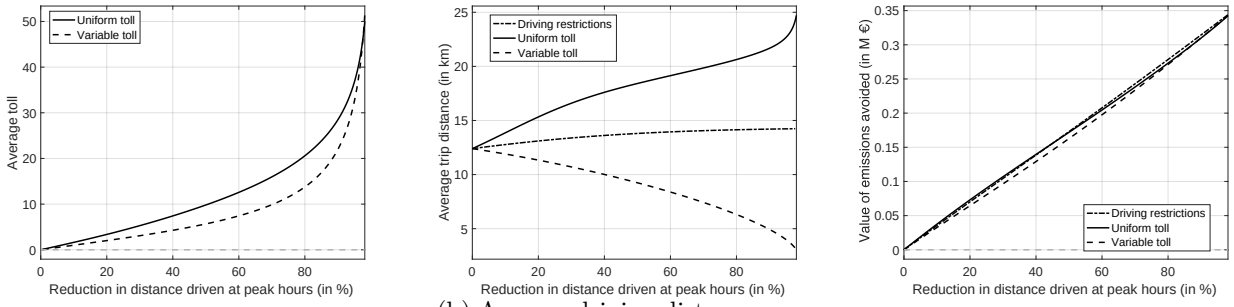

(a) Average toll

(b) Average driving distance, conditional on driving at peak hours

(c) Value of emissions avoided

Figure 5 presents the total consumer surplus losses using distributional weights (the inverse of income) and the difference in consumer surplus changes between the top and bottom 10% of the income distribution. First, we see that using distributional weights does not affect the policy ranking nor the consumer surplus change magnitudes, as seen in Panel (a).

Panel (b) indicates that all policies are always progressive as they generate more consumer surplus losses to high-income individuals. We also notice that the progressivity increases with the policy stringency level. Finally, driving restrictions generate the largest differences between low and high-income individuals. Since wealthy individuals are the least sensitive to trip cost, they are less vulnerable to price instruments and have lower consumer surplus losses from paying tolls. By forcing individuals to reduce their driving habits, driving restrictions hurt more high-income individuals who rely more on their cars than low-income individuals.

Figure 5: Distributional outcomes

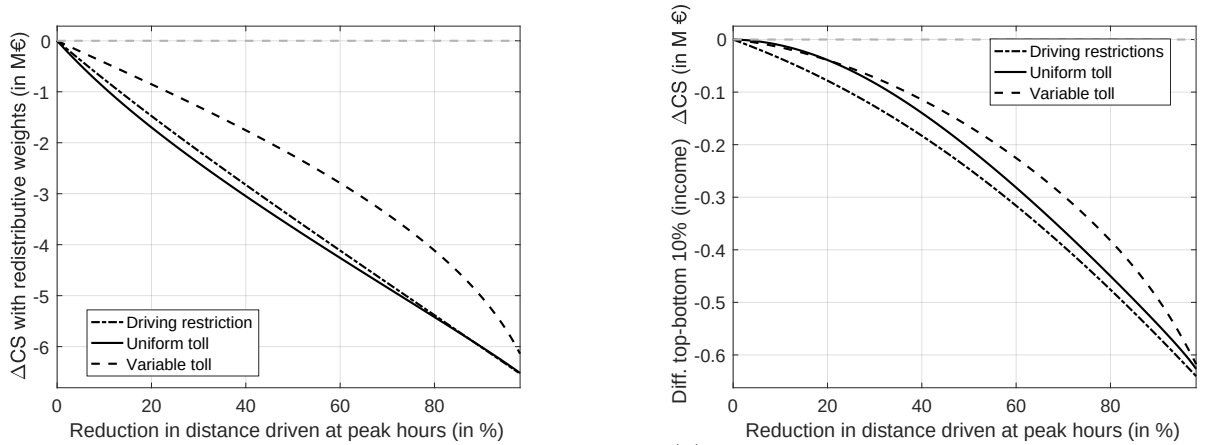

(a) Consumer surplus with distributional weights

(b) Difference in ΔCS between the top and bottom 10% of the income distribution

Figure 6 presents how the welfare changes of each policy are distributed across individual residential location. Panel (a) shows that the far suburbs are the most affected by driving

restrictions, followed by the close suburbs, and finally, the city center. The ranking remains constant across stringency levels.

Panel (b) shows the distribution of welfare under uniform tolls. For mild stringency levels, the welfare gains are higher in the far and close suburbs than in the city center. When traffic reduction becomes larger than 26%, the ranking reverts, and individuals living in the city center are the least affected. Large speed gains compensate for the toll costs for long-distance drivers under mild stringency levels. Under higher toll values, the speed gains are insufficient to compensate for the toll cost. By contrast, the uniform toll is welfare-improving in the city center for traffic reduction below 55.2%.

Finally, Panel (c) shows the results for the variable toll. As for the uniform toll, for moderate policy stringency levels, welfare gains are higher in the far and close suburbs than in the city center. This highlights that the speed improvements are more valuable for individuals living in the suburbs, with typically longer commutes. However, when the policy stringency becomes very high, individuals in the suburbs experience high welfare losses since they do not have good alternatives to driving. By contrast, in the city center, individuals are almost always better off since substituting for other modes is not very costly in terms of consumer surplus loss.

Figure 6: Change in welfare by area

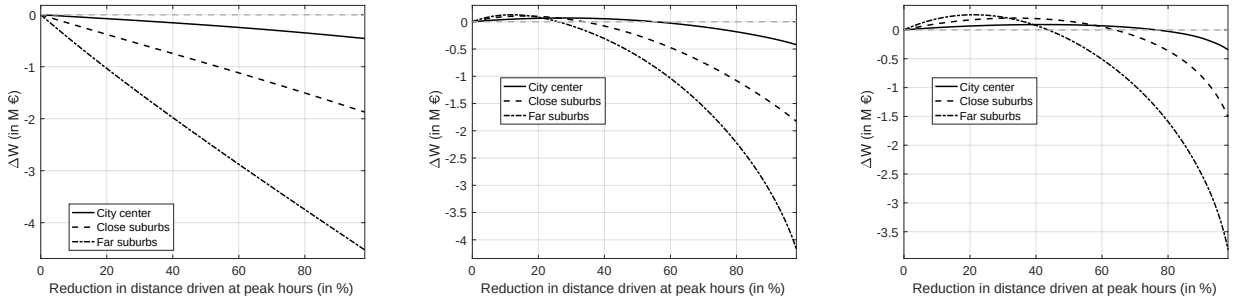

(a) Driving restrictions (b) Uniform tolls (c) Variable tolls

5.4 Measuring the efficiency of simple instruments

We analyze the performance of simple policy instruments by comparing them with the optimal policies. We first characterize optimal policies, and then we quantify the performance of simple policy instruments.

5.4.1 First-best personalized tolls

We define the optimal policy as the personalized tolls the social planner sets to maximize welfare. This is equivalent to imposing Pigouvian tolls that charge individuals their marginal

social costs.[28] We solve for welfare-maximizing tolls associated with every traffic reduction level. This is introduced through a constraint on the social planner problem. By comparing the welfare across policy stringency levels, we can find the traffic reduction level that achieves the highest welfare. We write the problem of a social planner maximizing welfare as:

$$\begin{aligned} & \max_{\mathbf{p}} \mathrm{W}(\mathbf{p}, \mathbf{v}(\mathbf{p})) \\ \text{such that} \quad & \textstyle\sum_{n=1}^{N_d} \omega_n k_n s_{n\mathbf{d}t_1}(p_n) = \bar{K}_{t_1}, \end{aligned}$$

where $\mathbf{p} = (p_1, ..., p_{N_d})$ is the vector of personalized tolls for the N_d drivers in our sample. $\bar{K}_{t_1}$ is the total number of kilometers driven at peak hours that the policy must achieve. The welfare function is composed by the consumer surplus, the toll revenue and the value of emissions avoided:

$$\mathrm{W}(\mathbf{p}, \mathbf{v}(\mathbf{p})) = \sum_n \omega_n CS_n(p_n, \mathbf{v}(\mathbf{p})) + \sum_n \omega_n p_n s_{n\mathbf{d}t_1}(p_n, \mathbf{v}(\mathbf{p})) - \sum_{t=t_1,t_2} \sum_n \omega_n e_n k_n s_{n\mathbf{d}t}(p_n, \mathbf{v}(\mathbf{p})),$$

where e_n denotes the emissions costs (in €/km) of individual n's car. We provide the Lagrangian of the problem and interpret the optimality conditions in Appendix E.3.3.

Because tolls influence individual decisions to drive and thus equilibrium speeds, we need to recompute traffic equilibrium for each toll vector along the optimization procedure. The traffic equilibrium creates links between an individual's utility and the other individuals' tolls. We overcome this challenge by rewriting the problem. The new formulation considers speeds as parameters and introduces the congestion technologies as additional non-linear constraints (in the spirit of the MPEC formulation of the BLP estimation of Dubé et al., 2012).[29] This leads to the following problem to solve:

$$\begin{aligned} & \max_{\{\mathbf{v},\mathbf{p}\}} \mathrm{W}(\mathbf{v}, \mathbf{p}) \\ \text{such that} \quad & \textstyle\sum_{n=1}^{N_d} \omega_n k_n s_{n\mathbf{d}t_1}(\mathbf{v}, p_n) = \bar{K}_{t_1} \\ & v_t^a = f^a\left(K_t^a(\mathbf{v}, \mathbf{p}) + K_0^a\right) \quad \forall a = 1, ..., A, \quad t = t_1, t_2. \end{aligned}$$

This problem is still a high-dimension non-linear optimization problem. However, the dependencies across individuals occur only through the equilibrium speed constraints. Additionally, we put some bounds on the toll values: tolls must be positive and below or equal €100.

[28] It is simple to calculate the Pigouvian tolls at the initial traffic equilibrium. However, these tolls would not be optimal since their implementation changes the traffic equilibrium and, thus, the value of the optimal Pigouvian tolls. Our method allows us to solve for equilibrium-consistent Pigouvian tolls.

[29] It is standard to use market-clearing conditions as constraints to the social planner optimization program when solving spatial equilibrium models, as noted by Fajgelbaum and Gaubert (2024).

5.4.2 Efficiency of variable tolls

Figure 7 compares the variable tolls and the welfare-maximizing policy. We restrict the set of policy stringency levels to those that generate positive welfare effects under variable tolls. These are policies reducing traffic up to 51.6%. Panel (a) provides the changes in welfare due to the policies. On average across policy stringency levels, the variable toll achieves 77.2% of the gains from personalized tolls and a maximum of 86.4%.[30] The variable toll has, therefore, very good performances.

Figure 7: Changes in welfare, consumer surplus, toll revenues and emissions avoided from variable tolls and welfare-maximizing personalized tolls

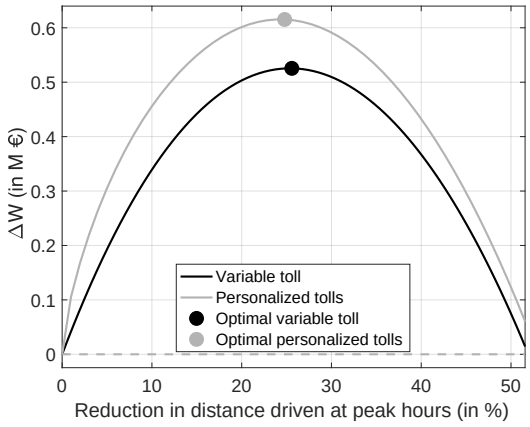

(a) Welfare

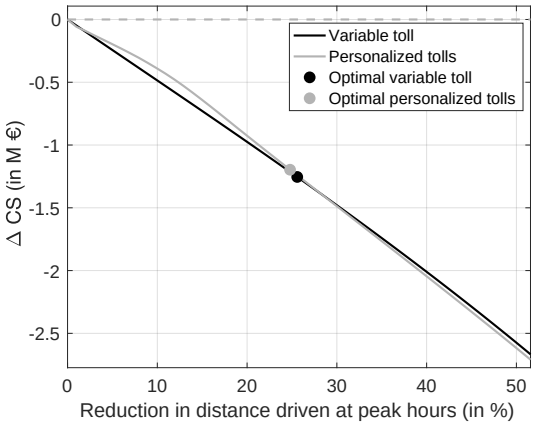

(b) Consumer surplus

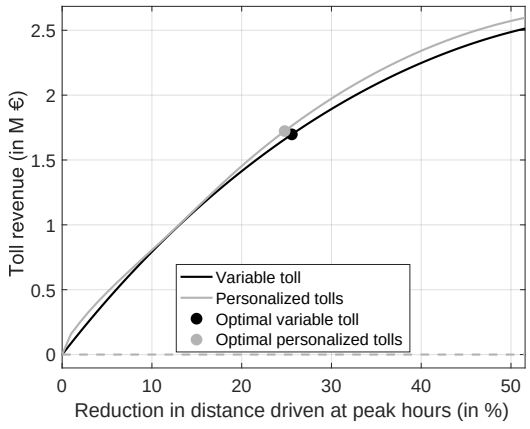

(c) Toll revenue

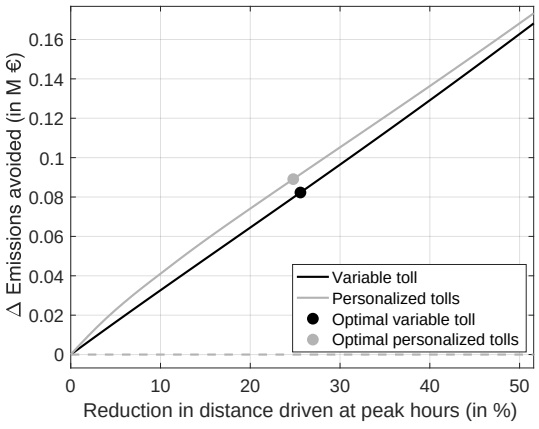

(d) Emissions avoided

When the policy stringency level becomes high, the shadow cost of the traffic constraint is very high, making the optimal individual toll almost equal to the shadow cost multiplied by the individual trip distance. This is why the personalized tolls converge to a toll scheme

[30] To calculate the difference in welfare across policy instruments, we need the same policy outcome grid. We approximate the welfare curves by Bernstein polynomials of degree eight.

linear in distance. By contrast, under a low policy stringency level, the shadow cost of the traffic constraint is low, and the individual-specific terms that define the optimal personalized tolls have more importance. This is apparent in the first-order condition associated with the optimality of tolls presented in Appendix E.3.3. The social planner sets lower tolls for individuals with the lowest emissions costs, who are more likely to be constrained to peak hour commutes, and lowest contributions to traffic in areas with high potential gains from speed improvements.

As in the previous section, we decompose welfare into its main components. Panel (b) shows that the welfare-maximizing tolls do not improve consumer surplus. Panel (c) indicates that the two types of tolls raise similar revenues, with the revenue being only slightly higher under personalized tolls. Panel (d) compares the policy instruments in terms of emissions avoided. We find small but significant improvements in emissions from personalized tolls. We can increase the gains from emissions avoided by 15.9% on average across policy levels.

5.4.3 Characteristics of the optimal policy

We further analyze the policy stringency level that achieves the best welfare outcome. First, we analyze the heterogeneity across personalized tolls to understand which dimensions of heterogeneity are taken into account by the social planner setting the personalized tolls. To do so, we regress the value of the toll on individual characteristics. Column (1) of Table 13 shows that individuals between 50 and 60 have slightly higher tolls than other age categories. Tolls increase with income for income below €2,400 and then decrease after €3,500. Tolls also increase with distance but the marginal effect of distance is decreasing. Individuals with high public transport speeds are offered higher tolls, while tolls are cheaper for individuals living further away from the city center. We find a positive association between the emissions costs and the tolls, reflecting that the social planner cares about reducing emissions. Finally, tolls significantly decrease with the probability of being flexible, reflecting that the social planner wants to limit inter-temporal substitution. However, we do not obtain a significant correlation with the probability of being constrained to peak-hour commutes. Overall, these characteristics explain 81% of the variance in personalized tolls. In Appendix E.3.4, we provide graphs of the relationships between personalized tolls and the main individual characteristics.

Table 13: Regression of personalized tolls on individual characteristics

	(1) W-maximizing tolls		(2) CS-maximizing tolls	
	Estimate	Std-err	Estimate	Std-err
Intercept	0.32†	0.166	-9.66**	2.73
Age $\in$]18, 30]	-0.036	0.067	-0.988	1.02
Age $\in$]30, 40]	-0.051	0.065	2.02†	1.04
Age $\in$]40, 50]	0.097	0.07	0.642	1.08
Age $\in$]50, 60]	0.174*	0.072	6.18**	1.14
Age $>$ 60	0.032	0.075	4.96**	1.22
Income $\in$ [800, 1,200[	0.133	0.089	4.72**	1.3
Income $\in$ [1,200, 1,600[	0.159†	0.09	4.42**	1.51
Income $\in$ [1,600, 2,000[	0.235*	0.118	-10.7**	1.86
Income $\in$ [2,000, 2,400[	0.362**	0.08	-2.39*	1.16
Income $\in$ [2,400, 3,000[	0.247**	0.071	-7.89**	1.13
Income $\in$ [3,000, 3,500[	0.296**	0.074	-17**	1.1
Income $\in$ [3,500, 4,500[	0.158*	0.078	-9.82**	1.22
Income $\geq$ 4,500	0.118	0.142	-5.61*	2.31
Distance	1.77**	0.06	2.74**	0.895
Dist-d_2 $\times$ (dist$\geq d_2$)	-0.442**	0.108	7.01**	1.67
Dist-d_3 $\times$ (dist$\geq d_3$)	-0.287	0.186	-11.8**	2.97
Dist-d_4 $\times$ (dist$\geq d_4$)	0.129	0.395	3.19	5.89
Speed public transport	0.115**	0.005	1.51**	0.075
Close suburbs	-0.806**	0.061	-1.75	1.09
Far suburbs	-2.24**	0.061	-7.88**	1.1
Emissions cost (cent/km)	0.123**	0.018	0.57*	0.287
Proba of being flexible	-0.549**	0.103	2.65†	1.54
Proba of being constrained to peak hour	0.116	0.128	0.804	2.02
R^2	0.807		0.428	

Notes: tolls in €, distance in 10 km, speed in public transport in km/hr and emissions cost in cent/km. The reference category is individuals below 18 with an income below €800 living in the city center.

Finally, we compare policy instruments without fixing the traffic reduction. For each policy instrument, we find the stringency level that maximizes welfare and thus compare the best outcome achievable by each policy instrument. To enrich the analysis we consider additional two-part tolls: with a fixed and a variable part, different values in the city center and the suburbs, and different values at peak and off-peak hours. We exclude driving restrictions from this analysis since they never improve welfare.

Table 14 provides the welfare gains achieved by the different tolls. The two-part toll with a fixed and variable part achieves 86.4% of welfare gains obtained under the welfare-maximizing personalized tolls. The simple variable toll reaches similar results, generating 85.4% of the maximum welfare gains. Between variable and two-part tolls, welfare is improved mainly through a raise in toll revenue that more than compensates for the extra losses in consumer surplus. Indeed, the two-part toll has a lower variable fee (€0.18 instead of €0.20), plus a fixed part of €0.39.

The location-specific toll is less efficient, generating 65.8% of potential welfare gains. This policy sets a much lower toll in the suburbs than in the city center (€1.65 and €4.4,

respectively). Consequently, traffic is reduced by only 15.2%, 9.1 percentage points less than the optimal policy, leading to more modest gains from emissions avoided. The relatively good performance of the location-specific toll comes from not reducing too much consumer surplus, which is achieved by considerably lowering the toll burden on individuals driving in the suburbs.

Finally, we explore the benefits of setting different tolls during peak and off-peak hours. The best time-specific tolls set a higher value at peak hours than the uniform toll (€2.61 against €2.25) and a toll of €1.37 during off-peak hours. By setting a toll during off-peak hours, the regulator reduces the incentives to substitute towards driving at off-peak hours. The regulator can then increase the toll at peak hours and raise a large toll revenue. Indeed, we see that the toll revenue is 37.8% higher than under the uniform toll. Additionally, this policy is efficient at reducing emissions by discouraging individuals from driving during off-peak hours; the gains from emissions reductions are 49.4% higher than under the uniform toll. The time-specific toll achieves 52.7% of the potential welfare gains, while the uniform toll generates only 46.1%.

Table 14: Comparison across optimal policies (conditional on a policy instrument)

	Traffic reduction (%)	ΔW	ΔCS	Toll revenue	Emissions avoided	%ΔW w.r.t. personalized tolls
(1) Personalized	24.3	0.615	-1.17	1.7	0.088	100
(2) Fixed and per-km	25.5	0.532	-1.37	1.82	0.083	86.4
(3) Per-km	25.6	0.525	-1.25	1.7	0.082	85.4
(4) Location-based	15.2	0.405	-1.22	1.57	0.057	65.8
(5) Time-specific	14	0.325	-1.9	2.15	0.078	52.7
(6) Uniform	14	0.284	-1.33	1.56	0.052	46.1

Note: (2) Fixed toll = 0.385, per-km toll = 0.18, (3) per-km toll = 0.205, (4) city-center toll = 4.4, suburb toll = 1.65, (5) peak hour toll = 2.61, off-peak hour toll = 1.37, (6) fixed toll = 2.25, all in €. Changes in welfare, consumer surplus, toll revenue and value of emissions avoided in million €.

5.4.4 Consumer surplus-maximizing policies

We study whether any policy can increase the aggregate consumer surplus by solving for consumer surplus-maximizing personalized tolls.[31] Figure 8 shows that a significant range of policy stringency levels can raise aggregate consumer surplus. These are policies reducing traffic up to 23.4%. However, the aggregate gains are relatively small, below €150,500, or €0.05 per driver. Under consumer surplus-maximizing tolls, the toll revenue is always zero. Since the social planner has no incentive to raise revenue, the consumer surplus-maximizing tolls are prohibitively high and never paid. A fraction of individuals receive zero tolls; these are individuals with the highest utility from driving. This consumer surplus-maximizing

[31]We could consider more objectives for the social planner, such as the sum of consumer surplus with redistributive weights or assigning different weights to the different components of the welfare. We leave this for future research.

policy is similar to imposing driving restrictions since, in the end, only a fraction of individuals drive for free. The critical difference with standard driving restrictions is that the social planner efficiently targets those individuals allowed to drive rather than randomly affecting individuals. The policy generates consumer surplus gains for individuals allowed to drive freely, more than compensating the consumer surplus losses from those assigned to high tolls.

Figure 8: Change in consumer surplus from variable and consumer surplus-maximizing tolls

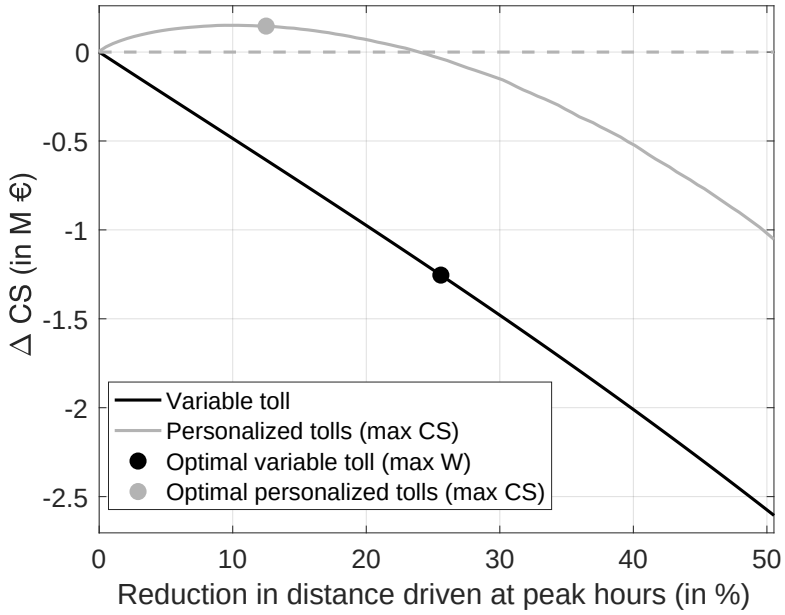

Column (2) of Table 13 shows the results of the regression of consumer surplus-maximizing tolls on individual characteristics. First, we see that individuals above 50 have higher tolls. Tolls are, however, non-monotonic with income. Wealthy individuals, with an income between €3,000 and €3,500, have the lowest tolls, while individuals with an income between €800 and €1,600 are offered the highest toll values. We also see that tolls increase with distance until 35 kilometers (d_3). The public transport speed significantly raises the toll while the distance to the city center decreases it. Individuals living in the far suburbs have a toll that is €7.9 lower than individuals living in the city center. Indeed, the social planner wants to reduce the consumer surplus losses of the individuals with the highest disutility from substituting away from driving. The emissions costs appear significant at the 5% level, which is related to the correlation between individual emission cost and other individual characteristics since emission reduction is not part of the social planner's objective. Finally, the social planner sets higher tolls for individuals that are more likely to be able to choose the departure time. Overall, the individual characteristics explain only 43% of the variation in personalized tolls. We complement this analysis with the graphs representing the relationships between personalized tolls and demographic characteristics in Appendix E.3.5.

5.5 Distributional effects

We set a benchmark policy stringency level to characterize the winners and losers and the location of environmental benefits under each type of policy. Because our model includes many layers of heterogeneity (in preferences, schedule constraints, availability and quality of public transport, trip characteristics, and congestion technologies), and as all these dimensions of heterogeneity interact, it is difficult to predict which policy instrument is favorable to which individuals. As in Section 5.3, we compare policy instruments holding fixed the traffic reduction achieved.

We use the policy stringency level that generates the highest welfare gains with welfare-maximizing personalized tolls as the benchmark. This generates a reduction of 24.3% of the traffic. We calibrate the fraction of cars banned, the uniform toll, and the variable road toll to achieve the same traffic reduction at peak hours. Table 15 below provides the policy parameters.[32] The variable toll of €0.19/km implies an average value of €2.47, much lower than the uniform toll. The maximum variable toll reaches €13.2 for the longest distance driven.

Table 15: Policy parameters for the benchmark stringency level

Outcome matched	Driving restriction	Uniform toll	Variable toll	Av. pers. toll max W
Distance, peak hours	34.9%	4.17	0.190	3.46

Note: Uniform and average personalized tolls in €, and variable tolls in €/km.

Heterogeneity in policy effects In Table 16, we provide the changes in consumer surplus at the individual level. We do not take into account the potential redistribution of the toll revenue since it would require important assumptions on how it is redistributed. We also ignore the benefits of the emissions avoided. We focus on individuals who own a car because they are the only ones affected by the policies. All policies lead to a small fraction of winners. The driving restriction improves individual consumer surplus for 8.5% of individuals. However, we see the maximum individual consumer surplus gain is small (€1.6) while the individual consumer surplus loss can be as high as €34.7. The second policy generating the largest number of winners is the variable toll, which increases the individual consumer surplus of 7.6% of individuals. The uniform toll increases the individual consumer surplus of only 4.3% of individuals. This policy instrument also appears to split the policy burden more equally across individuals as the individual consumer surplus losses are below €3.5. The personalized tolls generate the lowest share of winners across individuals (2.4%) and

[32]With two trips per day, the uniform toll implies a total cost of €8.2 per day, close to the London congestion charge between 2005 and 2011. The London toll implemented in 2003 was initially £5/day and increased to £8 in 2005, £10 in 2011, £11.5 in 2011, and £15 in 2020.

cause high individual consumer surplus losses (up to €7.6). But it also generates the highest consumer surplus gains (up to €8.4).

We finally focus on policy popularity and support from car owners. Assuming a policy is implemented, we ask which is most popular among car owners? For each potential driver, we select the policy that generates the largest individual consumer surplus change. The variable toll is most popular and is the favorite policy for 35.9% of the car owners. But this is far from the majority. Driving restriction is the second most preferred policy with 31.2% of the drivers in favor. Finally, personalized tolls are preferred by 28.6% of drivers. The uniform toll is the least preferred policy instrument, preferred by only 4.3% of drivers.

Table 16: Winners and losers across policies

	Driving restriction	**Uniform toll**	**Variable toll**	**Personalized tolls**
% ΔCS > 0	8.48	4.3	7.62	2.36
% ΔCS < 0	91.5	95.7	92.4	97.6
Min ΔCS (€)	-34.7	-3.51	-7.43	-7.57
Max ΔCS (€)	1.61	7.85	3.25	8.44
Policy support (in % potential drivers)	31.2	4.32	35.9	28.6

Who are the winners and losers? We characterize winners and losers by analyzing the association between consumer surplus changes and demographic characteristics. Figure 9 shows average consumer surplus with respect to income, age, and trip distance under each policy.[33] These graphs are helpful to understand who is the most negatively affected by the policies and whether different policies target different individuals.

Panel (a) of Figure 9 presents the distribution of average surplus loses across income levels. Under all four policies, we obtain slightly u-shaped curves, indicating that middle-income individuals are the most affected by traffic-reducing policies. However, the inflexion point is at a higher income level for variable and personalized tolls. Replacing driving restrictions or the uniform toll by optimal personalized tolls benefits the lowest-income individuals. In addition, the gains from personalized tolls relative to the variable toll increase with income.

Panel (b) shows the average consumer surplus change by age. The uniform toll has relatively homogeneous effects, while the per-kilometer and personalized tolls hurt middle-aged individuals the most. Finally, the driving restriction generates very high consumer surplus losses for middle-aged individuals. The gains from personalized tolls relative to the variable toll are mainly for individuals over 30 years old.

In Panel (c) we observe more heterogeneity of the policy effects on consumer surplus with respect to distance. The driving restriction and uniform toll have similar effects and favor

[33]We use local quadratic polynomials to smooth the curves.

very short and very long distance commuters. The driving restriction is better than the uniform toll for individuals with trip distances below 14 km but it is worse for those with longer trips. By contrast, under the variable and personalized tolls, the average consumer surplus change decreases with distance. This is to be expected due to the link between the value of these tolls and the distance driven.

Figure 9: Average surplus change and demographic characteristics

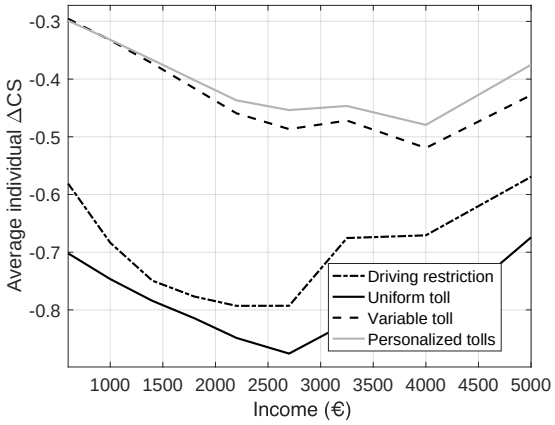

(a) Income

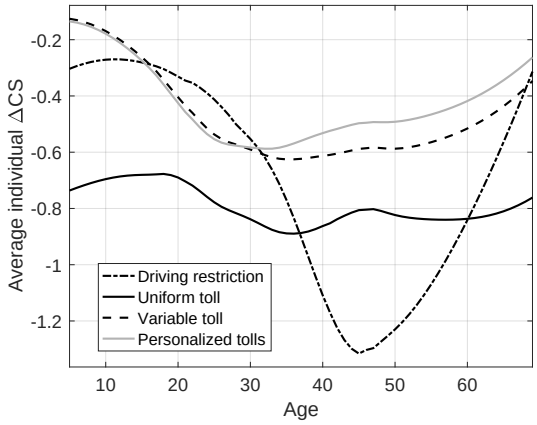

(b) Age

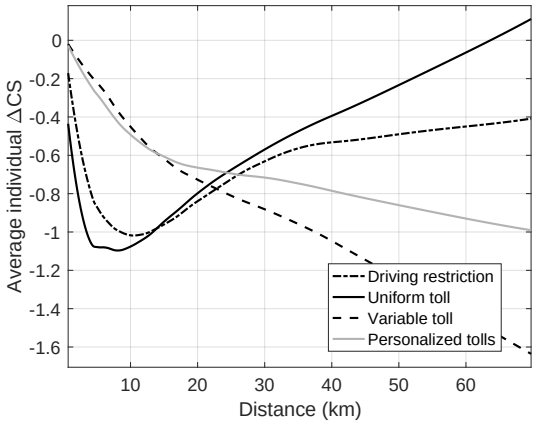

(c) Trip distance

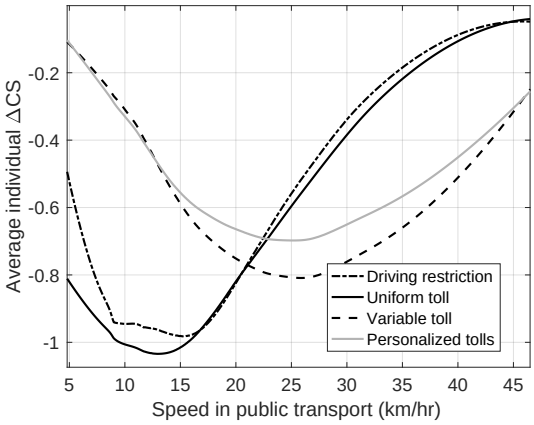

(d) Public transport speed

Finally, Panel (d) presents the average change in consumer surplus as function of the primary quality dimension for public transport, which is its speed. Individuals with the lowest public transport speed are the most affected by the uniform toll and driving restriction. By contrast, those with speeds between 20 and 30 km/hr are the most affected under the variable and personalized tolls.

In Appendix E.4.1, we examine the link between the change in consumer surplus, schedule constraints, and professional activity. We find that the driving restriction and the uniform toll hurt more individuals with a low probability of being able to choose a departure time, in

particular those with a high likelihood of being constrained to a peak hour commute. Among employed individuals, workers in education, health, public, retail, and private employees are the most affected by the policies.

Table 17: Changes in emissions under different policies

	Driving restriction	**Uniform toll**	**Variable toll**	**Personalized tolls**
Main emissions estimates				
ΔCO_2	-314	-330	-292	-328
%Far suburbs	88.8	85.3	86.7	76.5
%City center	7.31	9.94	8.16	15.1
%Close suburbs	3.92	4.75	5.1	8.44
ΔNO_X	-0.417	-0.417	-0.376	-0.418
ΔHC	-0.105	-0.112	-0.098	-0.112
ΔPM	-0.035	-0.034	-0.031	-0.035
ΔEq. NO_X	-0.945	-0.939	-0.849	-0.943
%Far suburbs	91.2	88.3	88.6	80
%City center	5.64	7.92	7.04	12.8
%Close suburbs	3.15	3.77	4.33	7.23
Alternative emissions estimates (Copert)				
ΔNO_X	-1.15	-1.21	-0.997	-1.12
ΔHC	-0.075	-0.083	-0.063	-0.077
ΔPM	-0.052	-0.054	-0.046	-0.051
ΔEq. NO_X	-1.93	-2.02	-1.69	-1.89
%Far suburbs	76.5	71	77.5	66.3
%City center	7.3	9.24	9.62	16
%Close suburbs	16.2	19.8	12.8	17.7
Relative importance of speed changes (Copert)				
NO_X	11	11.7	11	10.6
HC	20.4	20	23.2	21.5
PM	7.41	8.14	6.99	6.89
Eq. NO_X	9.56	10.3	9.41	9.1

Note: Δ emissions in tons. "Eq. NO_X" aggregates local pollutants into equivalent NO_X emissions. Relative importance in %.

Environmental impacts Table 17 presents the differences between policy instruments' efficiency in reducing carbon and local pollutant emissions. The four policies have roughly the same impact: they reduce carbon emissions by 292 to 330 tons of CO_2 emissions and local pollutant emissions decrease by 0.85 to 0.95 tons of equivalent NO_X emissions.[34] We decompose citywide emissions by computing the share emitted in each area of the city (close, far suburbs, and city center). Most of the gains come from traffic reduction in the far suburbs (between 76.5% and 88.8% for CO_2 emissions and 80% and 91.2% for local pollutants). Moreover, there is a large difference between the distribution of emissions gains between the personalized tolls and the other policy instruments. The personalized tolls generate more emissions reductions in the city center and the close suburbs since it allows individuals with long-distance commutes and inefficient public transport alternatives to drive more.

[34]We group NO_X, HC and PM into an equivalent NO_X emissions measure using the social costs as weights.

As a robustness check, we measure policy effects on emissions using our alternative estimates of car local pollutant emissions that depend on driving speeds (see Appendix C.4.2). We obtain a larger reduction in emissions, but the heterogeneity patterns across pollutants and policies remain identical. However, we find that the gains from the emissions reduction in the far suburbs are lower. By increasing speeds in the far suburbs, the emissions increase. Overall, the speed improvements are responsible for a small share of the total decrease in emissions, representing at most 23.2% for HC emission changes and 10.3% for equivalent NO_X emissions. In Appendix E.4.2, we analyze additional aggregate policy outcomes: the substitution patterns across transportation modes, travel time changes, speed changes, and the marginal costs of congestion. The marginal costs of congestion at peak hours are lower under the policies than initially, illustrating the importance of calculating equilibrium-consistent Pigouvian tolls.

5.6 Robustness and additional policy instruments

We also study welfare consequences of implementing policies across both periods and provide the results in Appendix E.5.1. Policy rankings remain the same, but the regulations generate larger consumer surplus losses for individuals since inter-temporal substitution is no longer possible. Consequently, we find a lower set of uniform and variable toll levels that are welfare-improving.

In Appendix E.5.2, we check the sensitivity of the results to changes in overcrowding levels on public transport. We consider the benchmark variable toll and two scenarios where overcrowding levels increase by 15% and 30%. These assumptions are rather extreme since public transport usage at peak hours increases by 5.9% in our benchmark. We find minimal changes in the transportation mode shares and equilibrium speeds. The total consumer surplus loss would be 9.2% and 18.4% higher in the two scenarios, but the policy would still be welfare-improving.

In Appendix E.5.3, we modify the schedule constraints by either allowing all individuals to choose their departure time or restricting them to fixed (but stochastic) departure times. The results show that removing schedule constraints lowers welfare gains from the policies, while the gains increase with more schedule constraints. The results may seem counter-intuitive, but reinforcing schedule constraints raises the toll revenue more than it decreases consumer surplus. We also notice that reinforcing schedule constraints implies a lower traffic reduction at peak hours but generates higher gains from emissions avoided. This is due to a smaller increase in the distance driven during off-peak hours.

Finally, in Appendix E.5.4, we check the sensitivity of the results to changes in the

unobserved part of traffic. As expected, if policies reduce unobserved traffic, we see lower consumer surplus losses and higher welfare gains. This suggests that our welfare gains estimates can be interpreted as lower bounds.

We choose to focus on three simple policy instruments that have been implemented in practice. However, our model could analyze more policies or changes in the transportation environment. We outline a few additional counterfactual results, where a detailed analysis is provided in Appendix F. In Appendix F.1, we study an auction resembling Shanghai's vehicle license regulation (see Li, 2018). Using this policy to achieve the same traffic reduction would not lead to welfare gains. In Appendix F.2, we compare the standard driving restrictions with two attribute-based policies: one banning older vehicles and one banning diesel cars. The diesel-based policy generates the highest welfare gains between the three policies. This is because diesel cars are owned by individuals more likely to pay the toll, raising the toll revenue. In Appendix F.3, we briefly study changes to public transport. Finally, additional scenarios are discussed in Appendix F.4.

6 Conclusion

Combining data from two waves of a detailed transportation survey, Google Directions, TomTom, and passenger flow in railway public transit, we estimate a nested logit model to represent the transportation decisions of individuals for their daily trips to work or places of study in the Paris metropolitan area. The estimated parameters confirm the importance of trip duration for individual decisions and reveal a large degree of schedule inflexibility, making it challenging to discourage individuals from driving at peak hours. We combine this transportation mode choice model with a flexible reduced-form congestion model that predicts how road speeds vary when the number of drivers changes in different parts of the city. We simulate the effects of simple transportation policies on welfare and its different components and find that all the regulations decrease consumer surplus. Simple driving restrictions decrease consumer surplus less than uniform road tolls because they force everyone to contribute to traffic reduction. Meanwhile, variable tolls are always the best policy instruments for welfare and consumer surplus because they target long distance drivers, which makes them efficient at reducing traffic. Variable tolls achieve 85.4% of the potential welfare gains from the optimal policies, suggesting it is an efficient policy instrument.

References

Agarwal, N. (2015). An empirical model of the medical match. *American Economic Review 105*(7), 1939–1978.

Akbar, P. and G. Duranton (2017). Measuring the cost of congestion in highly congested city: Bogota. *CAF – Working paper*.

Allen, T. and C. Arkolakis (2022). The Welfare Effects of Transportation Infrastructure Improvements. *The Review of Economic Studies*.

Almagro, M., F. Barbieri, J. C. Castillo, N. G. Hickok, and T. Salz (2024). Optimal urban transportation policy: Evidence from Chicago. Technical report, National Bureau of Economic Research.

Anderson, M. L. (2014). Subways, strikes, and slowdowns: The impacts of public transit on traffic congestion. *American Economic Review 104*(9), 2763–96.

Anderson, M. L. and L. W. Davis (2020). An empirical test of hypercongestion in highway bottlenecks. *Journal of Public Economics 187*, 104197.

Arnott, R., A. De Palma, and R. Lindsey (1990). Economics of a bottleneck. *Journal of Urban Economics 27*(1), 111–130.

Arnott, R., A. D. Palma, and R. Lindsey (1993). A structural model of peak-period congestion: A traffic bottleneck with elastic demand. *The American Economic Review 83*(1), 161–179.

Barahona, N., F. A. Gallego, and J.-P. Montero (2020). Vintage-specific driving restrictions. *The Review of Economic Studies 87*(4), 1646–1682.

Barwick, P. J., S. Li, A. Waxman, J. Wu, and T. Xia (2024). Efficiency and equity impacts of urban transportation policies with equilibrium sorting. *American Economic Review 114*(10), 3161–3205.

Basso, L. J. and H. E. Silva (2014, November). Efficiency and substitutability of transit subsidies and other urban transport policies. *American Economic Journal: Economic Policy 6*(4), 1–33.

Batarce, M. and M. Ivaldi (2014). Urban travel demand model with endogenous congestion. *Transportation Research Part A: Policy and Practice 59*, 331 – 345.

Bento, A., K. Roth, and A. R. Waxman (2020). Avoiding traffic congestion externalities? The value of urgency. Working paper, National Bureau of Economic Research.

Berry, S., J. Levinsohn, and A. Pakes (1995). Automobile Prices in Market Equilibrium. *Econometrica 60(4)*, 889–917.

Bou Sleiman, L. (2021). Are car-free centers detrimental to the periphery? Evidence from the pedestrianization of the Parisian riverbank. Technical report, Center for Research in Economics and Statistics.

Buchholz, N., L. Doval, J. Kastl, F. Matějka, and T. Salz (2024). The value of time: Evidence from auctioned cab rides. Technical report, National Bureau of Economic Research.

Cardell, N. S. (1997). Variance components structures for the extreme-value and logistic distributions with application to models of heterogeneity. *Econometric Theory 13*(2), 185–213.

Carstensen, C. L., M. J. Hansen, F. Iskhakov, J. Rust, and B. Schjerning (2022). A dynamic equilibrium model of commuting, residential and work location choices. *Topics in Urban Economics: Non-Market Valuation and Location*, 35.

Cook, C. and P. Z. Li (2023). Value pricing or lexus lanes? the distributional effects of dynamic tolling. Technical report.

COPERT methodology report (2020). Emep/eea air pollutant emission inventory guidebook 2019 - update oct. 2021. *EEA*.

Couture, V., G. Duranton, and M. A. Turner (2018). Speed. *Review of Economics and Statistics 100*(4), 725–739.

Crawford, G. S., R. Griffith, and A. Iaria (2021). A survey of preference estimation with unobserved choice set heterogeneity. *Journal of Econometrics 222*(1), 4–43.

Davis, L. W. (2008). The effect of driving restrictions on air quality in Mexico City. *Journal of Political Economy 116*(1), 38–81.

De Palma, A. and R. Lindsey (2006). Modelling and evaluation of road pricing in Paris. *Transport Policy 13*(2), 115–126.

De Palma, A., R. Lindsey, and G. Monchambert (2017). The economics of crowding in rail transit. *Journal of Urban Economics 101*, 106–122.

De Palma, A., F. Marchal, and Y. Nesterov (1997). Metropolis: Modular system for dynamic traffic simulation. *Transportation Research Record 1607*(1), 178–184.

Dubé, J.-P., J. T. Fox, and C.-L. Su (2012). Improving the numerical performance of static and dynamic aggregate discrete choice random coefficients demand estimation. *Econometrica 80*(5), 2231–2267.

Dubois, P., R. Griffith, and M. O'Connell (2018). The effects of banning advertising in junk food markets. *The Review of Economic Studies 85*(1), 396–436.

Engelson, L. and M. Fosgerau (2016). The cost of travel time variability: Three measures with properties. *Transportation Research Part B: Methodological 91*, 555–564.

Fajgelbaum, P. and C. Gaubert (2024). Optimal spatial policies. Technical report.

Galdon-Sanchez, J. E., R. Gil, F. Holub, and G. Uriz-Uharte (2021). Benefits and costs of driving restriction policies: The impact of Madrid Central on congestion, pollution and consumer spending. Working paper.

Gale, D. and H. Nikaido (1965). The jacobian matrix and global univalence of mappings. *Mathematische Annalen 159*(2), 81–93.

Gallego, F., J.-P. Montero, and C. Salas (2013). The effect of transport policies on car use: Evidence from Latin American cities. *Journal of Public Economics 107*, 47 – 62.

Geroliminis, N. and C. F. Daganzo (2008). Existence of urban-scale macroscopic fundamental diagrams: Some experimental findings. *Transportation Research Part B: Methodological 42*(9), 759 – 770.

Goldszmidt, A., J. A. List, R. D. Metcalfe, I. Muir, V. K. Smith, and J. Wang (2020). The value of time in the United States: Estimates from nationwide natural field experiments. Working paper, National Bureau of Economic Research.

Hall, J. D. (2018). Pareto improvements from lexus lanes: The effects of pricing a portion of the lanes on congested highways. *Journal of Public Economics 158*, 113–125.

Hall, J. D. (2021). Can tolling help everyone? estimating the aggregate and distributional consequences of congestion pricing. *Journal of the European Economic Association 19*(1), 441–474.

Hall, J. D. and I. Savage (2019). Tolling roads to improve reliability. *Journal of urban economics 113*, 103187.

Hang, D., D. McFadden, K. Train, and K. Wise (2016). Is vehicle depreciation a component of marginal travel cost?: A literature review and empirical analysis. *Journal of Transport Economics and Policy 50*(2), 132–150.

Hanna, R., G. Kreindler, and B. A. Olken (2017). Citywide effects of high-occupancy vehicle restrictions: Evidence from "three-in-one" in Jakarta. *Science 357*(6346), 89–93.

Hansen, B. E. (2014, 02). Nonparametric Sieve Regression: Least Squares, Averaging Least Squares, and Cross-Validation. In *The Oxford Handbook of Applied Nonparametric and Semiparametric Econometrics and Statistics*. Oxford University Press.

Haywood, L. and M. Koning (2015). The distribution of crowding costs in public transport: New evidence from Paris. *Transportation Research Part A: Policy and Practice 77*, 182–201.

Herzog, I. (2023). The city-wide effects of tolling downtown drivers: Evidence from London's congestion charge. Working papers.

Hintermann, B., B. M. Schoeman, J. Molloy, T. Götschli, A. Castro, C. Tchervenkov, U. Tomic, and K. W. Axhausen (2024). Pigovian transport pricing in practice. Technical report, WWZ Working Paper.

Javaudin, L. and A. de Palma (2024). Metropolis2: Bridging theory and simulation in agent-based transport modeling. Technical report, THEMA (THéorie Economique, Modélisation et Applications).

Jia, Z., C. Chen, B. Coifman, and P. Varaiya (2001). The PeMS algorithms for accurate, real-time estimates of g-factors and speeds from single-loop detectors. In *ITSC 2001. 2001 IEEE Intelligent Transportation Systems*, pp. 536–541. IEEE.

Kilani, M., S. Proost, and S. Van der Loo (2012). Tarification des transport individuels et collectifs à Paris. rapport final de recherche PREDIT.

Kilani, M., S. Proost, and S. Van der Loo (2014). Road pricing and public transport pricing reform in Paris: Complements or substitutes? *Economics of Transportation 3*(2), 175–187.

Koch, N., N. Ritter, A. Rohlf, and B. Thies (2023). Machine learning from big gps data about the heterogeneous costs of congestion. *Available at SSRN 4526796*.

Kreindler, G. (2024). Peak-hour road congestion pricing: Experimental evidence and equilibrium implications. *Econometrica 92*(4), 1233–1268.

Li, S. (2018). Better lucky than rich? Welfare analysis of automobile licence allocations in Beijing and Shanghai. *The Review of Economic Studies 85*(4), 2389–2428.

Loder, A., L. Ambühl, M. Menendez, and K. W. Axhausen (2017). Empirics of multi-modal traffic networks–using the 3D macroscopic fundamental diagram. *Transportation Research Part C: Emerging Technologies 82*, 88–101.

Mangrum, D. and A. Molnar (2020). The marginal congestion of a taxi in new york city. Technical report.

McFadden, D. (1974). The measurement of urban travel demand. *Journal of public economics 3*(4), 303–328.

Ostermeijer, F., H. Koster, L. Nunes, and J. van Ommeren (2022). Citywide parking policy and traffic: Evidence from amsterdam. *Journal of Urban Economics 128*, 103418.

Petrin, A. and K. Train (2010). A control function approach to endogeneity in consumer choice models. *Journal of marketing research 47*(1), 3–13.

Reynaert, M. and J. M. Sallee (2021). Who benefits when firms game corrective policies? *American Economic Journal: Economic Policy 13*(1), 372–412.

Rosaia, N. (2024). Competing platforms and transport equilibrium. Technical report.

Russo, A., M. W. Adler, F. Liberini, and J. N. van Ommeren (2021). Welfare losses of road congestion: Evidence from rome. *Regional Science and Urban Economics 89*, 103692.

Small, K. A. (2012). Valuation of travel time. *Economics of transportation 1*(1-2), 2–14.

Small, K. A., E. T. Verhoef, and R. Lindsey (2007). *The economics of urban transportation*. Routledge.

Small, K. A., C. Winston, and J. Yan (2005). Uncovering the distribution of motorists' preferences for travel time and reliability. *Econometrica 73*(4), 1367–1382.

Tarduno, M. (2022). For whom the bridge tolls: Congestion, air pollution, and second-best road pricing. Working papers.

Tassinari, F. (2024). Low emission zones and traffic congestion: evidence from Madrid Central. *Transportation Research Part A: Policy and Practice 185*, 104099.

Train, K. E. (2009). *Discrete choice methods with simulation*. Cambridge university press.

Tsivanidis, N. (2022). The aggregate and distributional effects of urban transit infrastructure: Evidence from Bogota's TransMilenio. Working paper.

Van Den Berg, V. and E. T. Verhoef (2011). Winning or losing from dynamic bottleneck congestion pricing?:

The distributional effects of road pricing with heterogeneity in values of time and schedule delay. *Journal of Public Economics 95*(7), 983–992.

Van Essen, H., L. Van Wijngaarden, A. Schroten, D. Sutter, C. Bieler, S. Maffii, M. Brambilla, D. Fiorello, F. Fermi, R. Parolin, et al. (2019). *Handbook on the external costs of transport, version 2019*. Number 18.4 K83. 131.

Yang, J., A.-O. Purevjav, and S. Li (2020). The marginal cost of traffic congestion and road pricing: Evidence from a natural experiment in Beijing. *American Economic Journal: Economic Policy 12*(1), 418–53.

Appendix (for online publication only)

A Index of mathematical notation

Table 18: Index of the mathematical notations used in the paper

Symbol	Description
	Indices
$n \in N$	Individual
$t \in T$	Departure time period
$t_1, t_2 \in T$	Peak hours and off-peak hours
$\mathcal{T}_n \subseteq T$	Set of all periods accessible by n
$\mathcal{T}_1, \mathcal{T}_2, \mathcal{T}_{12}$	Combinations of period available (peak hours, off-peak hours, both)
$j \in J$	Transportation mode
$\mathcal{J}_n \subseteq J$	Set of all transportation modes accessible by n
$\mathbf{d}$	Index for driving
$c, c(n) \in C$	Socio-professional category (for an individual n)
$\mathcal{C}$	Set of individuals with socio-professional category c
$k(n)$	Type of fuel of individual n's car
$a \in A$	Area (Highways, city center, ring roads, close suburbs, far suburbs)
$q \in Q$	Bernstein basis polynomials index
p	Polynomial index selected to minimise MSFE
$i \in I$	Observation of speed, occupancy rate and instruments
l	Public transit line
	Variables
X_{njt}	Mode and departure period characteristics
u_{njt}	Utility
ϵ_{njt}	Preference shock
$\tilde{\epsilon}_{njt}$	Period-specific preference shock
ζ_{nj}	Mode-specific preference shock
s_{njt}	Probability of choosing mode j and period t for individual n
D_{nj}	Expected utility of the mode (nest) j
ω_n	Weight of individual n
π_{nl}	Probability of being able to access combination of periods $\mathcal{T}_l$
k_n^a	Trip distance in area a for individual n
k_n	Trip distance for individual n
K_t^a	Kilometers driven from our sample in area a and time t
K_{0t}^a	Unobserved kilometers driven in area a and time t
f	Congestion technology
κ	Tuning parameter for the equilibrium speed algorithm
v_t^a	Speed in area a and period t
$\mathbf{v}$	Speed vector
$\mathbf{g}$	Contraction function
K	Lipschitz coefficient
$\phi_{c(n)}$	Probability of being schedule-constrained for individual n with SPC $c(n)$
$\pi_{c(n)}$	Probability to be constrained to peak hours for individual n with SPC $c(n)$, conditional on being schedule-constrained
$\boldsymbol{\pi}$	Vector of probabilities to be constrained to peak hours, conditional on being schedule-constrained
μ_c	Fraction of individuals with SPC c commuting during peak hours
y_{njt}	Indicator when mode j and period t are chosen by n
duration	Trip duration
ρ_{nt}	Individual and period-specific speed shocks
ν_i	Unobserved speed shock from road traffic data
τ_i	Occupancy rate for road traffic data
τ_t^a	Occupancy rate at period t in area a
B_q	Bernstein basis polynomials
$\hat{e}_i$	Prediction error for estimating congestion technology
h	Leverage value for estimating congestion technology
$\mathcal{B}$	Matrix containing Bernstein polynomials
$\mathbf{p}$	Vector of personalized tolls (for all individuals)
fc	Fuel consumption of car in litres/km
ft	CO_2 emissions per litre of fuel
CO_2	CO_2 emissions
c	Overcrowding level
Υ	Train capacity
ψ	Hourly number of passengers
ns	Number of train stations
$\xi_{n\mathbf{d}t}$	Mode-specific preference shock for driving (for the control function specification)
$\hat{\epsilon}$	Residual independent of duration (for the control function specification)
$Z_{n\mathbf{d}t}$	Instruments for the control function specification
η_{nt}	Duration shock after projecting duration on the instruments for the control function specification
M	Mean effective car length
h	Length of traffic sensor
W	Welfare = consumer surplus + toll revenue + value of emissions avoided
CS_n	Individual consumer surplus
ΔCS_n	Change in individual consumer surplus
ΔCS	Change in aggregate consumer surplus
N_d	Number of potential drivers
e_{nt}	Emissions per kilometer for individual n at period t
	Parameters
β_n	Mode and departure period characteristics
α_n	Sensitivity to trip cost
σ	Nest parameter
γ	Instrument parameter for the control function specification
θ	Set of parameters for demographic characteristics and the nest parameter
c_q^a	Coefficients of estimated congestion technology
ϕ^a	Scale parameter for the mapping between distance and road occupancy rate
$\sigma^{\hat{\epsilon}}$	Variance of $\hat{\epsilon}$ for the control function specification
$\boldsymbol{\lambda}$	Lagrange multipliers vector for road speed constraint
μ	Lagrange multiplier for total distance driven constraint

B Additional details on the model

B.1 Uniqueness of the model equilibrium case with one period and one area

We consider here the case of only one endogenous speed in the model. The equilibrium speed v is given by:

$$v - f\left(\sum_{n=1}^{N} \omega_n k_n s_{n\mathbf{d}}(v) + K_0\right) = 0$$

We define $g(v) := v - f\left(\sum_{n=1}^{N} \omega_n k_n s_{n\mathbf{d}}(v) + K_0\right)$. If the non-linear equation admits a solution, the solution is unique if the function is monotonic, i.e., if $|g'(v)| > 0 \; \forall v \in [\underline{v}, \overline{v}]$. The derivative is:

$$g'(v) = 1 - \underbrace{f'\left(\sum_{n=1}^{N} \omega_n k_n s_{n\mathbf{d}}(v) + K_0\right)}_{\leq 0} \times \sum_{n=1}^{N} \omega_n k_n \underbrace{\frac{\partial s_{n\mathbf{d}}(v)}{\partial v}}_{\geq 0},$$

which is always positive for $v \in [\underline{v}, \overline{v}]$ as long as the speed function is weakly decreasing in the occupancy rate and the probability of driving increases with speed. The assumption that K_0 is fixed is not crucial, the result is still valid as long as K_0 increases in speed.

B.2 Uniqueness of the model equilibrium case with multiple periods and one area

Now, we consider a model with a single area but multiple time periods which are substitutes for individuals. In this setting we have a system of T non-linear equations, $\mathbf{g}(\mathbf{v}) = 0$, where:

$$g_t(\mathbf{v}) := v_t - f\left(\sum_{n=1}^{N} \omega_n k_n s_{n\mathbf{d}t}(\mathbf{v}) + K_{0t}\right)$$

We want to show that the Jacobian of the system is a Leontieff matrix, i.e. the diagonal terms are positive and the off-diagonal terms are non-positive. First we compute the diagonal terms, which is the same as the previous derivative and is always greater than 1:

$$\frac{\partial g_t}{\partial v_t} = 1 - \underbrace{f'\left(\sum_{n=1}^{N} \omega_n k_n s_{n\mathbf{d}t}(\mathbf{v}) + K_{0t}\right)}_{\leq 0} \times \sum_{n=1}^{N} \underbrace{\omega_n k_n \frac{\partial s_{n\mathbf{d}t}(\mathbf{v})}{\partial v_t}}_{\geq 0}.$$

Then, we compute the off-diagonal terms, which are always negative due to the substitutability between the different time periods:

$$\frac{\partial g_t}{\partial v_{t'}} = \underbrace{-f'\left(\sum_{n=1}^{N}\omega_n k_n s_{n\mathbf{d}t}(\mathbf{v}) + K_{0t}\right)}_{\leq 0} \times \sum_{n=1}^{N} \underbrace{\omega_n k_n \frac{\partial s_{n\mathbf{d}t}(\mathbf{v})}{\partial v_{t'}}}_{\leq 0}.$$

The Jacobian of $\mathbf{g}(\mathbf{v})$ is thus a Leontieff matrix and by Theorem 5 from Gale and Nikaido (1965) it is a P-matrix. We then apply the main theorem of Gale and Nikaido (1965) (Theorem 1) that states that if the Jacobian of a system of non-linear equations is a P-matrix, the system has a unique solution in its bounded support.

C Additional information on data and sample construction

C.1 Information about the EGT data

The EGT constitutes publicly available data upon request on ADISP.[35] The 2010 survey was conducted from 2009 to 2011 between October and May, excluding school holidays. Due to the Covid crisis, the 2020 survey was stopped and only contains observations collected in 2019. Instead of relying on a trip diary where surveyed individuals self-report their trips, the EGT relies on pollsters visiting households and recording the information about trips from the previous day.

The 2010 survey initially contains 35,175 individuals and 124,262 trips, while the 2020 survey contains 10,470 individuals and 35,656 trips. In our final sample, we keep the first work or study-related trip. We drop trips if one of the variables we need for the model is missing (origin, destination, departure time, professional activity, residence location, or income class). We also drop trips using less common transportation modes that are not included in our choice set (e.g., taxis, boats). We also drop individuals who took their first work or study trip outside the morning time window (defined as 5:45-10:15 a.m.). Finally, we exclude trips with distances lower than 700 meters or higher than the 99$^{\text{th}}$ percentile of the distance distribution (72.7 km). Our final sample consists of 15,480 individuals, of which 12,359 are from the 2010 survey and 3,121 from the 2020 survey.

The 2010 survey maps the Paris region into a grid with 1,489,347 squares to locate individual trips' origins and destinations. The size of the square edge is 100 meters. Thus, we use the

[35] Enquête Globale Transport (EGT) - 2010 and Enquête Globale Transport (EGT) - 2020, DRIEA, ADISP, see http://www.progedo-adisp.fr/.

GPS coordinates of the centroids of the grid squares. This approach limits any trip geocoding inaccuracy to a maximum of 70 meters. The 2020 survey provides GPS coordinates with three decimals, equivalent to an accuracy of 100 meters. The 2010 survey divides the region into 112 zones, where 400 to 500 individuals are interviewed to have representativity at the zone level. However, such zones are not used in the 2020 survey, leading to some zones with very few trips. We regroup some zones according to the following algorithm. In each iteration, we aggregate the zone with the smallest number of observations with the neighboring zone with the smallest number of observations. We iterate until no zone has less than 50 departing trips (pooling both survey waves). After this process, the region is divided into 93 zones.

C.2 Details about TomTom and Google Directions queries

Google Directions and TomTom Directions APIs provide directions and expected travel times associated with a given origin and destination pair of GPS coordinates at a specified departure time. The data from these API services have been used previously in the transportation literature (see Kreindler, 2024, Hanna et al., 2017, Akbar and Duranton, 2017, Tarduno, 2022, and Almagro et al., 2024). The public transport queries were done on November 9th, 2023, setting all trips to take place on Tuesday, November 21st, 2023, with a departure time at 9:30 a.m. We use TomTom data for driving times because this API gives 2,500 free queries daily. The car queries were done in November 2023, setting the trips to take place on Thursday 19th of September 2024 at 8:30 a.m. for peak hours and 6:30 a.m. for off-peak hours. For both modes, we winsorize the top and bottom 1% of the implied speeds from the queries. This allows us to avoid situations where the returned information from the APIs implies unrealistic speeds for the transportation modes.

TomTom queries for future dates use historical trip data and not live conditions. We may worry that TomTom modified its prediction algorithm after Covid. To address concerns regarding the impact of Covid on traffic and TomTom's predictions, we examine a subsample of queries that we also did before Covid, in August 2019 (for the future date of 11/19/2020) with Google Directions. On average, TomTom predicts trip speeds 8.5% lower than Google. These differences translate into TomTom queries having on average speeds lower than Google by 4.2 km/hr. This suggests that the Covid crisis did not significantly decrease trip duration predictions. Furthermore, the mild difference between the two APIs is reassuring about TomTom's reliability.

C.3 Additional information on the workforce survey

The workforce survey data is publicly available upon request on ADISP.[36] For the 2019 data, the information regarding employment starting and ending time flexibility comes in the additional survey module "Organisation du travail et Aménagement du temps de travail". For the 2022 survey, the information regarding work-hour flexibility appears in the primary survey data. We consider individuals to have a flexible starting time if they state that they fully decide their working hours or if they can decide their working hours within a specific time interval. We regroup several SPCs to have larger samples to estimate the probability of being flexible by SPC. In particular, we regroup farmers with agricultural workers, public executives with professors and information professions, intermediate professions across public and private sectors, civil employees with police and army officers, qualified workers across public and private sectors, unqualified workers across public and private sectors, and entrepreneurs with self-employed. This procedure reduces the number of SPCs from 32 to 16. We also have students in high school or below and students in higher education, so our final sample contains 18 SPCs.

C.4 Car fuel consumption and emissions

C.4.1 Baseline estimation method

The EGT data does not include the information for car fuel consumption. Fuel consumption and car emissions are linked through the formula:

$$fc_n = \frac{\mathrm{CO}_{2n}}{ft_{k(n)}},$$

where fc_n is the fuel consumption (in liter/km) for car n and $ft_{k(n)}$ reflects the quantity of CO_2 emissions (in gram) in a liter of fuel k (diesel or gasoline).[37] We thus estimate CO_2 emissions as well as local pollutants of each car in the EGT data with a prediction model. We rely on additional car registration data in the Paris metropolitan area from 2003 to 2018 that contains the main car characteristics, sales, and the value of CO_2 emissions.[38] We complement the car registration data with local pollutant emissions data by car model from the UK Vehicle Certification Agency.[39] All the emissions datasets are from official car

[36] "Module ad-hoc de l'enquête Emploi: organisation du travail et aménagement du temps de travail - 2019, INSEE, ADISP" and "Enquête Emploi en continu (version FPR) - 2022, INSEE, ADISP".

[37] It is equal to 2,287 g/L for gasoline cars and 2,686 g/L for diesel cars.

[38] These are proprietary data obtained from the French Car Manufacturers syndicate "CCFA" (for 2003-2008) and AAAData (for 2009-2018).

[39] Source: https://carfueldata.vehicle-certification-agency.gov.uk/downloads/archive.aspx.

manufacturer tests and may be different from real-time driving emissions, as pointed out by Reynaert and Sallee (2021).

We first match the French car registration data to the UK emissions data so that we can weigh each car model in the UK emissions data by their sales in the Paris metropolitan area in the prediction model. We rely on the following matching algorithm. (1) We aggregate the French car data by the year, brand, model name, fuel type, and CO_2 emissions. (2) We merge it with the UK emissions data by year, brand, model name, and fuel type. Since there are several versions for the same combination in the UK data, we select the closest neighbor based on cylinder capacity and CO_2 emissions. We drop observations for which either the percentage difference in CO_2 emissions or cylinder capacity between the two matches is larger than 10%. (3) For each pollutant, we drop car models for which the emission levels are above the corresponding Euro standard limit. We also drop cars whose emissions are lower than a tenth of the Euro norm value.

For hybrid cars and other fuel types (liquefied petroleum or natural gas), we observe that the top-selling models in France are not available in the UK emissions data. Thus, we rely on another dataset that provides car emissions data from 2012 to 2015. The data comes from the French environment agency ("ADEME").[40] We follow the same procedure described above but allow for more discrepancy between the potential matches by dropping observations only if the percentage difference in CO_2 emissions or cylinder capacity between the two matches is above 30%. We also rely on these ADEME data to obtain estimates of PM emissions for gasoline cars since the UK data only provides PM emissions for diesel cars.

With the final sample of car models with their corresponding sales and emissions, we estimate the prediction model. We specify the emissions level of a specific pollutant as a linear function of the horsepower, a linear time trend, and dummies for the years of changes in the emissions standard of this particular pollutant. We allow all the parameters to be different by fuel type. Finally, we regress the logarithm of the emission levels on car characteristics for PM emissions because PM data has more outliers. All regressions are weighted by the car model sales in Paris metropolitan area. Given the small sample size (91 observations) for hybrid cars and other fuels, we do not estimate a prediction model and instead use the sales-weighted average emission levels by fuel type. Emissions for electric vehicles are set to zero for all pollutants. For some individuals in EGT data, the car vintage and horsepower is missing. In such cases, we attribute the average vintage or horsepower values in the EGT sample conditional on the fuel type.

[40] Source: https://www.data.gouv.fr/fr/datasets/emissions-de-co2-et-de-polluants-des-vehicules-commercialises-en-france/. We prefer not to use it for conventional fuel cars because the sample period is limited.

C.4.2 Alternative method for emissions estimates

We follow an alternative method to estimate car emissions of local pollutants that depend on driving speed. We rely on Copert emissions factors for cars published in the COPERT methodology report (2020).[41] This report provides emission functions that link a car's emissions of local pollutants with its speed depending on fuel type, emission standard, and car segment (in four categories: mini, small, medium, and large).

The EGT data does not directly provide the car segments, so we predict them from the fiscal horsepower. We use our proprietary car data containing the horsepower and segment from 2003 to 2018. We specify and estimate an ordered logit model to predict the car segment from its horsepower.

Finally, we assign cars to an emission standard from their vintage: cars with a vintage before 2000 are under Euro 2 standards. From 2000 to 2005 they are under Euro 3 standards. From 2005 onward, they are subject to Euro 4 standards. Since both the Copert emissions data and the EGT data includes information on fuel types, we can directly match survey cars to the correct set of emission function parameters by fuel type. The Copert methodology also assumes electric vehicles do not emit pollutants.

Table 19 compares average observed and predicted emissions under both prediction methods. Our baseline method finds similar average CO_2 values to the observed ones. We find higher values for PM than observed, but this might be because the observations are for much more recent car models than in the EGT data. However, our baseline method and the Copert methodology provide similar estimates. Our method predicts lower NO_X than observed, while the alternative Copert method predicts higher values. It is the reverse for HC. Despite some differences at the pollutant level related to the emission prediction method, we do not think the benefits of reducing emissions will drastically differ.

[41] See https://www.emisia.com/utilities/copert/documentation/.

Table 19: Fit of the prediction models and comparison between average observed and predicted emissions

Pollutant	R^2	Gasoline			Diesel		
		Observed	Predicted	Predicted Copert	Observed	Predicted	Predicted Copert
CO_2	0.84	203	167		171	148	
NO_X	0.91	100	53	87.8	369	278	568
HC	0.47	100	81.1	29.3	110	36	14.2
CO	0.35	617	525	441	223	223	104
PM	0.9	0.4	2.2	1.9	3.2	23.9	30.1

Note: We obtain the same R^2 for diesel and gasoline since the estimation is performed on pooled data. "Observed" emissions are calculated on the CCFA data for the year 2003 (the average car vintage in the EGT sample) except for PM. We use the earliest years with available data for PM emissions: 2012 for gasoline and 2005 for diesel. For the Copert methodology, we assume a 45 km/hr speed. CO_2 in g/km. NO_X, HC, and PM in mg/km. All predicted values correspond to the weighted average of the final sample's observations from the 2010 survey.

C.5 Cost estimation

C.5.1 Driving costs for cars and motorcycles

We estimate the cost of using a car or a motorcycle by combining the trip distance from the itinerary provided by TomTom, estimates of the fuel consumption of household vehicles, and average fuel prices in 2011 from the National Survey Institute ("Insee").[42] For motorcycles, we assign the average fuel consumption by the number of cylinders, which is the only motorcycle characteristic we observe in the EGT data.[43] When a household has multiple vehicles, we assume the trip uses the most fuel-efficient one. We also assume each individual pays the total cost of the trip, regardless of the number of passengers.

Both for cars and motorcycles, we estimate additional costs related to vehicle depreciation, insurance, and maintenance. To decide which element to include and how, we follow the methodology from the American Automobile Association (AAA), which produces annual reports on the cost of driving for several countries, including France. While their estimates have been directly used in other studies (Almagro et al., 2024), we leverage the detailed information we have on individuals' cars, costs, and driving intensity to build our own estimates. This allows us to have more precise costs that are heterogeneous across individuals. From the list of non-fuel-related driving expenses suggested by the AAA, we account for car depreciation, maintenance, and insurance.[44] To estimate the depreciation cost, we exploit the same data used for emissions predictions to estimate the price of each car in the EGT sample. For cars, we follow Hang et al. (2016) and assume a 12-year, uniform depreciation

[42]Source for fuel prices: https://www.prix-carburants.developpement-durable.gouv.fr/petrole/se_cons_fr.htm.

[43]Source: French Energy Agency ("ADEME"). See https://www.statistiques.developpement-durable.gouv.fr/les-deux-roues-motorises-au-1er-janvier-2012.

[44]In the EGT, individuals report their "additional expenses including maintenance and insurance".

rate to obtain the yearly depreciation cost. For motorcycles, we assume a price of €1,500 and the same depreciation length and rate.[45] For the yearly maintenance and insurance costs, the EGT only provides six cost intervals at the household fleet level. We divide the values of the middle of the intervals by the size of the household's vehicle fleet.[46]

The EGT data contains the annual number of kilometers driven. To control for misreporting and extreme values, we assign each household to three possible values for cars: 7,500 km driven if the reported distance is below that value, 12,000 km if the reported distance is between 7,500 km and 17,500 km, and 17,500 km if the reported distance is larger than 17,500 km.[47] Since the average reported yearly distance driven with motorcycles is roughly half the distance driven with cars, we divide these thresholds by two for motorcycles. Finally, we divide the sum of the yearly depreciation, maintenance, and insurance costs by the assigned number of kilometers driven to obtain a cost per kilometer. We winsorize the top and bottom one percent of this cost per kilometer distribution. We obtain an average cost of depreciation, maintenance and insurance of €0.22 for 2010 and €0.27 for 2020. Finally, we obtain the total cost of driving by adding the fuel costs. We find an average cost per-kilometer of €0.31 in 2010 and €0.34 in 2020. For comparison, the 2010 AAA report finds a per-kilometer cost before taxes of €0.45 for gasoline cars. Our estimate is slightly below the AAA estimate because we do not include potential loan repayments and parking costs (we do not have the information in the EGT data). Our average is also likely to be lower than the national average since Parisians tend to drive smaller cars that are cheaper.

C.5.2 Public transport cost

The public transport network in Paris is operated by two companies: "RATP" mainly covers public transport inside Paris and close suburbs, while "SNCF" operates trains connecting Paris to suburban areas. During the period of the 2010 survey, the RATP pricing system relies on five pricing zones of trip origin and destination. We use the prices stated in the price guide of RATP for July 2011 and April 2020.[48] The ticket price using the SNCF network

[45]The average ownership length of a motorcycle in France is 12.2 years: https://www.onisr.securite-routiere.gouv.fr/etudes-et-recherches/vehicules/parc-des-vehicules/le-parc-deux-roues-motorises-des-menages#:~:text=L'%C3%A2ge%20moyen%20du%20parc,6%2C5%20ans%20en%202020.

[46]For households than own both cars and motorcycles, we count motorcycles as 0.8 cars, the value of the ratio between the reported cost for owners of a single motorcycle and a single car.

[47]In the 2010 report for France, the AAA uses an average of 9,363 km per year for conventional fuel cars. See https://www.automobile-club.org/actualites/la-vie-de-l-aca/budget-de-l-automobiliste-juin-2010.

[48]Source: "Guide tarifaire", July 2011, https://www.slideshare.net/quoimaligne/guide-tarifaire-ratp-sncf-ile-de-france-2011 and April 2020, https://www.iledefrance-mobilites.fr/medias/portail-idfm/9ae5b132-467f-404c-ac33-a6a5ffa679a8_16340_IDFM_guide_tarifaire_10x21_WEB.pdf.

depends on the exact stations of origin and destination rather than zones. Since there is no exhaustive data on the prices for all combinations of origin and destination train stations, we rely on a sample of ticket prices for 36 origin and destination pairs and estimate the train ticket price as a square function of the distance between stations. This regression has a good fit with an R^2 of 0.77. We use this function to predict prices for all origin-destinations pairs in the SNCF network. For 186 individuals, Google Directions API does not provide a public transport route, yet they report using public transport. We impute the driving distance to compute their train ticket cost and use their reported travel times in the survey. For all train tickets, if the distance is larger than the maximum trip distance in the sample of SNCF tickets, we cap the distance to be the same as the maximum of the ticket sample (41 km). We thus avoid predicting the ticket price for distances that lie outside the ticket sample used for estimation.

For individuals with a public transport subscription, we estimate a trip average cost by dividing the daily price of the subscription (obtained by dividing the subscription price by the relevant number of working days after accounting for holidays and bank holidays: 224) by two, which is the average number of trips taken in a day conditional on using public transport. For individuals without a subscription, missing information about their subscription coverage, or taking a trip outside their subscription coverage, we assume they pay the regular ticket price. The survey includes information on whether individuals can buy subsidized or reduced-price tickets, we use this information when computing the cost of public transport without subscription. Some itineraries require layovers between different services. Without a subscription, layovers between bus and tramway, as well as those between subway and commuter trains are included within a single ticket. Meanwhile, layovers such as bus-subway require the payment of an additional ticket. We account for these differences in our cost imputation.

In our final sample, 40.5% have a public transport subscription. Conditional on using public transport the share increases to 86%. There could be a selection effect on the estimation stage due to assigning to individuals that do not use public transport a higher cost of public transport than public transport users because of the subscription. We avoid this issue by predicting a cost of public transport net of the potential subscription rebate. For this, we estimate the price with potential subscription from the individual ticket price and some individual characteristics on the subsample of public transport users. The individual characteristics are age and distance, which are likely to affect the subscription rebate value and the likelihood of holding a subscription. We consider the deciles of age and trip distance distributions. The average public transport cost with subscription is €1.75 while the average cost without subscription is €3.21.

C.6 Public transport overcrowding

We compute a line-level measure of overcrowding in public railway transport. To do so, we rely on data provided by SNCF and RATP on the number of passengers at the metro or train station level. We use data for 2015, the oldest data available, and consider only the urban railway network, where overcrowding is the most problematic. The data only records validations from passengers that use an electronic metro card; there is no exhaustive data on passengers using tickets. Estimates suggest that the electronic validations represent two-thirds of the traffic for 2016; we expect the share to be even higher during morning peak and off-peak hours.[49] We exploit the variation in traffic between peak and off-peak hours across metro lines to estimate the role of overcrowding in transportation decisions. As long as traffic is homogeneously underestimated over the network and periods, omitting a portion of the traffic is not a major problem.

The data we use is composed of two separate datasets. The first contains daily entry flows of passengers at the railway station level. The second dataset contains "hourly profiles" at the station level: the distribution of validations (in %) across hours for different periods (business days outside holidays, business days during school holidays, and weekends).[50] By combining these datasets, we obtain daily and hourly estimates of the number of passengers in each metro station for regular business days. We exclude weekends, school holidays, public holidays, and two dates with a relatively low total number of entries.[51] Finally, we average traffic levels over 172 days. We use the passenger flow between 7:00-8:59 a.m. to represent peak hours and 6:00-6.59 a.m. for off-peak hours. We observe the number of passengers entering each station, but not the line they take. Thus, we allocate passengers to metro lines proportionally, using the annual traffic levels by lines as weights.

We also use schedule data that provides frequencies of trains at the station level for the second semester of 2015.[52] We count the average number of scheduled trains for each line (and direction) and for each hour. Additionally, we gather information about the passenger capacity of the train models used on each line.[53] The passenger capacity represents the number of passengers a train can carry, assuming four passengers per square meter. We

[49] See https://www.iledefrance-mobilites.fr/usages-et-usagers-des-titres-de-transport.

[50] We use the average profiles for the business days outside holidays for the second semester of 2015 since we noticed some problems with the data from the first semester 2015: the percentages did not sum to 100% for 20 stations.

[51] These record total daily traffic levels below a million, while the average is 7.5 million according to the official figures of the RATP. We interpreted this low number of passengers as indicating the occurrence of a strike.

[52] "General Traffic Feed Specification", see: https://transitfeeds.com/l/162-paris-france.

[53] We rely on Wikipedia and internal reports from the transport organization in the Paris area "STIF" containing information about the characteristics of the fleet of trains.

compute the total railway line capacity Υ_{lt} by multiplying the train's physical capacity by the number of trains per hour. Finally, the overcrowding level c_{lt} for line l, at period t is:

$$c_{lt} = \frac{\psi_{lt}}{2 \times \Upsilon_{lt} \times ns_l},$$

where ψ_{lt} is the hourly number of passengers in line l at time period t and ns_l is the number of stations. Since there are two directions, we multiply the total line capacity by two and use the total number of passengers going in both directions. We assume a uniform distribution of passengers entering and exiting each line and thus divide the measurement by each line's number of stations. Finally, we obtain individual overcrowding levels by weighting the overcrowding level of each line used in a trip by the time spent in that line. Finally, we provide in Table 20 the estimates of the overcrowding levels in the different metro and train lines. On average, we estimate the overcrowding level to be 0.73 at off-peak hours and 1.8 at peak hours. But these averages hide substantial heterogeneity across lines that provides key variation for estimating the sensitivity to overcrowding in public transport.

Table 20: Estimates of overcrowding levels in the railway public transit

Metro			**Suburb trains**		
Line	**Off-peak**	**Peak**	**Line**	**Off-peak**	**Peak**
1	0.27	1.21	A	0.78	2.08
2	0.29	1.31	B	0.52	1.12
3	0.35	1.58	C	0.39	1.2
3B	0.17	0.92	D	0.81	1.52
4	0.61	1.95	E	0.56	1
5	0.75	2.14	H	0.79	0.95
6	0.24	1.28	J	0.36	0.57
7	0.53	1.54	K	4.42	7.3
7B	0.2	1.06	L	0.7	2.19
8	0.26	1.17	N	0.79	1.42
9	0.28	1.12	P	2.17	3.63
10	0.19	1.32	R	0.8	1.1
11	0.56	2.08	U	2.08	4.59
12	0.31	1.63			
13	0.54	1.8			
14	0.43	1.46			
Average	0.37	1.47		1.17	2.2

C.7 Additional descriptive statistics

Table 21 provides a comparison between the durations and costs for the transportation modes available to each individual, in the final sample. Taking the car is the fastest option available to the largest fraction of individuals. However, the relatively low initial shares suggest that the high monetary cost dissuades many from choosing it. Public transport is not, on average, the fastest nor the cheapest alternative, yet it is the most used mode in both periods. The

public transport cost does not increase much with distance while the car or motorcycle costs linearly increase with distance. For this reason, the maximum price of public transport is lower than the maximum car and motorcycle costs.

The last panel of Table 21 presents the share of individuals with access to each transportation mode and the share of trips done with each one of the five modes, in each period. Across modes and periods, the differences between both years are at most two percentage points, confirming the similarity in transportation patterns across surveys. Car usage at peak hours in the 2020 survey has the largest decrease with respect to 2010, with a 2.47 percentage point decrease. This small reduction seems to go towards an increase in public transport and bicycle usage (1.39 and 0.66 percentage points respectively). This change could also be explained by a decrease of 4.88 percentage points on car availability between the two surveys.

Table 21: Average duration, cost and availability by transportation mode

Variable	**Mean**	**Median**	**Std. dev.**	**Min**	**Max**
Duration					
Bicycle	48.7	35.6	40.4	5.1	150
Public transport	41.9	37.8	23.6	2.58	266
Motorcycle	18.1	16.2	12.3	1.63	69.8
Walk	59.9	49	40	12.4	170
Car, peak	26.9	20.9	21.8	1.08	111
Car, non-peak	20.2	16.2	15.9	1.03	108
Cost					
Bicycle	0.68	0	0.8	0	1.74
Public transport	1.77	1.64	0.73	0.43	7.69
Motorcycle	3.3	2.14	3.48	0.1	26.9
Car	4.03	2.49	4.27	0.12	41.9
	Mode availability			**Shares**	
	2010	2020		2010	2020
Peak					
Bicycle	78.8	79.4		1.59	2.25
Public transport	86.1	87		34	35.4
Motorcycle	12.9	9.48		1.35	1.05
Walk	53.1	54.7		15.2	15.2
Car	78.8	73.9		24.4	21.9
Off-peak					
Bicycle	78.8	79.4		0.446	0.71
Public transport	86.1	87		11.7	13
Motorcycle	12.9	9.48		0.644	0.605
Walk	53.1	54.7		2.11	2.9
Car	78.8	73.9		8.46	6.97

Note: Durations in minutes, costs in €. Mode availability and initial shares in %. All statistics computed using survey weights.

D Additional estimation results

D.1 Control function approach for car travel times

There might be some endogeneity problems for individual trip durations. To formalize this issue, we consider that the source of endogeneity is due to unobservable individual preferences for driving that might be correlated to trip duration. For instance, if individuals like driving, they may locate in an area where the travel time is low. This is modeled as follows:

$$u_{n\mathbf{d}t} = \tilde{\beta}'_n \tilde{X}_{n\mathbf{d}t} + \beta_n^{\text{duration}} \text{duration}_{n\mathbf{d}t} + \xi_{n\mathbf{d}t} + \epsilon_{n\mathbf{d}t}$$

where $cov(\boldsymbol{\xi}_{\mathbf{d}t}, \mathbf{duration}_{\mathbf{d}t}) \neq 0$, $cov(\tilde{\mathbf{X}}_{\mathbf{d}t}, \boldsymbol{\xi}_{\mathbf{d}t}) = 0$ and $cov(\boldsymbol{\epsilon}_{\mathbf{d}t}, \mathbf{duration}_{\mathbf{d}t}) = 0$, $cov(\boldsymbol{\epsilon}_{\mathbf{d}t}, \boldsymbol{\xi}_{\mathbf{d}t}) = 0$. In short, only car trip duration is endogenous and the preference shock for driving can be decomposed as an exogenous iid term and another term that generates the correlation with duration.

We specify a control function as a linear function of a matrix of instruments Z. This matrix includes excluded instruments and individual characteristics which are also used to parametrize the preference heterogeneity. We rely on two sets of excluded instruments. First, we construct functions of other individual trip characteristics (other than duration), and choice sets at the origin or destination of an individual. The intuition is that choice set and trip characteristics should affect other individual decisions to drive, and thus, equilibrium speeds. But these variables should not affect individuals directly because what matters for an individual decision is only his own choice set and his own trip characteristics. We construct six instruments for the origin and the destination of an individual. These variables are the sum of other individual costs, overcrowding levels at peak hours and off-peak hours, trip distances, numbers of alternatives in the choice set and the share of other individuals with a car. The free-flow car trip duration (measured as trip duration at 3 a.m.) is the second set of excluded instruments. Finally, we use individual characteristics that shift preferences (income dummies, age dummies, a local linear function of distance and the socio-professional activity).

We use the same instruments for the duration at peak and off-peak hours. Formally, we have:

$$\text{duration}_{n\mathbf{d}t} = Z_{n\mathbf{d}t}\gamma_t + \eta_{n\mathbf{d}t}.$$

The important assumption is that $cov(\xi_{\mathbf{d}t}|Z_{\mathbf{d}t}) \neq 0$ but $cov(\eta_{\mathbf{d}t}, \xi_{\mathbf{d}t}) = 0$. In economic terms, the assumption is that once we condition the duration of individual trip on the instruments, the residual is uncorrelated with unobserved individual preferences. And we can express the

unobserved individual preference term as:

$$\xi_{n\mathbf{d}t} = \rho_t \eta_{n\mathbf{d}t} + \hat{\epsilon}_{n\mathbf{d}t},$$

with $cov(\hat{\epsilon}_{\mathbf{d}t}, \text{duration}_{\mathbf{d}t}) = 0$. Then, we can re-write the utility function as:

$$u_{n\mathbf{d}t} = \tilde{\beta}_n' \tilde{X}_{n\mathbf{d}t} + \beta_n^{\text{duration}} \text{duration}_{n\mathbf{d}t} + \rho_t \eta_{n\mathbf{d}t} + \hat{\epsilon}_{n\mathbf{d}t} + \epsilon_{n\mathbf{d}t}$$

The standard assumption would be to consider the joint distribution of the error terms to be normal: $(\eta_{\mathbf{d}t}, \xi_{\mathbf{d}t}) \sim N(0, \Sigma)$ so that $\hat{\epsilon} \sim N(0, \sigma^{\hat{\epsilon}})$. As it has been done previously in the applied literature, we set $\sigma^{\hat{\epsilon}} = 0$ and ignore $\hat{\epsilon}_{n\mathbf{d}t}$.

Table 22 provides the results of the regressions of driving durations at peak and off-peak hours on the instruments. The R^2 are very high, indicating strong predicting power of the instruments.

Table 22: First-stage regressions of durations on the instruments

	Peak hours		Off-peak hours	
	Parameter	**Std. error**	**Parameter**	**Std. error**
Intercept	20.9**	(2.19)	9.52**	(1.02)
Income ∈ [800, 1,200[	-0.057	(0.187)	-0.044	(0.09)
Income ∈ [1,200, 1,600[	-0.097	(0.187)	-0.059	(0.091)
Income ∈ [1,600, 2,000[	-0.157	(0.19)	-0.02	(0.094)
Income ∈ [2,000, 2,400[	0.067	(0.196)	-0.012	(0.099)
Income ∈ [2,400, 3,000[	-0.29	(0.212)	-0.199†	(0.108)
Income ∈ [3,000, 3,500[	-0.329	(0.216)	-0.238*	(0.107)
Income ∈ [3,500, 4,500[	-0.505*	(0.223)	-0.337**	(0.111)
Income ≥ 4,500	-0.185	(0.3)	-0.158	(0.153)
Age ∈]18, 30]	-0.929*	(0.379)	-0.486*	(0.195)
Age ∈]30, 40]	-1.08*	(0.427)	-0.693**	(0.219)
Age ∈]40, 50]	-1.26**	(0.425)	-0.808**	(0.218)
Age ∈]50, 60]	-1.21**	(0.428)	-0.718**	(0.22)
Age > 60	-1.45**	(0.52)	-0.971**	(0.261)
Distance	1.48**	(0.204)	-0.796**	(0.103)
(Dist-d_2) × (dist≥d_2)	0.876**	(0.277)	2.43**	(0.136)
(Dist-d_3) × (dist≥d_3)	-3.89**	(0.49)	-0.848**	(0.293)
(Dist-d_4) × (dist≥d_4)	-0.272	(1.01)	0.954	(0.826)
Craftspeople	-0.134	(1.85)	0.125	(0.882)
Shopkeepers	0.279	(0.906)	0.13	(0.435)
Entrepreneurs, self-employed	0.001	(0.801)	-0.052	(0.399)
Public executives	-0.262	(0.712)	-0.109	(0.343)
Private executives	0.363	(0.706)	0.079	(0.339)
Education, health	-0.111	(0.705)	0.097	(0.339)
Administrative professions	1.23†	(0.72)	0.561	(0.35)
Technicians	0.602	(0.743)	0.326	(0.361)
First-line supervisors	1.08	(0.848)	0.335	(0.413)
Public employees	0.194	(0.725)	0.231	(0.351)
Private employees	0.86	(0.73)	0.386	(0.356)
Retail employees	-0.528	(0.87)	-0.328	(0.43)
Services	1.4†	(0.786)	0.704†	(0.38)
Qualified workers	0.192	(0.727)	0.196	(0.35)
Unqualified workers	0.331	(0.816)	0.244	(0.379)
Students ≤ high school	-0.839	(0.802)	-0.381	(0.393)
Students in higher education	-0.397	(0.741)	-0.4	(0.364)
Sum of costs, at origin	0.261**	(0.061)	0.167**	(0.033)
Sum of overcrowding levels, peak, at origin	-2.19**	(0.454)	-2.08**	(0.237)
Sum of overcrowding levels, off-peak, at origin	2.45**	(0.612)	2.28**	(0.318)
Sum of distances, at origin	-4.44**	(0.581)	-1.36**	(0.29)
Sum of number of alternatives, at origin	-3.35**	(0.354)	-1.67**	(0.165)
Car ownership rate, at origin	15**	(0.813)	6.69**	(0.399)
Sum of costs, at destination	0.783**	(0.061)	0.375**	(0.028)
Sum of overcrowding levels, peak, at destination	10.9**	(0.483)	5.23**	(0.241)
Sum of overcrowding levels, off-peak, at destination	-15.4**	(0.783)	-7.16**	(0.384)
Sum of distances, at destination	-6.33**	(0.619)	-3.15**	(0.284)
Sum of number of alternatives, at destination	0.27	(0.337)	0.077	(0.153)
Car ownership rate, at destination	-18.2**	(1.01)	-8.02**	(0.49)
Free-flow duration	1.54**	(0.016)	1.25**	(0.009)
R^2	0.948		0.975	

*Note: The reference categories are individuals with age < 18, with an income below €800 and farmers. Duration and free-flow duration measured in 10 minutes. Significance levels: **: 1%, *: 5%, †: 10%.*

D.2 Robustness checks for the transportation mode choice model

We analyze the robustness of our estimates to several model assumptions. Table 23 provides the estimates of the average utility parameters, while Table 24 presents the implied values of travel time.

Weather controls We use historical hourly data from OpenWeather for the city of Paris to control for the possible role of weather on individual choices.[54] First, we match the OpenWeather data to the exact departure hour and date provided in the survey. Then, based on the distribution of temperatures in our sample, we construct temperature quintiles. For rain and snow, we create four categories based on the levels (in millimeter per hour): 0, less than 0.3, between 0.3 and 0.8, and more than 0.8. The weather dummies are then interacted with the bicycle and walk alternative constants, as these modes are the most susceptible to being affected by the weather shocks. The inclusion of weather controls has no significant impact on the average sensitivities to duration and cost and almost no impact on the distribution of valuations of travel time.

Travel time reliability Recent transportation literature has focused on the importance of the reliability of travel time for individual transportation decisions (Small et al., 2005, Engelson and Fosgerau, 2016, Hall and Savage, 2019, Bento et al., 2020). We study the role of preferences for travel time reliability in our model and how including this factor affects our estimates. We build a measure of travel time reliability by collecting real-time traffic data from TomTom for all trips in our sample that have car access, for every weekday between February 26$^{\text{th}}$, 2024, and March 22$^{\text{nd}}$, 2024. We query trip itinerary and durations at 6:30 a.m. (to represent off-peak hours) and at 8:30 a.m. (for peak hours). We construct a proxy of reliability by taking the standard deviation of the durations for each trip at each period.[55]. As seen from the estimation results, the average utility parameters remain close to the benchmark, and the distribution of the values of travel time is marginally lower.

Alternative model assumptions First, we consider a model where we modify the nest structure by allowing individuals to choose first between transportation modes and then peak and off-peak hours. This model allows for correlation in the preference shocks across departure times for a given mode. However, column (4) of Table 23 shows a high value for

[54]Source for weather data: https://openweathermap.org/.

[55]We also consider another reliability measure given by the difference between the 80$^{\text{th}}$ and 50$^{\text{th}}$ percentiles as suggested by Small et al. (2005). We choose to rely on the standard deviation because we obtain a better fit

the nest parameter (σ), almost equal to 1, indicating that the options within nests are almost independent and suggesting that our nesting structure is more relevant.

Then we consider two specifications were we modify our assumptions regarding the cost of the trip. In column (5) of Table 23, we analyze the effect of not including the additional cost per km driven (depreciation, maintenance, and insurance). We find larger average sensitivities to cost, which translate into a large decrease in the mean VOT, reaching only €3.8. In the second specification, column (6) of Table 23, we do not perform the correction for the cost of public transport subscriptions. This implies that individuals without subscription pay the full price, while individuals with subscription pay the average trip cost of their subscription. We find a large decrease in the average sensitivity of cost, leading to a large increase in the distribution of valuation of travel time, with a mean VOT of €326. Such high VOT values are unrealistic, supporting the relevance of our correction

Finally, we consider two possible changes to our choice set definition. First, we allow every individual to drive, even those who do not own a car. For those without a car, we attribute the average car cost in the sample. Then, we query the TomTom service for those trips for the travel times, as with the rest of the sample. As expected, adding a unavailable alternative changes the results by lowering the average utility of driving. As seen in column (7) of Table 23, this change leads to small changes in the average duration cost sensitivities. These changes lead to a small decrease in the average VOT, as seen in Table 24. The second change in the choice set definition corresponds to allowing only individuals who have a bicycle or a bike-sharing pass to use this mode. We see very small changes, in particular, the mean valuation for bicycling marginally increases. The distribution of valuations of travel time remains increases with respect to our benchmark and there is a significant increase in the nest parameter, implying less correlation between periods.

Table 23: Average estimated parameters under alternative model specifications

Coefficients	(1)		(2)		(3)		(4)		(5)		(6)		(7)		(8)	
Duration	-0.61**	(0.014)	-0.611**	(0.014)	-0.609**	(0.014)	-0.611**	(0.02)	-0.618**	(0.013)	-0.591**	(0.013)	-0.5910	(0.013)	-0.6140	(0.014)
Cost	-0.312**	(0.016)	-0.312**	(0.016)	-0.327**	(0.017)	-0.313**	(0.017)	-1.01**	(0.043)	-0.121**	(0.012)	-0.3290	(0.016)	-0.2930	(0.016)
Bicycle, peak	-3.47**	(0.075)	-3.47**	(0.075)	-3.44**	(0.075)	-3.47**	(0.1)	-3.3**	(0.077)	-3.53**	(0.077)	-3.410	(0.074)	-3.340	(0.077)
Public transport, peak	-1**	(0.062)	-0.897**	(0.091)	-0.973**	(0.062)	-0.995**	(0.062)	-0.332**	(0.079)	-1.21**	(0.063)	-0.9040	(0.059)	-0.9880	(0.062)
Motorcycle, peak	-3.43**	(0.112)	-3.33**	(0.13)	-3.33**	(0.112)	-3.46**	(0.133)	-3.49**	(0.114)	-3.65**	(0.117)	-3.440	(0.109)	-3.420	(0.113)
Car, peak	-2.68**	(0.527)	-2.59**	(0.527)	-2.78**	(0.535)	-2.68**	(0.529)	-3.3**	(0.545)	-2.99**	(0.54)	-3.810	(0.457)	-2.550	(0.517)
Car, off-peak	-3.88**	(0.544)	-3.79**	(0.543)	-3.83**	(0.552)	-4.02**	(0.534)	-4.62**	(0.56)	-4.3**	(0.593)	-5.030	(0.474)	-3.850	(0.541)
Public transport, off-peak	-1.9**	(0.174)	-1.78**	(0.181)	-1.8**	(0.172)	-2.07**	(0.085)	-1.16**	(0.154)	-2.22**	(0.296)	-1.760	(0.148)	-1.980	(0.202)
Walking, off-peak	-0.737**	(0.154)	-0.743**	(0.152)	-0.669**	(0.148)	-0.888**	(0.092)	-0.86**	(0.151)	-0.847**	(0.255)	-0.7480	(0.139)	-0.8260	(0.181)
Bicycle, off-peak	-4.15**	(0.16)	-4.17**	(0.159)	-4.07**	(0.156)	-4.27**	(0.149)	-4.08**	(0.16)	-4.32**	(0.242)	-4.080	(0.148)	-4.060	(0.176)
Motorcycle, off-peak	-3.73**	(0.162)	-3.62**	(0.173)	-3.6**	(0.157)	-3.83**	(0.161)	-3.8**	(0.159)	-4.02**	(0.226)	-3.740	(0.153)	-3.760	(0.178)
No. layovers in PT	-0.486**	(0.041)	-0.485**	(0.041)	-0.463**	(0.041)	-0.484**	(0.042)	-0.252**	(0.039)	-0.265**	(0.038)	-0.5110	(0.038)	-0.4110	(0.039)
Railway only	0.015	(0.063)	0.014	(0.063)	0.025	(0.063)	0.014	(0.064)	0.131*	(0.065)	0.107†	(0.063)	-0.0290	(0.06)	0.0420	(0.063)
PT overcrowding	-0.066*	(0.033)	-0.066*	(0.033)	-0.061†	(0.032)	-0.065†	(0.034)	0.06†	(0.034)	-0.004	(0.034)	-0.050	(0.031)	-0.0680	(0.033)
σ	0.816**	(0.16)	0.807**	(0.153)	0.762**	(0.159)	0.999**	(0.058)	0.87**	(0.135)	0.978**	(0.299)	0.8130	(0.136)	0.9070	(0.192)
Reliability					0.066**	(0.0174)										
Log-likelihood	-17,441		-17,417		-17,433		-17,441		-17,130		-17,600		-18,442		-17,416	

*Note: (1): Baseline model. (2): Weather controls. (3): Travel time reliability. (4): Departure periods as nests. (5): Only fuel cost for cars. (6): No public transport subscription correction for cost. (7): Car available to everyone. (8): Bicycle not widely availability. Walking at peak hours is the baseline alternative. Duration measured in 10 minutes. Cost in €. We provide the mean coefficients, the standard-errors are computed using the delta-method. Significance levels: **: 1%, *: 5%, †: 10%.*

Table 24: Values of travel time for the alternative specifications

	Min	**Q1**	**Mean**	**Median**	**Q99**	**Max**
(1) Baseline	1.58	2.74	17.9	16.4	52.8	90.3
Alternative specifications						
(2) Weather controls	1.58	2.58	17.4	15.6	54.1	91.3
(3) Reliability measure	1.54	2.52	15.9	14.6	46.4	71.2
Alternative specifications						
(4)Periods as nests	1.58	2.56	17.4	15.6	53.3	86.9
(5) Only fuel costs	0	0.942	3.8	3.72	6.78	7.17
(6) No public transport subscription correction	0	8.03	326	31.8	2,841	2,887
(7) Car widely availability	1.16	2.74	16.4	14	51	111
(8) Bicycle not widely availability	2.11	3.09	18.5	16.6	57	91.4

Note: in €/hr.

Assumption for schedule constraints The central assumption in our modeling of schedule constraints is that they are driven solely by socio-professional activity. To test this, we examine whether other individual characteristics beyond professional activity contribute to the likelihood of being schedule-constrained. Specifically, we regress the probability of being schedule-constrained on socio-professional activity and a range of individual factors, including age, education, gender, household composition, and population density. These additional characteristics account for just 2% of the variation in schedule constraints, a very small amount compared to the 29% explained by professional activity.

Table 25: Regressions of the probability of being schedule-constrained on professional activity and individual controls

	Only SPC		Additional controls	
	Parameter	**Std. error**	**Parameter**	**Std. error**
Administrative professions	-0.34**	(0.011)	-0.35**	(0.012)
Education, health	-0.53**	(0.011)	-0.56**	(0.011)
Entrepreneurs	-0.02	(0.014)	-0.09**	(0.014)
Farmers	-0.19**	(0.014)	-0.2**	(0.014)
First-line supervisors	-0.42**	(0.015)	-0.42**	(0.015)
Private employees	-0.51**	(0.012)	-0.51**	(0.012)
Private executives	-0.03*	(0.011)	-0.08**	(0.011)
Public employees	-0.74**	(0.011)	-0.71**	(0.011)
Public executives	-0.27**	(0.012)	-0.33**	(0.012)
Qualified workers	-0.68**	(0.011)	-0.66**	(0.011)
Retail employees	-0.78**	(0.013)	-0.72**	(0.013)
Services	-0.63**	(0.012)	-0.58**	(0.012)
Shopkeepers	-0.03*	(0.014)	-0.06**	(0.014)
Technicians	-0.36**	(0.012)	-0.38**	(0.012)
Unqualified workers	-0.76**	(0.012)	-0.7**	(0.012)
Age $\in$]18-25]			0.05*	(0.021)
Age $\in$]25-35]			0.15**	(0.021)
Age $\in$]35-45]			0.18**	(0.021)
Age $\in$]45-60]			0.21**	(0.02)
Age $>$ 60			0.29**	(0.021)
Primary school			-0.005	(0.01)
Middle school			0.03**	(0.009)
High school			0.05**	(0.009)
Post-secondary education			0.13**	(0.01)
$\geq$ Bachelor degree			0.13**	(0.01)
Male			0.03**	(0.004)
Couple with children			0.001	(0.004)
Single			0.01*	(0.003)
Population $\in$ [2-4.9[			-0.01	(0.007)
Population $\in$ [5-9.9[			-0.01	(0.008)
Population $\in$ [10-19[			-0.01	(0.008)
Population $\in$ [20-49[			-0.03**	(0.008)
Population $\in$ [50-99[			-0.03**	(0.008)
Population $\in$ [100-199[			-0.02*	(0.008)
Population $\in$ [200-2,000[			-0.02**	(0.005)
Paris			-0.02**	(0.006)
Intercept	0.89**	(0.009)	0.64**	(0.024)
R^2	0.29		0.31	

*Note: The reference group is comprised of craftspersons, individuals below 18 years old, individuals with no diploma, females, couples without children, and individuals living in rural areas. Population is in 1,000 inhabitants. Significance levels: **: 1%, *: 5%, †: 10%.*

D.3 Additional results on the value of time

We present the distributions of the value of travel time by age, income, and trip distance in Figure 10 using second-order local polynomials. Young individuals are associated with the lowest values of the opportunity cost of time. The VOT then increases with age, reaching its highest value around 45 years old. After that age, the VOT starts decreasing, and it becomes

around 20% lower than the maximum at age 70. We also see some heterogeneity in the VOT across income categories, but the heterogeneity is less pronounced. Poor individuals have the lowest valuations of time, on average, but the opportunity cost of time increases rapidly with income. The average VOT slightly decreases between incomes of €1,800 an income of €3,200, and then the average VOT increases. Regarding the VOT and distance, we see non-monotonic effects of distance. Short trips tend to be associated with a low valuation of travel time, which is consistent with the distribution of distances by age: the shortest commuters tend to be children in high-school or below. The VOT values rapidly increase with distance, decrease until 20 km, and rise again but more slowly.

Figure 10: Value of travel time and individual characteristics

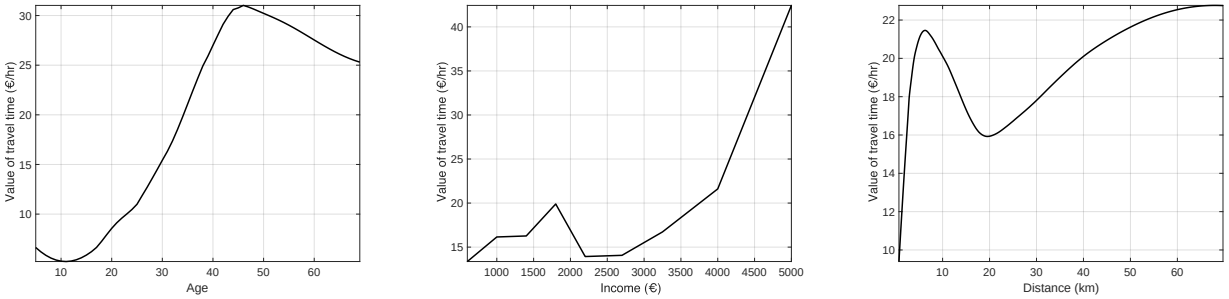

(a) Age (b) Income (c) Trip distance

D.4 Traffic sensor data and congestion technology estimates

D.4.1 Definition of the areas

Figure 11 displays the locations of the traffic sensor (black dots) as well as the definitions of the five areas in our model: city center (light grey), ring roads (the circles around the city center, in white), the close suburbs (dark grey), the far suburbs (the part with no color) and the highways (the dots connecting the suburbs to the city center). As shown in Figure 11, there is no traffic sensor in the suburbs outside the highways. The data comes from two different sources. The highway traffic data comes from the regional road maintenance agency (DRIF). Traffic data for Paris and the ring roads comes from the city of Paris.[56]

[56]Source: https://opendata.paris.fr/explore/dataset/comptages-routiers-permanents-historique/information/.

Figure 11: Traffic sensor locations and area definition

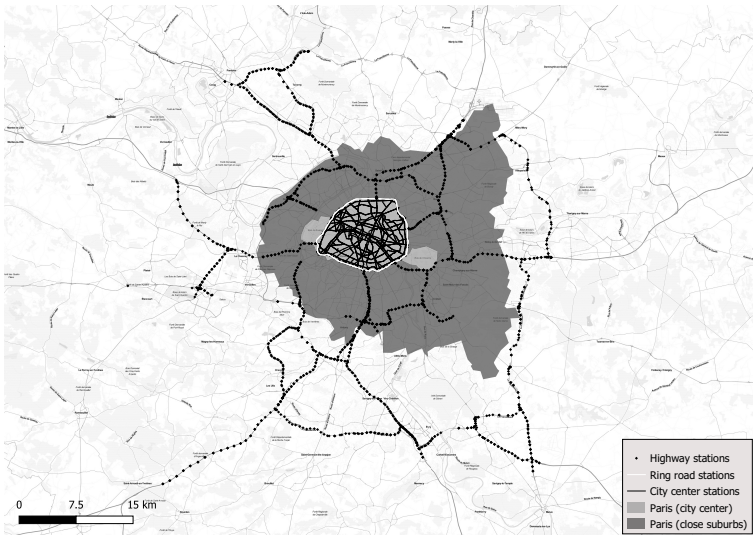

D.4.2 Fundamental equations of traffic

The traffic flow (number of vehicles passing per hour), traffic density (number of vehicles per kilometer and hour), and speed are related through the fundamental equation of traffic flow:

$$\text{traffic flow} = \text{speed} \times \text{traffic density}.$$

The road traffic density is related to the occupancy rate (the fraction of the road-lane occupied by a vehicle) using:

$$\text{traffic density} = \frac{\text{occupancy rate}}{M + h} \times \text{no. lanes}, \tag{16}$$

where M is the mean effective car length, representing the length of the car plus the space between two vehicles. h represents the length of a traffic sensor. The data on the highways contain all traffic variables but the data from the city center and the ring roads does not record speeds. We reorganize the fundamental equation above to obtain the speeds from occupancy rates and traffic flows:

$$\text{speed} = \frac{\text{traffic flow}}{\frac{\text{occupancy rate}}{M+h} \times \text{no. lanes}}. \tag{17}$$

D.4.3 Sample construction

For traffic observations from the highways connecting the far suburb to the city center, we restrict the sample to sensors that record traffic going in the direction of the city center.

We drop outliers in speed (below 0 or greater than the maximum highway speed limit, 130 km/hr) and occupancy rates (below 0% and above 50%). An occupancy rate of 50% represents extreme traffic conditions: the traffic monitoring institute in Paris defines traffic as pre-saturated from 15% and saturated from 30%. We follow the same approach when cleaning the data from Seine-Saint-Denis. We also detect inconsistent observations using the fundamental relationship between traffic flow, occupancy rates, and speed. More specifically, we combine Equations (16) and (17) to obtain the implied average car length plus sensor length from traffic flow, speed, and occupancy rate:

$$M + h = \frac{\text{occupancy rate} \times \text{speed} \times \text{no. lanes}}{\text{traffic flow}}.$$

We then drop observations in the top and bottom 1% of the implied length distribution, keeping 6.1 million observations.

The data on the city center traffic and the ring roads contain sensor measurements of traffic flows and occupancy rates only. Unfortunately, sensors cannot measure speed accurately because of traffic lights and multiple intersections.

Instead of relying on an assumption for the effective car length as often done in the literature (e.g., Geroliminis and Daganzo, 2008 or Loder et al., 2017), we rely on the highway data to predict the average car length plus sensor length in Paris. It has been documented by Jia et al. (2001) that the traffic composition varies over time, making the uniform car length assumption inappropriate. We rely on a prediction model for the average car length plus sensor length that we estimate using the highway data. Then, we use this model to predict hourly lengths in the city center and the ring roads. Our prediction model specifies the length as a function of the distance to the city center and day-of-the-week interacted with hour fixed effects. Because the relationship between the length and the distance to the city center may not be constant as we get closer to the city center, we rely on a piecewise linear specification with six intervals. This prediction model is estimated using 4.8 million observations from highway data, for which we observe the GPS coordinates of the traffic sensor obtain an R^2 of 0.18. For predictions, we set the distance to the city center to 0. We then get expected lengths specific to the hour and the day of the week. We do not directly observe the number of lanes in the city center traffic data, so we rely on additional data from Open Street Map. Finally, we exclude outliers in occupancy rate and estimated speed following the same criteria as before for the highway data.

Additional data from Seine-Saint-Denis For the additional data used to calibrate the linear combination technology for the close suburbs, we received data from the Directorate of

Roads and Travel of the Seine-Saint-Denis Department. The data for Seine-Saint-Denis has good coverage of that area of the close suburbs. However, measurements of traffic conditions are very noisy as they are provided in the form of intervals (e.g. speed intervals such as 0 to 30 km/hr rather than exact speeds). Therefore, it is not enough reliable to directly estimate a congestion technology, which is why we do not include those sensors in Figure 11.

The additional data covers 71 sensors across the Seine-Saint-Denis department. For each sensor, data for one week is provided (ranging from January 25$^{\text{th}}$ 2023 to April 20$^{\text{th}}$ 2023). For each sensor, the number of vehicles (cars and trucks) going at different speed intervals is recorded each hour. The first speed interval is 0-30 km/hr and then each interval has a 10 km/hr range. We compute the average hourly speed of a sensor by taking the average across the midpoints of each interval, weighted by the number of vehicles in the interval. However, this average hourly speed is a noisy measure of the actual speed, as the intervals are fairly large. In particular, the first interval from 0 to 30 km/hr is large enough to hide important speed variation during the most congested periods. The data includes roads lengths, average speeds, and flows, but no occupancy rate measure. We rearrange Equation (16) to express occupancy rate as a function of the observed variables and we assume a mean car length of 5.9 meters (the average car length we estimated for Paris). We drop observations following the same criteria as for the city center sensors.

Finally, we compute average speed and occupancy rates by weighting each sensor by the average traffic flow of the sensor. We find an average speed of 34.9 km/hr and an occupancy rate of 14.1 % at peak hours, while we find a speed of 36.6 km/hr and an occupancy rate of 11.4 % at off-peak hours.

Additional data for the instrumental variables We use data on accidents recorded by the National interministerial road safety observatory (ONISR).[57] It contains the date and time of every accident that involved at least one vehicle and where at least one person required medical care. The information in the dataset comes from the corresponding police reports of the accidents. During the period 2016 to 2017, the dataset records 25,439 accidents in the Paris metropolitan area. Additional instruments rely on weather changes. We use data on weather conditions in Paris at the hourly level from OpenWeatherMap.[58]

[57]Source: https://www.data.gouv.fr/fr/datasets/bases-de-donnees-annuelles-des-accidents-corporels-de-la-circulation-routiere-annees-de-2005-a-2022/.

[58]See https://openweathermap.org/.

D.4.4 Fit of the congestion technology models

Table 26 represents the number of observations used to estimate the congestion technologies for each area and the fit of the models, measured by the R^2. The three congestion technologies have good fits with R^2 between 0.18 for the city center and 0.65 for the ring roads. The lower R^2 in the city center probably reflects more idiosyncrasies in traffic speed: traffic lights and intersections generate heterogeneous traffic flows, implying heterogeneous speeds.

Table 26: Fit of the congestion technology by area

Area	Number of observations	R^2	Degree
Highways	3,844,145	0.63	8
Ring roads	1,197,679	0.65	7
City center	5,124,452	0.18	3

Note: "Degree" represents the degree of the polynomial.

D.5 Additional results on checking the equilibrium uniqueness

D.5.1 Formula for the Jacobian

We provide here the analytical formula for the Jacobian of the contraction defined as:

$$g_t^a(\mathbf{v}, \kappa) = \kappa v_t^a + (1-\kappa) f^a(\mathbf{v}).$$

We can identify, in the Jacobian, three types of derivatives: $\frac{\partial g_t^a(\mathbf{v},\kappa)}{\partial v_t^a}$, $\frac{\partial g_t^a(\mathbf{v},\kappa)}{\partial v_t^{\tilde{a}}}$ and $\frac{\partial g_t^a(\mathbf{v},\kappa)}{\partial v_{t'}^{\tilde{a}}}$.

$$\frac{\partial g_t^a(\mathbf{v},\kappa)}{\partial v_t^a} = \kappa + (1-\kappa) \underbrace{f^{a\prime}\left(\sum_{n=1}^N \omega_n k_n^a s_{n\mathbf{d}t}(\mathbf{v}) + K_{0t}^a\right)}_{\leq 0} \times \sum_{n=1}^N \underbrace{\omega_n k_n^a \frac{\partial s_{n\mathbf{d}t}(\mathbf{v})}{\partial v_t^a}}_{\geq 0}$$

$$\frac{\partial g_t^a(\mathbf{v},\kappa)}{\partial v_t^{\tilde{a}}} = (1-\kappa) \underbrace{f^{a\prime}\left(\sum_{n=1}^N \omega_n k_n^a s_{n\mathbf{d}t}(\mathbf{v}) + K_{0t}^a\right)}_{\leq 0} \times \sum_{n=1}^N \underbrace{\omega_n k_n^a \frac{\partial s_{n\mathbf{d}t}(\mathbf{v})}{\partial v_t^{\tilde{a}}} \mathbb{1}\{k_n^{\tilde{a}} > 0\}}_{\geq 0}$$

$$\frac{\partial g_t^a(\mathbf{v},\kappa)}{\partial v_{t'}^{\tilde{a}}} = (1-\kappa) \underbrace{f^{a\prime}\left(\sum_{n=1}^N \omega_n k_n^a s_{n\mathbf{d}t}(\mathbf{v}) + K_{0t}^a\right)}_{\leq 0} \times \sum_{n=1}^N \underbrace{\omega_n k_n^a \frac{\partial s_{n\mathbf{d}t}(\mathbf{v})}{\partial v_{t'}^{\tilde{a}}} \mathbb{1}\{k_n^{\tilde{a}} > 0\}}_{\leq 0}$$

Given the functional form assumptions we make on the demand model, the derivatives of the

probability of driving at period t_1 with respect to speeds at period t_1 and t_2 are given by:

$$\frac{\partial s_{n\mathbf{d}t_1}(\mathbf{v})}{\partial v^a_{t_1}} = \left[\phi_n \pi_n \sigma s_{n\mathbf{d}t_1|\mathcal{T}_1}(1 - s_{n\mathbf{d}t_1|\mathcal{T}_1}) + (1-\phi_n) s_{n\mathbf{d}t_1|\mathcal{T}_{12}} \left(1 - (1-\sigma)\frac{s_{n\mathbf{d}t_1|\mathcal{T}_{12}}}{s_{n\mathbf{d}t_1|\mathcal{T}_{12}} + s_{n\mathbf{d}t_2|\mathcal{T}_{12}}} - \sigma s_{n\mathbf{d}t_1|\mathcal{T}_{12}}\right)\right]$$
$$\times \left(-\frac{k^a_n}{(v^a_{t_1})^2}\rho_{nt_1}\right) \times 6 \times \frac{\beta^{\text{duration}}_n}{\sigma}$$
$$\frac{\partial s_{n\mathbf{d}t_1}(\mathbf{v})}{\partial v^a_{t_2}} = (1-\phi_n) s_{n\mathbf{d}t_1|\mathcal{T}_{12}} \left(-(1-\sigma)\frac{s_{n\mathbf{d}t_2|\mathcal{T}_{12}}}{s_{n\mathbf{d}t_1|\mathcal{T}_{12}} + s_{n\mathbf{d}t_2|\mathcal{T}_{12}}} - \sigma s_{n\mathbf{d}t_2|\mathcal{T}_{12}}\right)$$
$$\times \left(-\frac{k^a_n}{(v^a_{t_2})^2}\rho_{nt_2}\right) \times 6 \times \frac{\beta^{\text{duration}}_n}{\sigma}$$

That the factor 6 corresponds to converting speeds in km/hr into tens of minutes, which is the unit of duration in the individual utility.

D.5.2 Additional results on the equilibrium solving algorithm

We show additional numerical results about the convergence by plotting the average number of iterations needed to converge for the possible values of κ between 0.5 and 0.95. More specifically, we draw ten different initial speed values from a uniform distribution over $[\underline{\mathbf{v}}, \overline{\mathbf{v}}]$ and solve for the speed equilibrium with different values for the tuning parameter. We always converge to the same equilibrium speeds, suggesting that our algorithm is likely to be a contraction for lower values of κ than the one we use. Figure 12 indicates the number of iterations and the convergence time depending on the tuning parameter. The graphs are very similar when we introduce any policy. The number of iterations and the time increases exponentially with κ.

Figure 12: Average number of iterations and convergence times (across 10 simulations)

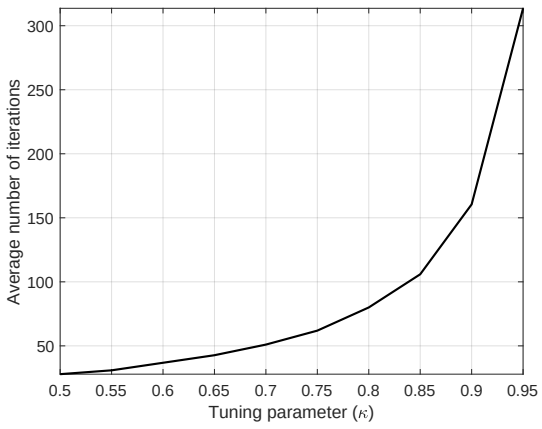

(a) Number of iterations

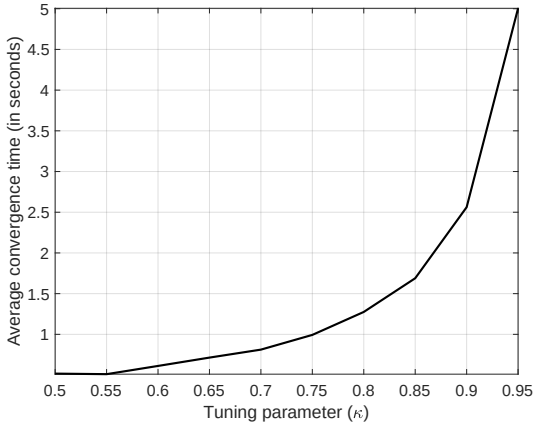

(b) Average convergence time

E Additional results on the policy effects

E.1 Consumer surplus and welfare definitions

To evaluate the impacts of transportation policies on individuals, we rely on changes in consumer surplus, which measure compensating variations. The consumer surplus per trip for individual n is defined as the expected utility of the choice that maximizes the utility conditional on the set of periods available $\mathcal{T}_n$. It is:

$$CS_n|\mathcal{T}_n = \frac{1}{|\alpha_n|} \log\left(\sum_{j \in \mathcal{J}_n} \exp(\sigma \log(D_{nj}))\right),$$

where $D_{nj} = \sum_{t \in \mathcal{T}_n} \exp\left(\frac{\beta_n' X_{njt}}{\sigma}\right)$ is the expected utility of the best departure period within $\mathcal{T}_n$ for transportation mode j. α_n is the parameter of sensitivity to the trip cost, which converts the utility into monetary terms. There is a constant utility term that cannot be identified and is normalized to 0 in the expression above.

The variation of consumer surplus eliminates the constant and thus is identified and given by:

$$\Delta CS_n|\mathcal{T}_n = \frac{1}{|\alpha_n|}\left[\log\left(\sum_{j \in \mathcal{J}_n^1} \exp(\sigma \log(D_{nj}^1))\right) - \log\left(\sum_{j \in \mathcal{J}_n^0} \exp(\sigma \log(D_{nj}^0)\right)\right].$$

Where $\mathcal{J}_n^1$ and D_{nj}^1 represent respectively the choice set and the expected utility of transportation mode j under the counterfactual scenario, while $\mathcal{J}_n^0$ and D_{nj}^0 represent their initial values.

In our model with stochastic constraints, the change in individual consumer surplus is thus:

$$\Delta CS_n = (1-\phi_n)\Delta CS_n|\mathcal{T}_{12} + \phi_n\pi_n\Delta CS_n|\mathcal{T}_1 + \phi_n(1-\pi_n)\Delta CS_n|\mathcal{T}_2.$$

We can further decompose the variation in consumer surplus into a partial policy effect which measures the policy effect at constant initial speeds, and an equilibrium speed effect under the implemented policy. To make the expression clearer, we make apparent the dependence between the driving speeds and the utilities associated with the transportation modes $D_{nj}^0(\mathbf{v_0})$ and $D_{nj}^1(\mathbf{v_1})$, where $\mathbf{v_0}$ and $\mathbf{v_1}$ represent the initial and final vectors of speeds.

The decomposition is given by:

$$\Delta CS_n|\mathcal{T}_n = \frac{1}{|\alpha_n|}\Bigg[\underbrace{\log\left(\sum_{j\in\mathcal{J}_n^1}\exp\left(\sigma\log\left(D_{nj}^1(\mathbf{v_0})\right)\right)\right)-\log\left(\sum_{j\in\mathcal{J}_n^0}\exp\left(\sigma\log\left(D_{nj}^0(\mathbf{v_0})\right)\right)\right)}_{\text{policy effect at constant speed}}$$
$$\underbrace{+\log\left(\sum_{j\in\mathcal{J}_n^1}\exp\left(\sigma\log\left(D_{nj}^1(\mathbf{v_1})\right)\right)\right)-\log\left(\sum_{j\in\mathcal{J}_n^1}\exp\left(\sigma\log\left(D_{nj}^1(\mathbf{v_0})\right)\right)\right)}_{\text{equilibrium speed effect}}\Bigg]$$

Our welfare change outcome is simply the sum of consumer surplus changes, the potential toll revenue and the monetary value of emissions avoided:

$$\Delta W = \sum_{n=1}^{N}\omega_n\left(\Delta CS_n + \sum_{t=\{t_1,t_2\}}\left(p_{nt}s_{n\mathbf{d}t}^1 + \left(e_{nt}^1 s_{n\mathbf{d}t}^1 - e_{nt}^0 s_{n\mathbf{d}t}^0\right)k_n\right)\right),$$

where p_{nt} is the toll for individual n and period t. e_{nt}^0 represents the cost of emissions, per kilometer, for individual n and period t in the initial situation and e_{nt}^1 in the counterfactual situation. The emission costs are function of the period and the policy environment because in some specifications the emissions levels depend on the speeds. $s_{n\mathbf{d}t}^0$ and $s_{n\mathbf{d}t}^1$ represents the probability to drive in period t under the initial situation, and the counterfactual policy respectively.

E.2 Social costs of emissions

The values for the social costs of emissions come from a 2019 report from the European Commission (Van Essen et al., 2019). The values for NO_X and PM correspond to the "transport city" and "transport metropole" values for those pollutants in Table 14 of the report. For hydrocarbons (HC), we take the value for non-methane volatile organic compound (NMVOC), which includes hydrocarbons. Finally, for CO_2 , we use the "high" cost estimate from Table 24 in the report.

Table 27 presents the average social cost in cents of euro per km driven for the vehicles in the final sample (using the baseline emissions estimates). Gasoline cars have, on average, a lower social cost from emissions than diesel cars. For gasoline cars, CO_2 is the main component of the cost of emissions with a 92.9% share. For diesel vehicles, CO_2 only accounts for 62.3% of emissions costs, while PM and NO_X jointly represent 37.6%.

Table 27: Social costs of emissions per kilometer driven

	Gasoline	Diesel
Average cost per km	3.4	4.53
Cost composition (in %)		
CO_2	92.9	62.3
NO_X	4.15	16.4
HC	0.36	0.12
PM	2.63	21.2

Note: Average cost in cents of euro per km. All statistics computed using survey weights, restricting the sample to the 2010 EGT survey, and using the baseline estimates of vehicles' emissions.

E.3 Additional results on the comparison across stringency levels

E.3.1 Importance of endogenous speeds

In Figure 13, we compare our model's predictions for the proportion of individuals driving with those from a naive model that would consider speeds and, thus, trip durations fixed. All scenarios and stringency levels deliver biases under exogenous speeds: we overestimate the number of individuals substituting away from using their cars at peak hours and underestimate those who choose to drive at off-peak hours. The improvement of equilibrium speeds indeed dampens the incentives to stop driving.

Figure 13: Predicted car shares as function of the policy stringency level

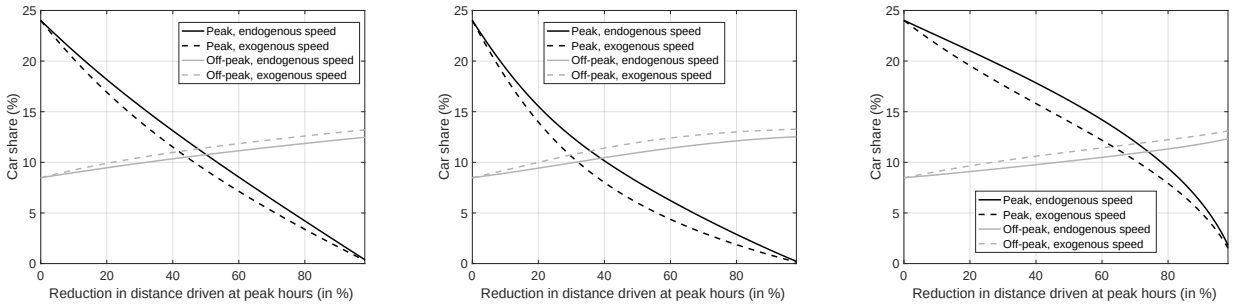

(a) Driving restrictions (b) Uniform tolls (c) Variable tolls

To further highlight the importance of considering the equilibrium speed adjustments, we compare the toll revenues predicted under constant speeds with the predictions from our model. The results in Figure 14 below suggest that not accounting for the speed changes significantly underestimates the number of individuals paying the toll and the toll revenue. Moreover, the magnitude of the bias increases with the policy stringency levels, reflecting the increasing role of speed adjustments.

Figure 14: Predicted toll revenues under endogenous and exogenous speeds

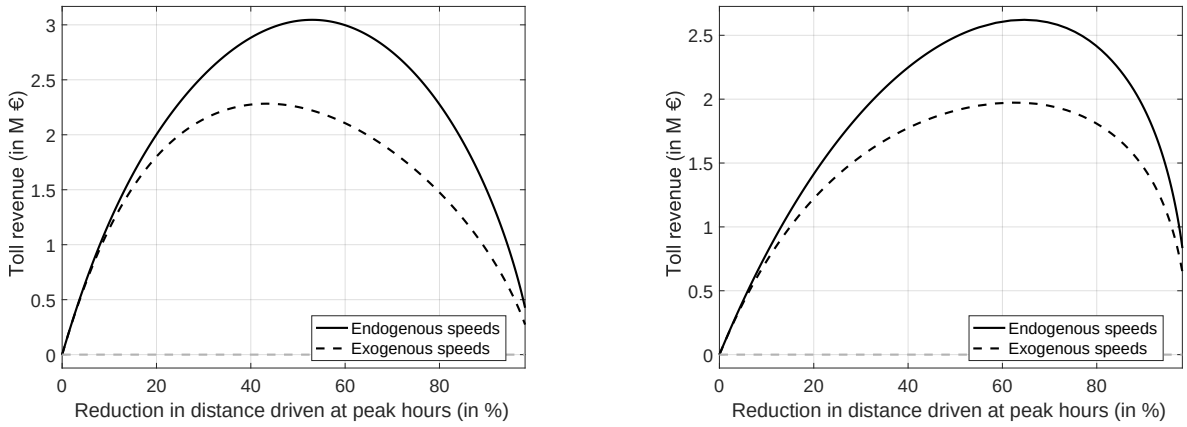

(a) Uniform tolls

(b) Variable tolls

E.3.2 Additional outcomes of the policy effects

We provide the equilibrium speeds for the city center, ring roads, and highways in Figure 15. As expected, the speeds increase with the policy stringency level at peak hours, while at off-peak hours, they decrease. This is the consequence of important shifts towards driving at off-peak hours. The speed at peak hours increases the most on the highways while there is much less speed improvement in the city center. At the same time, the off-peak hour speed in the city center is almost constant, reflecting that individuals driving in the city center have better alternatives to cars. By contrast, those who drive on the highways and ring roads are more likely to substitute for driving during off-peak hours.

Figure 15: Speeds under the different policies and stringency levels

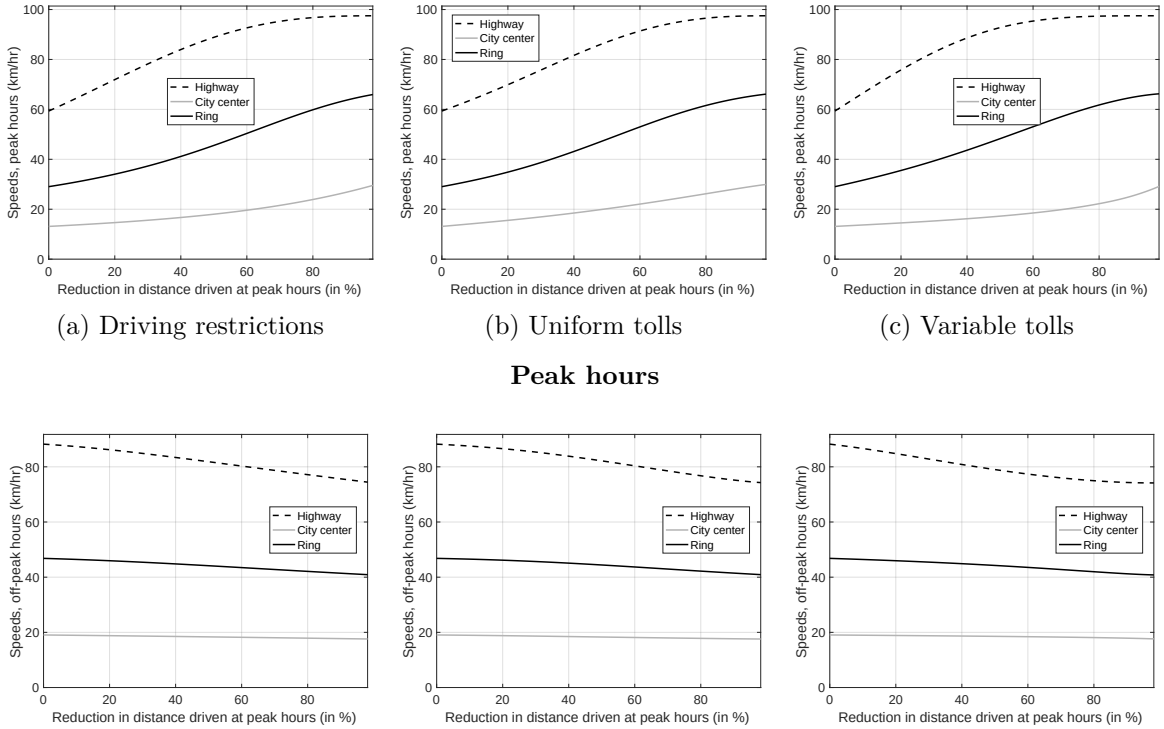

(a) Driving restrictions (b) Uniform tolls (c) Variable tolls

Peak hours

(d) Driving restrictions (e) Uniform tolls (f) Variable tolls

Off-peak hours

Lastly, we provide in Figure 16 the gains from speed improvements and emissions avoided relative to the change in consumer surplus. We find that the gains from speed account for 44.7% of the consumer surplus losses associated with the most lenient variable toll. The gains decrease rapidly with the policy stringency level because individuals are discouraged from driving and do not benefit from improved speeds. The gains from speeds under uniform tolls and driving restrictions are modest relative to the large consumer surplus losses and account for less than 27.1%. Finally, when the policy stringency is very high, the speed changes become negatively valued since the majority of drivers drive during off-peak hours when speeds are lower than initially.

In Panel (b) of Figure 16, we see that the benefits of the emissions avoided are small relative to the consumer surplus losses. The environmental benefits compensate less than 7% of the consumer surplus losses. The relative importance decreases under the variable toll while it increases under uniform tolls and driving restrictions. The emissions values must be between 14 and 28 times higher to justify the policies from the standpoint of consumer surplus and environmental benefits.

Figure 16: Relative gains from speed improvements and emissions avoided

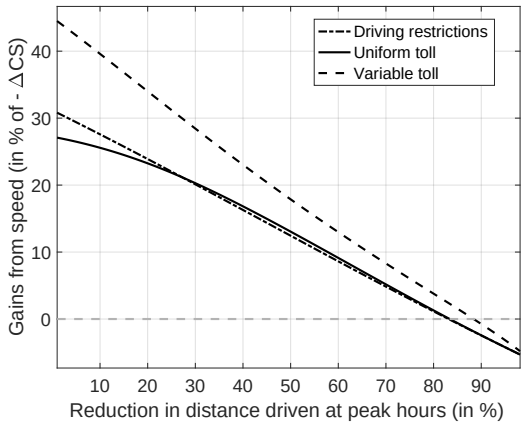

(a) Gains from speed improvements relative to consumer surplus losses

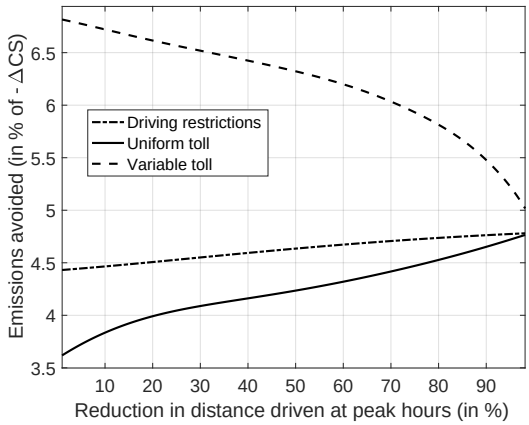

(b) Gains from emissions avoided relative to consumer surplus losses

E.3.3 Social planner problem

The welfare function is composed by the consumer surplus (CS), the toll revenue (T) and the value of emissions avoided (E):

$$\mathrm{W} = \underbrace{\sum_n \omega_n CS_n(p_n, \mathbf{v}(\mathbf{p}))}_{CS} + \underbrace{\sum_n \omega_n p_n s_{n\mathbf{d}t_1}(p_n, \mathbf{v}(\mathbf{p}))}_{T} - \underbrace{\sum_{t=t_1,t_2} \sum_n \omega_n e_n k_n s_{n\mathbf{d}t}(p_n, \mathbf{v}(\mathbf{p}))}_{E}$$

The following Lagrangian represents the social planner's program:

$$\mathcal{L}(\mathbf{p}) = CS(\mathbf{p}, \mathbf{v}(\mathbf{p})) + T(\mathbf{p}, \mathbf{v}(\mathbf{p})) - E(\mathbf{p}, \mathbf{v}(\mathbf{p})) - \lambda \left(\sum_{n=1}^{N} \omega_n k_n s_{n\mathbf{d}t_1}(p_n, \mathbf{v}(\mathbf{p})) - \bar{K}_{t_1} \right)$$

The first-order conditions associated to the Lagrangian representing the problem above are:

$$\frac{\partial (CS + T - E)}{\partial p_n} + \sum_t \sum_a \frac{\partial (CS + T - E)}{\partial v_t^a} \frac{\partial v_t^a}{\partial p_n} - \lambda \omega_n k_n \frac{\partial s_{n\mathbf{d}t_1}}{\partial p_n} - \lambda \sum_t \sum_a \sum_{n'} \omega_{n'} k_{n'} \frac{\partial s_{n'\mathbf{d}t_1}}{\partial v_t^a} \frac{\partial v_t^a}{\partial p_n} = 0,$$

$\forall p_n$. The equation above highlights the congestion externalities: the level of p_n directly individual n's outcomes and indirectly everyone's outcomes through the speeds.

We can express the derivatives of the different welfare components:

$$\frac{dCS}{dp_n} = \underbrace{\omega_n \frac{\partial CS_n}{\partial p_n}}_{\text{mg. direct change indiv. cons. surplus}} + \underbrace{\sum_t \sum_a \sum_{n'} \omega_{n'} \frac{\partial CS_{n'}}{\partial v_t^a} \frac{\partial v_t^a}{\partial p_n}}_{\text{mg. indirect change agg. cons. surplus}} .$$

The first term represents the direct effect of increasing p_n on consumer surplus for individual n.

The second term reflects congestion externalities on aggregate consumer surplus: increasing the toll for individual n affects everyone's consumer surplus through speed changes. Speeds at peak hours increase while speeds during off-peak hours increase. We expect the marginal change in aggregate consumer surplus to be positive when the policy is not too strict. However, for high policy stringency levels, individuals are more likely to drive during off-peak hours than during peak hours, and the marginal change in aggregate consumer surplus turns negative. The marginal individual consumer surplus change from a price increase is:

$$\frac{\partial CS_n}{\partial p_n} = -s_{n\mathbf{d}t_1}.$$

Next, we turn to the change in toll revenue:

$$\frac{dT}{dp_n} = \underbrace{\omega_n \frac{\partial T_n}{\partial p_n}}_{\text{mg. direct change in toll revenue from } n} + \underbrace{\sum_t \sum_a \sum_{n'} \omega_{n'} p_{n'} \frac{\partial s_{n'\mathbf{d}t_1}}{\partial v_t^a} \frac{\partial v_t^a}{\partial p_n}}_{\text{mg. indirect change in total toll revenue}},$$

where:

$$\frac{\partial T_n}{dp_n} = \underbrace{s_{n\mathbf{d}t_1}}_{\text{positive effect on toll revenue}} + \underbrace{p_n \frac{\partial s_{n\mathbf{d}t_1}}{\partial p_n}}_{\text{negative on toll revenue through substitution}}.$$

In the expression above, we see the standard two effects of increasing the toll: a positive effect that increases the toll revenue by $\omega_n s_{n\mathbf{d}t_1}$, and a negative effect that reduces the toll revenue proportionally because individuals substitute to other modes and periods. If we consider the sum of consumer surplus and toll revenue, the direct impact of the toll on consumer surplus and the positive effect on the toll revenue cancel out. Since the toll revenue is entirely redistributed, the value of the toll is neutral from the sum of consumer surplus and the toll revenue point of view. We thus have:

$$\frac{\partial (CS_n + T_n)}{\partial p_n} = p_n \frac{\partial s_{n\mathbf{d}t_1}}{\partial p_n}.$$

Finally, we look at the derivative with respect to the emissions cost:

$$\frac{dE}{dp_n} = \underbrace{\omega_n e_n k_n \frac{\partial (s_{n\mathbf{d}t_1} + s_{n\mathbf{d}t_2})}{\partial p_n}}_{\text{mg. direct change in emissions from } n} + \underbrace{\sum_t \sum_a \sum_{n'} \omega_{n'} e_{n'} k_{n'} \frac{\partial (s_{n'\mathbf{d}t_1} + s_{n'\mathbf{d}t_2})}{\partial v_t^a} \frac{\partial v_t^a}{\partial p_n}}_{\text{mg. indirect change in emissions from all indiv.}}$$

In the previous equation, we see that what matters regarding emissions is how much the total probability of driving changes from p_n. If individuals only substitute inter-temporally and keep driving, we obtain no reduction in emissions.

We can rewrite the Lagrangian first-order condition as:

$$\omega_n p_n \frac{\partial s_{n\mathbf{d}t_1}}{\partial p_n} - \omega_n e_n k_n \frac{\partial (s_{n\mathbf{d}t_1} + s_{n\mathbf{d}t_2})}{\partial p_n} - \lambda \omega_n k_n \frac{\partial s_{n\mathbf{d}t_1}}{\partial p_n}$$
$$+ \sum_t \sum_a \sum_{n'} \omega_{n'} \left(\frac{\partial CS_{n'}}{\partial v_t^a} + p_{n'} \frac{\partial s_{n'\mathbf{d}t_1}}{\partial v_t^a} - e_{n'} k_{n'} \frac{\partial (s_{n'\mathbf{d}t_1} + s_{n'\mathbf{d}t_2})}{\partial v_t^a} - \lambda k_{n'} \frac{\partial s_{n'\mathbf{d}t_1}}{\partial v_t^a} \right) \frac{\partial v_t^a}{\partial p_n} = 0$$

Intuitively, the social planner sets the toll to equalize its marginal benefits to the its marginal costs:

$$\underbrace{-\omega_n e_n k_n \frac{\partial (s_{n\mathbf{d}t_1} + s_{n\mathbf{d}t_2})}{\partial p_n} - \lambda \omega_n k_n \frac{\partial s_{n\mathbf{d}t_1}}{\partial p_n}}_{\text{marginal direct benefits}} + \underbrace{\sum_t \sum_a \sum_{n'} \omega_{n'} \left(\frac{\partial CS_{n'}}{\partial v_t^a} + p_{n'} \frac{\partial s_{n'\mathbf{d}t_1}}{\partial v_t^a} \right) \frac{\partial v_t^a}{\partial p_n}}_{\text{marginal indirect benefits}}$$
$$= \underbrace{-\omega_n p_n \frac{\partial s_{n\mathbf{d}t_1}}{\partial p_n}}_{\text{marginal direct costs}} + \underbrace{\sum_t \sum_a \sum_{n'} \omega_{n'} \left(e_{n'} k_{n'} \frac{\partial (s_{n'\mathbf{d}t_1} + s_{n'\mathbf{d}t_2})}{\partial v_t^a} + \lambda k_{n'} \frac{\partial s_{n'\mathbf{d}t_1}}{\partial v_t^a} \right) \frac{\partial v_t^a}{\partial p_n}}_{\text{marginal indirect costs}}$$

The marginal benefits include the direct reduction in emissions, the relaxation of the traffic level constraint, and the indirect effects on aggregate consumer surplus and toll revenue. The marginal costs of increasing p_n are related to the direct decrease in toll revenue from substitution, the indirect increase in everyone's emissions, and the tightening of traffic constraints from improved speeds.

If we ignore the indirect effects from congestion externalities, we obtain the following equation that defines the optimal toll:

$$p_n = e_n k_n \left(1 + \frac{\partial s_{n\mathbf{d}t_2} / \partial p_n}{\partial s_{n\mathbf{d}t_1} / \partial p_n} \right) + \lambda k_n,$$

which indicates that p_n should be proportional (with the same factor λ) to the number of kilometer driven if the emissions costs are small relative to the shadow cost of reducing traffic.

E.3.4 Welfare-maximizing personalized tolls and individual characteristics

Figure 17 shows the distribution of personalized tolls across demographics using quadratic local linear regressions. On the same graph, we provide the average variable toll that achieves the same traffic level as a benchmark. We see that the personalized tolls set higher values for middle-aged individuals and high-income individuals. We notice the same pattern arising under variable toll, indicating that most heterogeneity is related to distance heterogeneity. When looking at the relationship between tolls and distance, we see that personalized tolls

provide cheaper tolls to long-distance commuters. Both variable and personalized tolls increase with speed in public transport. However, the difference between personalized and variable tolls increases with speed, indicating that the social planner favors individuals with inefficient public transport alternatives. When investigating the relation between the personalized tolls and schedule constraints, we find that the social planner sets higher tolls for individuals with a high probability of being flexible and a low probability of being constrained to peak-hour commutes.

Figure 17: Welfare-maximizing tolls and demographic characteristics

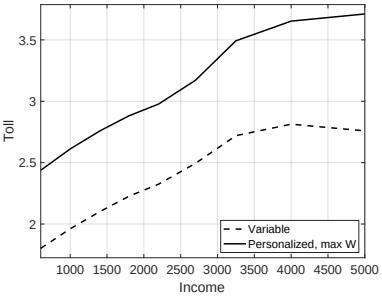

(a) Income

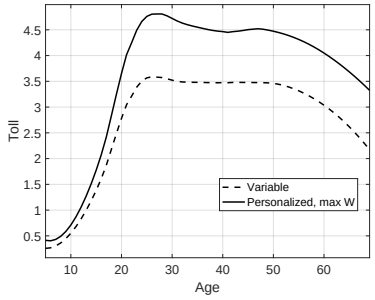

(b) Age

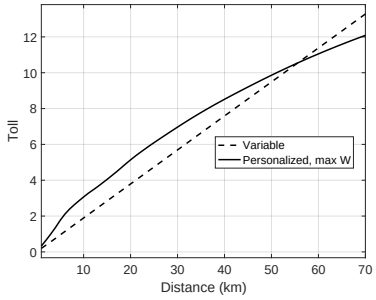

(c) Trip distance

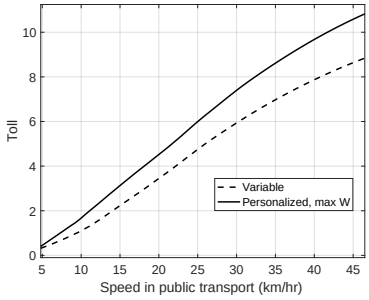

(d) Speed in public transport

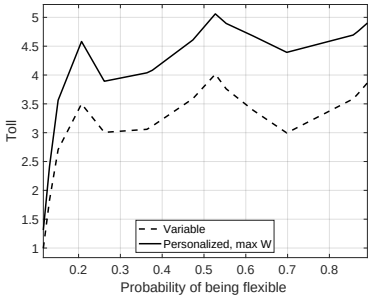

(e) Flexibility

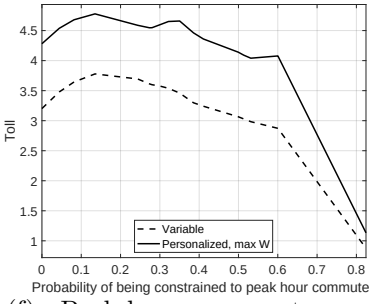

(f) Peak-hour commute constraint

E.3.5 Consumer surplus-maximizing personalized tolls and individual characteristics

Figure 18 shows that the tolls increase with income, but the heterogeneity across income levels is much lower than the one related to age. The social planner sets very low tolls for young individuals, while individuals between 20 and 30 are associated with the highest tolls. When looking at the relationship between tolls and distance, we see that personalized tolls rapidly increase with distance and decrease. Personalized tolls increase with speed in public transport, the highest average tolls are for individuals with a public transport speed above 40 km/hr. This highlights the importance of the public transport alternative for the consumer surplus loss. When investigating the relation between the personalized tolls and

schedule constraints, we find that the social planner sets higher tolls for individuals with a high probability of being flexible and a low probability of being constrained to peak-hour commutes.

Figure 18: Consumer surplus-maximizing tolls and demographic characteristics

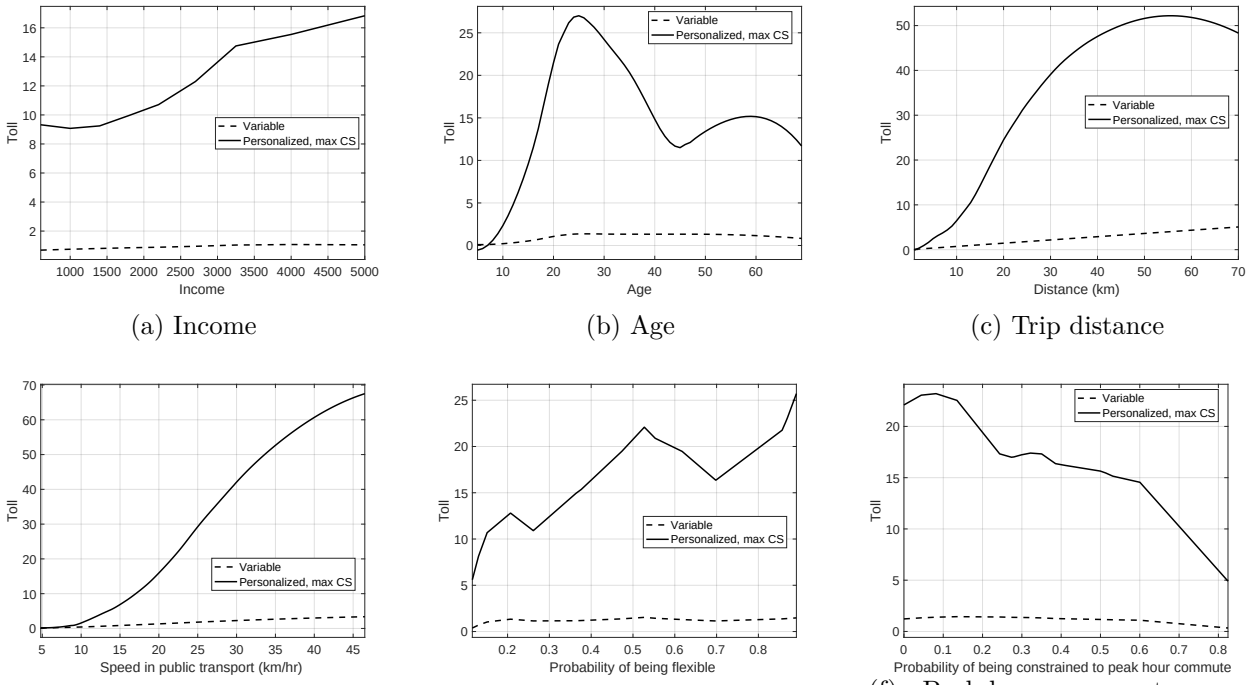

(a) Income (b) Age (c) Trip distance

(d) Speed in public transport (e) Flexibility (f) Peak-hour commute constraint

E.4 Additional results for the benchmark policy levels

E.4.1 Change in consumer surplus, professional activity and schedule constraints

Table 28 provides the average variation in consumer surplus by professional activity at the benchmark stringency level across policies. Among employed individuals, workers in education, health, public, retail, and private employees are the most affected by the policies. Figure 19 provides the average consumer surplus variation across the range of probabilities characterizing the schedule constraints. Panel (a) presents the variation according to the probability of being able to choose the departure time. Panels (b) and (c) show the variation in average consumer surplus according to the probabilities of being constrained to commute at peak or off-peak hour respectively. We find that the driving restriction and the uniform toll hurt more individuals with a low probability to be able to choose a departure time, in particular those with a high probability to be constrained to peak hour commute.

Table 28: Average consumer surplus change by professional activity

Socio-professional activity	Driving restriction	Uniform toll	Variable toll	Personalized tolls
Farmers	-2.31	-1.59	-0.624	-0.472
Craftspersons	-0.587	-0.769	-0.48	-0.361
Shopkeepers	-0.376	-0.523	-0.38	-0.273
Entrepreneurs, self-employed	-0.415	-0.531	-0.357	-0.323
Public executives	-0.48	-0.547	-0.322	-0.326
Private executives	-0.452	-0.526	-0.422	-0.367
Education, health	-0.959	-0.871	-0.433	-0.411
Administrative professions	-0.548	-0.534	-0.396	-0.39
Technicians	-0.652	-0.691	-0.529	-0.453
First-line supervisors	-0.802	-0.659	-0.641	-0.503
Public employees	-0.859	-0.667	-0.322	-0.367
Private employees	-0.75	-0.661	-0.401	-0.427
Retail employees	-0.863	-0.644	-0.355	-0.369
Services	-0.515	-0.432	-0.144	-0.154
Qualified workers	-0.749	-0.579	-0.403	-0.394
Unqualified workers	-0.615	-0.447	-0.269	-0.291
Average	-0.491	-0.568	-0.311	-0.306

Figure 19: Average surplus change and schedule constraints

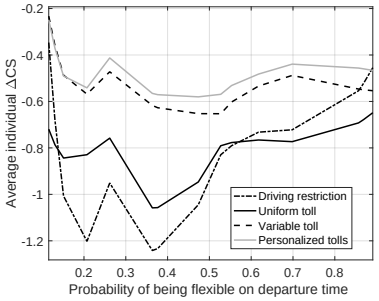

(a) Flexibility

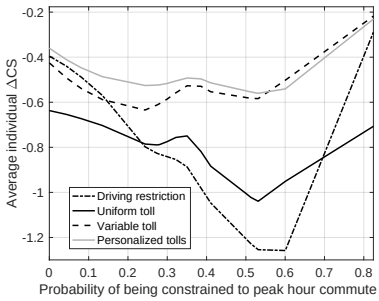

(b) Peak-hour commute constraint

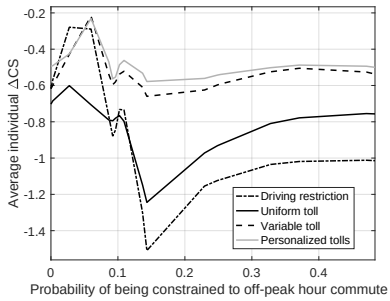

(c) Off-peak hour commute constraint

E.4.2 Additional aggregate outcomes

The aggregate shares of transportation modes are reported in Table 29. They reveal a moderate inter-temporal modal shift towards driving at off-peak hours. The share of individuals commuting during off-peak hours rises by at most 1.2 percentage points. The share of car users at peak hours drops under all policies, but the magnitudes differ. For example, driving restrictions and uniform tolls decrease the number of car users by 7 and 9.9 percentage points, respectively. By contrast, the variable toll and personalized tolls only reduce it by 3.7 and 4.3 percentage points, respectively. The variable and personalized tolls indeed discourage individuals with long distances from driving; therefore, the number of drivers remains relatively high. For the same reason, we observe important differences in the modal shifts across policies: driving restrictions and the uniform toll increase the fraction of individuals who walk and take public transport more than the variable toll.

Table 29: Predicted shares of the transportation modes under different policies

	Initial	**Driving restriction**	**Uniform toll**	**Variable toll**	**Personalized tolls, max W**
Pub. transport, peak	33.7	37.1	37.7	35.7	36.2
Car, peak	24	17	14.2	20.3	19.7
Walk, peak	14.9	16.4	18.3	15.3	15.4
Bicycle, peak	1.88	2.21	2.39	2	2.02
Motorcycle, peak	1.28	1.48	1.52	1.4	1.42
Pub. transport, off-peak	11.6	11.9	12	11.9	11.9
Car, off-peak	8.48	9.66	9.65	9.23	9.11
Walk, off-peak	2.77	2.83	2.9	2.78	2.79
Bicycle, off-peak	0.566	0.584	0.596	0.573	0.576
Motorcycle, off-peak	0.756	0.788	0.801	0.79	0.794
Total car	32.5	26.7	23.8	29.6	28.8
Total pub. transport	45.4	49	49.7	47.6	48.1
Total peak hours	75.8	74.2	74	74.7	74.8
Total off-peak hours	24.2	25.8	26	25.3	25.2

Note: in %.

Impacts on individual trip durations We complement the analysis by looking at how the policies impact expected travel times in Table 30 below. First, there is a large difference in the total travel time increase across policies: under the variable and personalized toll, it is only 11.7 and 12.5 thousand hours against 58 and 85.7 thousand hours under the driving restriction and the uniform toll, respectively. This reflects the more extensive substitution for driving at off-peak hours for long-distance commuters under the variable and personalized tolls. Indeed, driving during off-peak hours remains relatively fast but it generates consumer surplus losses because of the disutility for commuting during off-peak hours. In addition, individuals drive faster due to speed improvements.

All policies increase the average travel time; driving at peak hours becomes faster, but individuals rely less on this mode. We observe important dispersion in travel time change and a skewed distribution. Travel time increases are as high as more than 1.5 hours under variable and personalized tolls. Under all policies, some individuals reduce their expected trip durations. The variable toll has the largest share of individuals with reduced travel times, with 53.6% of the individuals, followed by personalized tolls with 50.2%. The driving restriction and uniform toll reduce travel time for 34.5 and 38.8% of individuals, respectively.

Table 30: Change in trip duration under the policies

	Driving restriction	Uniform toll	Variable toll	Personalized tolls, max W
Total Δduration (in 1,000 hrs)	58	85.7	11.7	12.5
Min Δduration	-4.78	-8.13	-8.5	-11.4
Mean Δduration	1.15	1.7	0.233	0.249
Max Δduration	60	91.3	115.8	118.8
% Δduration > 0	65.5	61.2	46.4	49.8
% Δduration < 0	34.5	38.8	53.6	50.2

Note: Δduration are in minutes, except "Total Δ duration". The shares of individuals with an increase/decrease in trip duration are for potential drivers.

Speed changes We analyze the speed changes by area in Table 31. The variable toll most improves the speed on the highways at peak hours (+19.7 km/hr). The variable toll is also better than the driving restriction and uniform toll at improving the speed on the ring roads at peak hours. However, it raises speeds in the city center and the suburbs at peak hours less than these alternative policy instruments. This occurs because the individuals who drive on the highways and ring roads tend to drive long distances and are discouraged from using their cars at peak hours. However, they do not have good transportation alternatives, so they drive during off-peak hours. Personalized tolls have different effects on speeds than variable tolls: they most enhance the speeds at peak hours in the city center and the ring roads.

Across the regulations, the areas with the smallest improvements are the city center and the suburbs, revealing the low scope for speed improvements from the congestion technologies in these areas. The speeds at off-peak hours decrease in all areas but remain much higher than the initial levels at peak hours. This reflects the imperfect substitution between driving at peak and off-peak hours as individuals face important schedule constraints.

Table 31: Predicted speeds under the different policies

	Area	Initial	Driving restriction	Uniform toll	Variable toll	Personalized tolls, max W
Peak hours	Highways	59.3	74.7	72.4	79	77.7
	City center	13.1	15	16.1	14.8	17.6
	Ring roads	29	35.4	36.4	37.1	44.1
	Close suburbs	16.2	18	18.5	17.4	18.1
	Far suburbs	24.8	26.8	26.8	26.4	26.1
Off-peak hours	Highways	88.2	85.6	86.1	83.9	85.3
	City center	19.1	18.7	18.7	18.8	18.5
	Ring roads	46.8	45.7	46	45.8	45
	Close suburbs	20.3	19.9	19.9	20	19.9
	Far suburbs	28.8	28.3	28.3	28.3	28.5

Note: in km/hr.

Marginal costs of congestion Table 32 presents the marginal congestion costs for each area and period under the different policies. We provide the marginal costs associated with adding one average driver in each area to account for differences in area sizes. All

policies reduce the marginal costs of congestion at peak hours and increase the marginal costs during off-peak hours. The reductions are quite large and heterogeneous across policies. The personalized tolls are particularly efficient at reducing the marginal congestion costs on the highways and ring roads (-60.8% and -60.5%). The marginal costs at off-peak hours are always lower than at peak hours, reflecting the mild intertemporal substitution of drivers.

Table 32: Marginal costs of congestion under the different policies

	Area	Initial	Driving restriction	Uniform toll	Variable toll	Personalized tolls, max W_2
Peak hours	Highways	4.39	1.96	2.39	1.58	1.72
	City center	4.26	3.28	3.11	3.64	2.6
	Ring roads	4.24	2.81	2.82	2.68	1.67
	Close suburb	1.57	1.06	1.06	1.29	1.14
	Far suburb	0.893	0.569	0.637	0.681	0.724
Off-peak hours	Highways	0.683	0.888	0.83	1.01	0.894
	City center	1.81	1.9	1.86	1.84	1.91
	Ring roads	1.2	1.32	1.26	1.28	1.36
	Close suburb	0.599	0.668	0.654	0.633	0.643
	Far suburb	0.323	0.388	0.369	0.375	0.353

Note: marginal costs associated to adding an average driver, in €.

E.5 Robustness checks for the policy simulations

E.5.1 All-day policies

In this section, we analyze the impacts of policies applied during the entire morning across all stringency levels as in Section 5.3. For this exercise, the traffic reduction is computed from the sum of kilometers driven at peak and off-peak hours. Figure 20 presents the main outcomes of interest across the three policies for all stringency levels. Panel (a) shows that the ranking between policies regarding welfare remains the same as before. However, policies enhance welfare for a smaller set of stringency levels. Indeed, we obtain welfare gains for traffic reductions below 26% with the uniform toll and 45% with the variable toll.

Panel (b) reveals that, as before, no policy increases the aggregate consumer surplus. Additionally, we see that consumer surplus losses are much higher than those of the peak-hour policies. For instance, with a variable toll and for a traffic reduction of 20%, consumer surplus loss is €2 million if the policy is applied all day against €0.98 million if it is only applied at peak hours. This highlights the role of departure time substitution in mitigating consumer surplus losses.

Finally, Panel (c) shows similar trends in terms of toll revenue between peak and all-day policies. The toll revenues are much higher with policies applicable to all day, as we obtain €1.4 million for a variable toll at peak hour that reduces traffic by 20% and €2.4 million under a variable toll applied all day that reduces traffic by the same percentage.

Figure 20: Change in welfare, consumer surplus, and toll revenue under all-day policies

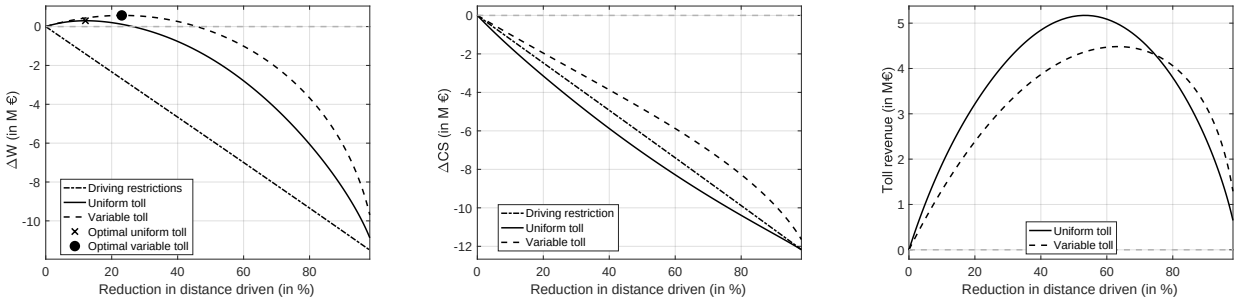

(a) Welfare (b) Consumer surplus (c) Toll revenue

Figure 21 presents the change in emissions, average tolls, and average distance driven across stringency levels for the all-day policies. We find graphs similar to those for the peak-only policies presented in Figure 4. Panels (a) and (b) show that gains from emissions reductions almost double, while the average toll is a bit higher for all-day policies than for peak-hour policies. From Panel (c), the average number of kilometers driven per trip remains similar between all-day and peak-only policies across all stringency levels. This result signals that the individuals targeted by the policies do not vary depending on whether the policy applies only at peak hours or all day. We take these results as evidence that the main results from our analysis of peak policies apply to all-day policies.

Figure 21: Additional policy outcomes under all-day policies

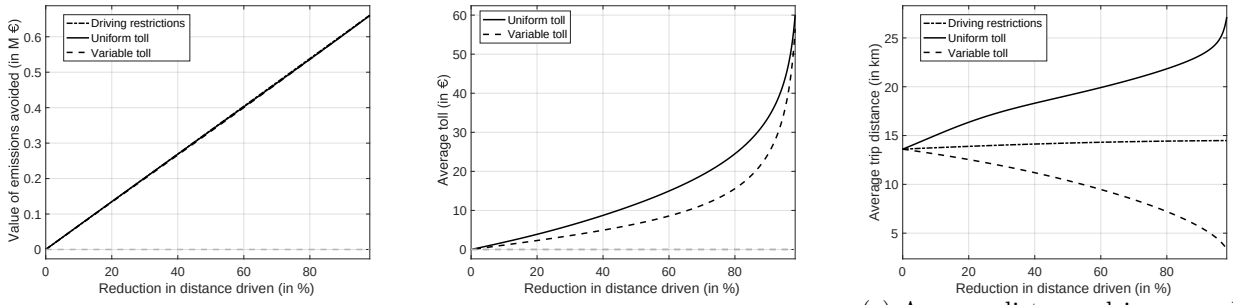

(a) Value of emissions avoided (b) Average toll (c) Average distance driven, conditional on driving

E.5.2 Increase in public transport overcrowding

We analyze how the welfare effects of the benchmark variable toll are modified when overcrowding in railway public transit increases. We consider the policy to be followed by a 15% and 30% increase in the overcrowding levels in public transport. These factors are much higher than what we should realistically expect since the benchmark variable toll raises the average probability of using public transport by only 5.9% at peak hours and 2.3% during off-peak hours. Table 33 shows that the toll revenue remains almost constant under the

three scenarios since the share of individuals driving is barely affected by the change in the overcrowding level. However, the consumer surplus decreases by 9.2% and 18.4% more than in the baseline setting. Yet, we still obtain that the variable toll is a welfare-enhancing policy.

Table 33: Effects of the variable toll with overcrowding level changes in public transit

	Baseline	**Overcrowding +15%**	**Overcrowding +30%**
Total ΔCS (M€)	-1.19	-1.3	-1.41
ΔCS at constant speed	-1.74	-1.84	-1.95
ΔCS from speed	0.55	0.543	0.536
Total ΔwCS (M€)	-1.04	-1.14	-1.24
Tax revenue (M€)	1.64	1.64	1.65
Value emissions avoided (M€)	0.078	0.077	0.075
ΔW = ΔCS + Tax rev. - ΔE (M€)	0.525	0.418	0.311
% ΔCS = 0	21.2	9.19	9.19
% ΔCS > 0	6	3.16	2.28
% ΔCS < 0	72.8	87.7	88.5

Note: The share of individuals with positive/negative/no consumer surplus change are relative to the entire population.

E.5.3 Removing schedule constraints

In this robustness check, we analyze the incidence of our estimated schedule constraints on the policy effects. We keep the same model parameters except that the probabilities of being schedule-constrained are set to zero for everyone and then to one for everyone. We solve the equilibrium without policy and with the benchmark variable toll for each scenario regarding the ability to choose the departure time. Table 34 shows that the toll generates lower consumer surplus losses when we remove the schedule constraints. This is intuitive because consumers are able to do more inter-temporal substitution to avoid paying the road toll. As a consequence, the toll revenue is lower, which makes the change in welfare lower than with our estimated schedule constraints.

Under full schedule constraints, we find the reverse. The variable toll generates more consumer surplus losses and more toll revenue than in the baseline situation, resulting in higher welfare gains. However, we see that the policy efficiency, in terms of traffic reduction, is lower under full schedule constraints than with less schedule constraints. These results show that the schedule constraints matter for the policy efficiency but not so much for the magnitude of the welfare gains.

Table 34: Welfare effects of the variable toll under different schedule constraints

	Baseline	**No schedule constraints**	**Full schedule constraints**
Total ΔCS (M€)	-1.19	-1.15	-1.25
ΔCS at constant speed	-1.74	-1.66	-1.89
ΔCS from speed	0.55	0.514	0.639
Total ΔwCS (M€)	-1.04	-1.01	-1.06
Toll revenue (M€)	1.64	1.59	1.78
Value emissions avoided (ΔE, M€)	0.078	0.072	0.087
ΔW = ΔCS + Tax rev. - ΔE (M€)	0.525	0.51	0.622
Dist. driven at peak hours (10,000 km)	8.63	8.38	9.39

E.5.4 Change in unobserved traffic

We now measure the welfare consequences of the benchmark variable toll when considering the unobserved part of the traffic changes. More specifically, we assume the unobserved part of the traffic homogeneously decreases by 24% at peak hours and increases by 14% during off-peak hours. These factors correspond to the average changes in traffic under the variable toll. Table 35 shows that the value of the speed improvements is 80.5% higher when we consider the change in the unobserved traffic. Despite that, the variable toll still reduces aggregate consumer surplus by €749,000. The toll revenue increases by 12.1%: speed gains are larger, so individuals are willing to pay more to drive. Ultimately, the welfare gains are much higher than without adjustment of the unobserved traffic despite a lower gain from emissions reductions.

Table 35: Welfare effects of the variable toll with changes in unobserved traffic levels

	Baseline	**Change in K_0^a**
Total ΔCS (M€)	-1.19	-0.749
ΔCS at constant speed	-1.74	-1.74
ΔCS from speed	0.55	0.992
Total ΔwCS (M€)	-1.04	-0.671
Tax revenue (M€)	1.64	1.84
Value emissions avoided (M€)	0.078	0.065
ΔW = ΔCS + Tax rev. - ΔE (M€)	0.525	1.15
% ΔCS > 0	7.62	24.6
% ΔCS < 0	92.4	75.4

F Additional policy instruments

F.1 Auctioned driving license

We consider a simple uniform second-price auction to allocate a fixed number of driving licenses. The equilibrium price is the highest rejected bid. This auction format implies that individuals bid their true license valuation, which is determined by the difference between their expected utility with and without the right to drive. We assume individuals perfectly

anticipate the speed improvements, but they do not know their preference shocks before submitting their bids.

The uniform toll is well-suited to a comparison with the auction as they both put a price on the right to drive. However, there is an essential difference from the perspective of individuals. Under the toll, individuals decide to drive after their schedule, mode, and departure time preference shocks are realized. While under the auction, individuals have to submit their bid for the license before receiving their preference shocks and lose the ability to react in case of extreme preference shocks.

We use an iterative algorithm to solve for the license price together with the equilibrium speeds for a given quota of driving licenses. Our algorithm cannot find a stable equilibrium for some values of the quota of driving licenses. We thus select the quota of driving licenses that implies the closest outcome to the one obtained in our main policies. Then, we re-calibrate the uniform toll to match the traffic reduction exactly across policies. We find that the uniform toll of €4.2 achieves the same traffic reduction (24.4%) as introducing a quota of driving licenses that allow 28.8% of the cars on the road. The equilibrium license price is €3.

Since individuals who get the license pay for it regardless of how often they decide to drive at peak hours, the policy generates considerably higher consumer surplus losses. Individuals can no longer react to good or bad realisations of their preference shocks for driving. Indeed, the driving license regulation causes 70.6% more consumer surplus losses than the uniform toll. The license generates 17.7% more revenue and 24.6% more values from emissions avoided. However, these benefits are insufficient to compensate for the large consumer surplus loss, causing a net welfare loss of €0.95 million, while the uniform toll enhances welfare. Finally, this policy generates only two percent of winners, indicating that the cost of a driving license is too high relative to the gains from speed for most individuals.

Table 36: Welfare effects of a uniform toll and auctioned driving license

	Uniform toll	**License**
Total ΔCS (M€)	-2.18	-3.72
ΔCS at constant speed	-2.8	-4.45
ΔCS from speed	0.616	0.732
Total ΔwCS (M€)	-2.01	-3.42
Toll/license revenue (M€)	2.27	2.67
Value emissions avoided (M€)	0.088	0.11
ΔW = ΔCS + Tax rev. + ΔE (M€)	0.173	-0.945
% ΔCS $>$ 0	4.29	2.04
% ΔCS $<$ 0	95.7	98

F.2 Attribute-based driving restrictions

Low emission zone policies are widely used in Europe.[59] They impose driving restrictions based on fuel type and vintage combinations to remove the most pollutant cars from the roads. Attribute-based policies are thus more cost-efficient at reducing emissions but generate greater heterogeneity across individuals than simple driving restrictions. We study the trade-off policymakers face by comparing the standard driving restrictions against two attribute-based policies: one banning all vehicles below a particular vintage and one banning diesel cars with a certain probability. While individuals are likely to change their cars in response to such policy, as shown by Barahona et al. (2020), we abstract from any effect on the fleet's composition.

As before, we calibrate the policies to reach the same traffic reduction. Since car vintage is a discrete variable, we cannot precisely match the expected number of kilometers at peak hours with only this parameter. We use the strictest vintage and assume that individuals are subject to the policy with a probability lower than one. This technical assumption can be interpreted as the frequency at which the policy is implemented. The policy parameter for diesel-based restriction is the probability of being restricted for a diesel-car owner. The calibrated parameters are as follows: the vintage cut-off is 2004, and the policy should be applied 87.6% of the time. This regulation restricts 48.5% of the population. The diesel-based restriction should be applied 52.8% of the time and affects 59.4% of the people.

As Table 37 suggests, the vintage-based policy generates €2.09 million of consumer surplus losses versus €1.85 million for the untargeted driving restriction. The diesel-based restriction causes lower consumer surplus losses than the vintage one (€1.78 million). Under the vintage- and diesel-based regulations, 51.5% and 41% of the potential drivers experience a consumer surplus increase, respectively. Targeted driving restrictions put the traffic reduction burden on only a fraction of the potential drivers. By contrast, standard restrictions share the traffic reduction burden on a larger number of individuals. We see that the vintage-based driving restriction can generate a consumer surplus loss of up to €90 while the maximal surplus loss is €34 under standard driving restrictions.

The vintage-based restriction is more efficient at reducing emissions. This is not the case for diesel-based driving restrictions that generate lower gains from emissions avoided. Indeed, diesel cars emit more harmful local pollutants but less carbon emissions. However, since the emissions value is small relative to the consumer surplus loss, the diesel-based policy remains

[59] For instance, in 2024, 66 German cites and 16 French cities are under low emission zone restrictions. Madrid, Barcelona, Milan, Rome, and Naples are additional examples of large cities with this type of policy. Source: https://urbanaccessregulations.eu/countries-mainmenu-147. Last accessed: 09/18/2024.

the best policy for welfare.

Table 37: Welfare effects of standard and attribute-based driving restrictions

	Standard	**Vintage-based**	**Diesel-based**
Total ΔCS (M€)	-1.88	-2.12	-1.81
ΔCS at constant speed	-2.42	-2.7	-2.31
ΔCS from speed	0.538	0.574	0.508
Total ΔwCS (M€)	-1.78	-2.47	-1.71
Value emissions avoided (M€)	0.085	0.11	0.096
ΔW = ΔCS + ΔE (M€)	-1.79	-2.01	-1.71
% ΔCS > 0	8.48	51.5	41
% ΔCS < 0	91.5	48.5	59
Min ΔCS (€)	-34.7	-91.1	-53.8
Max ΔCS (€)	1.61	7.2	5.88

F.3 Improving public transport

The main analysis of the paper focuses on policies targeting drivers. Our model can also provide insights into how improvements to public transport can mitigate consumer surplus losses related to traffic-reducing policies. However, we do not evaluate public transport improvements and their effects at the same level of detail as Almagro et al. (2024), who have a micro-founded model that determines bus trip durations from bus frequencies and traffic.

We consider four scenarios. First, we improve public transport coverage by allowing the 13.8% of individuals who initially do not have access to public transport to use a hypothetical public transport service.[60] In the second scenario, we target improvement in public transport by assigning the median public transport speed to individuals below that value. In the third scenario, we consider a homogeneous improvement that raises all individual speeds by 23.2%. This speed improvement factor is such that the targeted and homogenous speed improvements generate the same average speeds. Finally, in the last scenario, we make public transport free.

For each scenario, we measure the changes in outcomes by comparing the traffic equilibria with and without the benchmark variable toll, both under the new public transport environment. The welfare effects from the variable toll under different public transport environments are provided in Table 38. Public transport improvements reduce consumer surplus losses from the toll. The consumer surplus losses are the lowest under the homogeneous speed improvement. However, because public transport has become more attractive, individuals are less likely to pay the toll, considerably reducing the revenue raised. Moreover, reducing consumer surplus losses does not compensate for the lower toll revenue, generating lower welfare gains. Nevertheless, we obtain positive welfare effects from the toll, indicating that even after the public transport environment improvement, there is a gain from road pricing.

[60] We use the median characteristics of public transport: a speed of 15.1 km/hr, a price of €1.63, overcrowding levels of 120% at peak hours and 36% at off-peak hours, one layover, and not using the railway system only.

Note also that this welfare measure does not include public transport revenue, which would increase in the first three scenarios. Across scenarios, the share of winners from the toll decreases after improvements to public transport have been implemented. Changing the public transport environment does not reduce the magnitudes of the largest consumer surplus losses but reduces the maximum gains. This is because the gains from speeds are lower under an improved public transport environment, not compensating for the toll paid.

Table 38: Welfare effects of the benchmark variable toll under public transport improvements

	Baseline	**(1)**	**(2)**	**(3)**	**(4)**
Total ΔCS (M€)	-1.19	-1.19	-1.15	-1.13	-1.14
ΔCS at constant speed	-1.74	-1.74	-1.68	-1.53	-1.6
ΔCS from speed	0.55	0.548	0.522	0.409	0.454
Toll revenue (M€)	1.64	1.63	1.57	1.39	1.47
Value emissions avoided (Δ E, M€)	0.078	0.078	0.079	0.084	0.078
ΔW = ΔCS + Toll rev. + ΔE (M€)	0.525	0.524	0.498	0.346	0.404
% ΔCS > 0	7.62	7.61	7.46	6.03	5.93
% ΔCS < 0	92.4	92.4	92.5	94	94.1
Min ΔCS (€)	-7.43	-7.43	-7.42	-6.61	-7.48
Max ΔCS (€)	3.25	3.26	3.37	1.32	1.81

Note: (1): Coverage improvement. (2): Targeted speed improvement. (3): Homogeneous speed improvement. (4): Free access.

F.4 Discussion about the scope of the model

Change in road congestion technology Recent urban policies consist of pedestrianization of specific roads, as well as their conversion into bike lanes. By reducing the road capacity for cars, such policies reduce speed for the same level of traffic. We can model such policies as changes in the congestion technologies, either through parallel shifts of the curves or a proportional decrease in speed along the curve. Alternatively, we could also model improvements to road congestion technology, such as a road capacity increase or autonomous vehicles that would make traffic smoother.

Pricing a fraction of the road Hall (2018) and Hall (2021) suggest that setting a toll on a fraction of the roads is efficient because it induces self-selection of individuals according to their sensitivity to travel time against price. We could consider introducing a toll on a fraction of $1/h$ of the roads in area a. We denote by a_1 the tolled road and a_2 the free one. Conditional on driving, individual n chooses the tolled road if $\beta_n^{\text{duration}}\text{duration}_{n\mathbf{d}a_1} + \alpha_n p_{a_1} \geq \beta_n^{\text{duration}}\text{duration}_{n\mathbf{d}a_2}$ (abstracting from the departure time choice). Once we know the chosen road conditional on driving, we can also calculate the probabilities of driving and the expected traffic level on each road. Since capacity is divided by h, the speed on road a_1 is $v^{a_1} = f^a(h\phi^a K^{a_1} + K_0^a)$, where K^{a_1} is the traffic level on road a_1. The factor h reflects the road capacity reduction: the same number of kilometers driven implies a higher level of traffic.

Carpooling We have recently seen some initiatives to encourage carpooling. The U.S. has, for instance, a long tradition with high occupancy lanes in 27 metropolitan areas. While our model cannot predict the impacts of dedicating special lanes to carpooling and how individuals decide whether or not to carpool, we can still evaluate the benefits of carpooling under some simple assumptions. For instance, assuming that everyone has to carpool with three other people, a carpooling requirement amounts to considering that individuals are only driving one-fourth of their kilometers. Thus, it is equivalent to modifying the mapping parameter between the number of kilometers driven and the occupancy rate in Equation (14) to $\tilde{\phi}^a = \phi^a/4$. The model can easily accommodate different cost-sharing assumptions and include detours that increase driving times. However, endogeneizing the decision to carpool is beyond the scope of the model.

Modifying work conditions We could consider policies incentivizing working from home a fraction of the time. We can model this similarly to carpooling. For instance, if we assume individuals work from home one (random) day per week, it reduces the expected number of kilometers driven by 20%. This is equivalent to modifying the mapping parameter in equation (14) between the number of kilometers driven and the occupancy rate to $\tilde{\phi}^a = \frac{4}{5}\phi^a$. We can also deal with heterogeneous individual-specific remote work propensity. We would consider the number of kilometers of individual n to be $\tilde{k}_n = (1 - \delta_n)k_n$, where δ_n represents the fraction of the time individuals work from home. However, endogeneizing the choice of working from home is outside the scope of the model.

Parking cost and availability Recent literature shows the importance of parking prices and availability on traffic levels (Ostermeijer et al., 2022). The model can easily evaluate the effect of increasing parking prices through targeted increases in the costs of car trips. However, it would be more challenging to predict the impacts of policies affecting parking availability since we do not model the parking choice and we ignore the potential parking time in the car trip durations.